Future Operation of the GB High-pressure Gas Network with Hydrogen

Amirreza Azimipoor

School of Engineering

Cardiff University

A thesis submitted for a degree of

Doctor of Philosophy

November-2025

Acknowledgement

I sincerely thank my supervisors, Prof Meysam Qadrdan and Prof Nick Jenkins, for their unwavering support and guidance throughout my PhD journey. Their invaluable advice, patience, and encouragement have been instrumental in my success.

I deeply thank my colleague, Dr Tong Zhang for her invaluable mentorship and support. Her guidance and encouragement have been crucial to my growth as a researcher.

I am sincerely thankful of Dr Muditha Abeysekera for his feedback on my research and for allowing be to be a participant at Supergen community.

I am profoundly grateful to my parents for their unwavering support and encouragement throughout my PhD. Their love, patience, and belief in my abilities have been my foundation.

To all who have helped me during these challenging times, I cite parts of the poem “I turn death into…” by Ahmad Shamlou, a contemporary Iranian poet:

“…In you, there were lilies and rain.
In me, daggers and roars.
In you, fountains and fantasy.
In me, mere and murk.

…In your passageway I sang a different song.

…I turned love into a song
More sonorous than death
More sonorous than life
I turned death into a song.”

Summary

The UK has the ambition to Utilise the existing high-pressure gas network infrastructure for hydrogen (H_2) gas transportation. This thesis presents a comprehensive study on using the Great Britain (GB) high-pressure gas network for hydrogen transmission, employing a detailed, unsteady-state simulation model of GB high-pressure gas network developed in Synergi Gas software.

The impacts of hydrogen transmission via the grid were investigated through three studies. The first study examined centralised hydrogen injection, where hydrogen was injected at 20% volumetric concentration at nine natural gas supply points. The second study explored distributed hydrogen injection, where hydrogen produced using excess wind energy was injected at 28 wind farm locations at 20% volumetric concentration cap. Subsequently, the transmission of pure hydrogen through the existing high-pressure gas network was also investigated.

Comparison of the injection studies revealed that distributed hydrogen injection leads to inhomogeneous and varying hydrogen concentrations in different locations of the grid and across the time horizon. The case studies indicated that while the high-pressure gas network can accommodate 20% volumetric hydrogen without compromising pressure or significantly affecting compressor energy consumption, transmitting pure hydrogen increased compressor energy consumption and reduced linepack levels.

Further analysis focused on use of deblending technologies in the GB high-pressure gas network. Deblending refers to technologies that separate hydrogen and natural gas to deliver a specific concentration of gas to the end-user. The case studies considered deblending for gas delivery to power stations (requiring natural gas free of hydrogen), industrial sites (requiring pure hydrogen), and Local Distribution Zones (LDZs) (requiring natural gas with a fixed 20% hydrogen volumetric rate).

The cost of deblending varied based on the type of gas demanded by the end-user. As Industrial sites demanded pure hydrogen, large volumes of mixed gas were processed to produce pure hydrogen, leading to a high specific energy consumption. Delivering gas to other end-users produced significantly lower specific energy consumption, suggesting that deblending is more practical for delivering to power stations and LDZs

Table of Contents

List of Figures

List of Tables

Nomenclature

Abbreviations

ATR	Auto-thermal reformation (a chemical hydrogen production method)
ALEC	Alkeline Electrolysis
Bar-g	Bar-gauged (pressure unit equal to 10^5 Pa)
BWRS	Benedict-Webb-Rubin-Starling
CCGT	Combined-cycle gas turbine
CCS	Carbon Capture and Storage
EHB	European Hydrogen Backbone
ESO	Electricity System Operator
FES	Future Energy Scenarios (a document published by the GB national energy system operator, NESO.
GTYS	Gas Ten-Year Statement (published annually by National Gas, the GB gas transmission operator)
GWh	Giga Watt Hour
IQR	Interquartile Range
LDZ	Local Distribution Zone (receiving gas from the high-pressure gas network)_
LNG	Liquified Natural Gas
Mm^3/d	Millions of Standard Cubic Meters per Day
Mm^3/h	Millions of Standard Cubic Meters per Hour
MWh	Megawatt- hour
NTS	National Transmission System (the GB high-pressure gas network)
NREL	National Renewable Energy Laboratory

OPEX	Operating Expenditure
PEM	Proton Exchange Membrane (a type of electrolyser)
P2G	Power to Gas (for hydrogen production)
SEC	Specific energy consumption
SMR	Steam Methane Reformation (a chemical hydrogen production process)
Vol	Volumetric

Symbols

A	The cross-sectional area of the pipe [m^2]
a	Gas flow exponent [1.3]
D	Diameter [m]
d	Day (as a unit of time)
C	Total molar concentration [mol.m^{-3}]
$\mathfrak{D}_{ij}$	Maxwell–Stefan binary diffusivity [m²·s⁻¹]
ε	Absolute roughness of a pipe [assumed 0.067mm]
F	Frictional force
h	Hour (as a unit of time)
H_2	Hydrogen molecule
k_F	Friction factor of pipe
k_{ij}	Interaction coefficient of components i and j in benedict-Webb-Rubin-Starling equation of state
L_t	Linepack at timestep t [Mm^3]
L_0	Starting linepack [Mm^3]
l	Specified length of pipe [m]
m_i	Molar fraction of gas molecule i

$\mathrm{n^e}$	Polytropic exponent [1.3]
p	Pressure [bar-g]
p_b	Compressor station's base pressure [bar-g]
p_m	Average pressure of the pipeline [bar-g]
p_s	Pressure at standard conditions [bar-g]
p_2	Compressor station's discharge pressure [bar-g]
p_1	Compressor station's suction pressure [bar-g]
$p(0)$	Pressure at the beginning of pipe [bar-g]
$p(l)$	Pressure at the length l of the pipe [bar-g]
$\dot{m}$	Mass flow rate [kg/s]
q	Standard volumetric flow rate [m^3/s]
q_i^h	Standard volumetric flow rate of the H_2 injection stream at the injection site[m^3/s]
q_i^c	Standard volumetric flow rate of the incoming stream at injection site[m^3/s]
q_i^o	Standard volumetric flow rate of the outgoing stream from the injection site[m^3/s]
q_d^i	Standard volumetric flow rate at inlet of the deblending site
q_d^p	Standard volumetric flow rate at product stream of the deblending site
q_d^r	Standard volumetric flow rate at reject stream of the deblending site
X_d^i	Volumetric percentage of hydrogen at inlet of deblending site
Y_d^i	Volumetric percentage of natural gas at inlet of deblending site
J_i	Diffusive molar flux of species I [$mol \cdot m^{-2} \cdot s^{-1}$]
N_d^p	Volumetric percentage of hydrogen at product stream of deblending site

M_d^p	Volumetric percentage of natural gas at product stream of deblending site
H_d^r	Volumetric percentage of hydrogen at the reject stream of deblending site
G_d^r	Volumetric percentage of natural gas at the reject stream of deblending site
q_t	Standard volumetric flow rate at timestep t [m^3/s]
q_0	Standard volumetric flow rate at timestep 0 [m^3/s]
R	Specific gas constant [J/Kg K]
Re	Reynolds number of the flow
t	Time-step [s]
Γ_{ij}	Thermodynamic factor matrix
θ	Temperature [K]
θ_c	Critical temperature [K]
θ_s	Temperature at standard conditions [K]
u	Total number of components in the gas mixture
V	Volume of gas [m^3]
$\bar{V}_i$	Partial molar volume of species i [$m^3 \cdot mol^{-1}$]
v	Gas velocity [m/s]
W	Compressor power consumption [W]
x	distance along the pipe [m]
Z	Gas compressibility factor
Z_S	Gas compressibility factor at standard conditions [assumed 0.95]
$Z(0)$	Gas compressibility factor at the beginning of the pipe

$Z(l)$	Gas compressibility factor at the length l of the pipe
η	The efficiency of a compressor [assumed 0.8]
θ	Temperature [K]
ρ_s	Mass density at standard conditions [Kg/m^3]
ρ_m	Molar density [mol/m^3]
A_0, B_0, C_0, D_0, E_0 $\alpha_0, \gamma, a, b, c, \beta$	Benedict-Webb-Rubin-Starling coefficients.

Chapter One. Introduction

1.1. Anticipated role of hydrogen in the GB energy system

The UK is committed to reducing its carbon emissions to net zero by 2050 [1]. Hydrogen is expected to play a crucial role in achieving this target, as the UK government has set out plans to develop 10 GW of low-carbon hydrogen supply capacity by 2030 [2]. The UK electricity transmission network operator estimates that, under certain scenarios, annual hydrogen demand could reach as high as 478 TWh by 2050 [3].

Hydrogen demand is expected to increase first in industrial clusters before expanding nationwide [3]. Heavy industries that rely on high-temperature processes are likely to switch to blends of hydrogen and natural gas [3]. In addition, heavy-goods vehicles and large cargo ships are expected to replace conventional fuels with various forms of hydrogen [2]. The UK government also plans to use hydrogen for power generation by 2050 [2]. Furthermore, households in parts of the UK may adopt hydrogen for heating [2,3]. Together, these developments indicate that hydrogen will be required across the country. To meet this growing demand, multiple hydrogen production methods will be deployed, with production sites distributed geographically across Britain.

Hydrogen can be produced through various methods. In recent years, it has been colour-coded based on the production method for easier identification.

Large-scale hydrogen production is projected to use natural gas as a feedstock. Steam methane reforming (SMR) is the most established technology and currently generates most of the UK's hydrogen. SMR is a chemical process in which methane reacts with steam in two stages, ultimately producing hydrogen and carbon dioxide[4]. Hydrogen produced via SMR is referred to as grey hydrogen.

Carbon capture and storage (CCS) technologies could be used to collect and store the carbon-dioxide produced by the SMR technology. hydrogen produced with SMR paired with CCS technology is known as blue hydrogen.

The primary disadvantage of SMR is that capturing carbon dioxide emissions is limited to about 95% efficiency[5].

Consequently, alternative technologies are under development, although they are not yet commercially viable. One such technology is the auto-thermal reformer (ATR), which also produces carbon dioxide. ATR facilities enable more effective and less energy-intensive carbon capture, with capture rates approaching 100% [5]. Hydrogen produced via ATR combined with CCS is also referred to as blue hydrogen.

Another promising method is the pyrolysis of natural gas, which yields solid carbon. By collecting and storing this carbon, the process can theoretically achieve a 100% carbon capture rate[5]. Hydrogen produced in this way is referred to as turquoise hydrogen.

Another group of technologies under development are electrolysers, which use direct electric current to split water into hydrogen and oxygen. The approaches to electrolysis vary. Alkaline electrolysers and proton exchange membrane (PEM) electrolysers are the two technologies currently available commercially [6].

Hydrogen produced by electrolysers powered by renewable sources such as wind or solar is known as green hydrogen. [6].

The chemical processes for hydrogen production—SMR, ATR, and pyrolysis—require large amounts of natural gas. In Great Britain, these facilities are best located at the eight natural gas supply terminals, all of which are situated along the shoreline. In addition, these technologies require the capture and storage of their carbon by-products. The natural gas supply terminals offer another advantage: they are located near depleted gas and oil reservoirs, which provide an efficient means of storing the captured CO_2 from SMR and ATR processes.

The deployment of electrolysers will be geographically distributed across Great Britain, reflecting the widespread distribution of wind generation. Most offshore and onshore wind resources are located in Scotland, with significant concentrations also expected to develop in Northeast England and South Wales.

1.2. Role of the national transmission system in transporting hydrogen

Since both the demand and supply points of hydrogen are geographically dispersed across Britain, an efficient means of transmission is required. Figure 1.1 shows the high-pressure gas network in Great Britain. It illustrates how natural gas is transmitted through an extensive system of pipelines extending over 7,630 km [7]. The network includes eight supply terminals in total—two liquefied natural gas (LNG) import terminals and six terminals connected to gas

extraction fields. In addition, there are three interconnectors: Moffat (to Ireland), BBL (to the Netherlands), and INT (to Belgium). These interconnectors link the network to neighbouring systems and can function as both supply and demand points. Moffat is unidirectional, while the other two are bidirectional. [7].. The network has 24 compressor stations that actively maintain pressure levels within an operational range. [9]

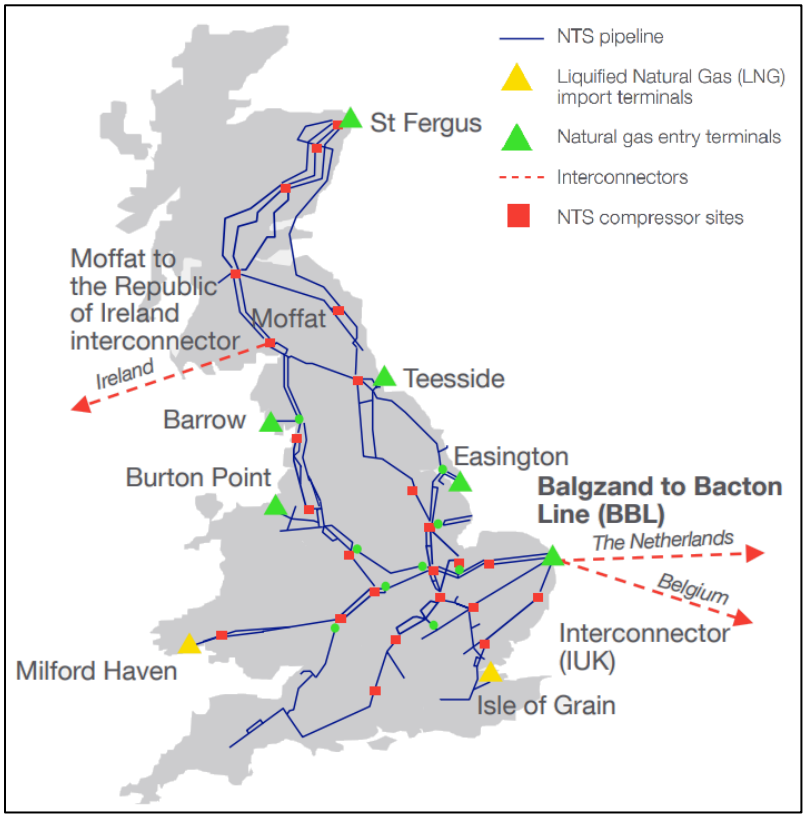

Figure 1.1. Map of the high-pressure gas network of the GB [8] .

The NTS transmits more than 930 TWh of natural gas annually [9], collecting gas from geographically dispersed locations. Supply points include gas fields in Scotland and Northeast England, LNG import sites in South Wales and Southeast England, storage sites in Southwest England, and interconnectors in Northern and Eastern England [7]. he NTS delivers this gas to power stations, large industrial sites, and local distribution zones (LDZs), which in turn supply lower-pressure consumers such as residential households [9].

National Gas plans to utilise the NTS for transmitting hydrogen [10], with three main ambitions: :

1. **Blended transmission (from 2025):** The company aims to repurpose the existing transmission grid to carry hydrogen–natural gas blends with up to 20% hydrogen by

volume[10]. This limit is based on *Future Grid Phase 1*, a comprehensive investigation into the safety of using hydrogen across all types of assets in the high-pressure network[11].In short, end-users can consume gas safely with hydrogen up to 20% vol without the need for any change to the appliances. Also, gas network components, pipes, regulators and compressors can tolerate up to 20% volumetric hydrogen in the blend. The study found that end-users can safely consume gas blends containing up to 20% hydrogen without modifying their appliances. Similarly, network components—such as pipes, regulators, and compressors—can tolerate up to 20% hydrogen by volume. The 20% threshold therefore guarantees safety and minimises disruption for both operators and consumers. Hydrogen will be injected into the NTS directly at points of production.

2. **Dedicated hydrogen transmission (by 2035–2050):** The company aims to repurpose up to one-third of the existing high-pressure gas network to transmit pure hydrogen by 2035 [12], with a nationwide hydrogen transmission network expected to be in place by 2050 [12].
3. **Deblending technologies:** National Gas is also investigating deblending technologies within the NTS. These systems control the hydrogen concentration in the blended gas delivered to consumers. Such control is especially important for sensitive users, such as CCGT power stations, which require stable gas compositions.

1.3. Research questions

These three ambitions raise four research questions:

1. How would increasing volumes of hydrogen in the gas network affect the operation of the high-pressure system—for example, pressure levels, linepack, and compressor energy consumption during a typical winter day?
2. Given that hydrogen supply will be geographically dispersed across Britain, how does the location of hydrogen injection influence the volumetric percentage of hydrogen in each region?
3. Which factors affect the specific energy consumption of deblending technologies in the high-pressure gas network?
4. If National Gas employs deblending technologies to deliver tailored hydrogen–natural gas concentrations to consumers, what would be the energy consumption of a gas network with multiple deblending facilities?

1.4. Thesis structure

This thesis is structured as follows to answer the research questions:

Chapter two reviews academic studies on the challenges of operating existing high-pressure gas networks with hydrogen. It also examines the modelling approaches used to tackle these challenges, highlighting those most relevant to the work presented in this thesis.

Chapter three introduces the unsteady-state simulation model of the GB high-pressure gas network, developed using Synergi Gas software. The model is highly granular, consisting of 279 nodes and 24 compressor stations. It was calibrated by comparing simulated hourly linepack values with real operational data, providing confidence that the model accurately represents system behaviour.

Chapter four investigates the impacts of hydrogen injection into the grid through three studies. The first is a centralised hydrogen injection study, in which hydrogen is introduced at the same nodes where natural gas enters the NTS. In this scenario, hydrogen is injected continuously at 20% by volume of the gas mix at every supply point throughout the day. The second is a distributed hydrogen injection study, which assumes hydrogen production from excess wind energy. In this case, injection points are co-located with wind farms across Great Britain, with hydrogen injected at 20% by volume of the gas mix at each location. The third is a 100% hydrogen transmission study, in which the high-pressure gas network is modelled to transport only hydrogen.

Chapter five investigates the use of deblending technology in the NTS by conducting two case studies. Deblending is sensitive to hydrogen concentration in mix-gas and the volumetric flowrate at inlet. To investigate this effect, one case study simulates the NTS on a winter day, while the other study simulates the NTS on a summer day, providing differences in both factors impacting deblending energy consumption. The energy consumption of each NTS deblending facility is determined using National Gas data. In all the deblending case studies, hydrogen is injected at a 20% volumetric rate at a point co-located with wind farms across the GB. Both case studies investigate the same use cases of deblending technology in the NTS: deblending for power stations, which provides natural gas with no hydrogen; deblending for industrial sites, which provides pure hydrogen; and deblending for LDZ sites, which provides natural gas with fixed 20% hydrogen volumetric rate.

Chapter six provides the conclusions, highlighting the remaining knowledge gaps and ways to further research on transmitting hydrogen with existing high-pressure network infrastructure.

Chapter Two. Review of the research questions and modelling techniques to simulate hydrogen transmission via pipeline

This literature review is divided into three sections. The first discusses issues related to transporting hydrogen via pipeline and summarises the research questions that have already been widely addressed. The second highlights the technical challenges of transporting hydrogen using the existing natural gas infrastructure and specifies the research questions this thesis seeks to answer. The third reviews the modelling techniques available to address these challenges, outlining which methods have been applied to each research question.

2.1. Transport of hydrogen via pipeline

Transporting hydrogen has long been recognised as a challenge and has therefore attracted substantial research. In particular, the economic aspects of hydrogen transportation have received considerable attention, with numerous studies conducted in this area. [13–16].

The economic feasibility of hydrogen transmission depends on factors such as the transmission distance, the volume of hydrogen transported, and the frequency of demand. Within Great Britain, two main methods are expected to be used: (1) compressed gas trucking and (2) pipeline transmission[14]:

1) **Compressed gas trucking** is more cost-effective for short distances (below 50 km) and for intermittent demand throughout the year. Composite storage vessels have a capacity of 500–1,300 kg of hydrogen per trailer. The levelised cost of hydrogen transported by truck is estimated at £2.10–£4.09/kg [14].

   Pipeline transmission becomes more cost-effective for larger volumes and continuous supply over distances between 50 km and 1,000 km. The levelised cost of hydrogen transported by pipeline is estimated at £0.26–£0.31/kg[14]. Given the UK's extensive high-pressure gas network, repurposing parts of the system for hydrogen transmission could reduce costs even further.

The economic feasibility of using existing pipeline infrastructure for hydrogen delivery, as opposed to constructing new pipelines, was evaluated in the European Hydrogen Backbone

report [17]. The study found that repurposing existing natural gas pipelines costs only 33–38% as much as building new ones. It also provides estimated unit capital costs for small (20-inch, ~500 mm), medium (36-inch, ~900 mm), and large (48-inch, ~1,200 mm) pipelines. These estimates are based on data collected from a wide range of European high-pressure gas network operators, rather than simulation. A summary of these cost analyses is available in a report by ACER[18].

Repurposing existing natural gas pipelines for hydrogen transport presents several technical challenges, the most significant being hydrogen embrittlement. This phenomenon causes metal to become brittle, potentially leading to pipeline failure. Although the exact mechanism remains unclear, research indicates that higher steel grades and welds are particularly susceptible.

Mitigation strategies include adding small amounts of impurities, such as oxygen, to the hydrogen stream and incorporating non-metallic inclusions in the steel to trap hydrogen. Various steel grades are currently being tested for hydrogen compatibility, with the UK's FutureGrid study aiming to demonstrate the feasibility of using existing pipelines to transport pure hydrogen.

Another challenge is hydrogen permeation, in which hydrogen escapes through pipeline walls at a rate roughly three times higher than that of natural gas. Such leakage undermines climate goals but can be mitigated using hydrogen traps or polymer coatings.

A further issue is gas stratification, which occurs when hydrogen and natural gas do not mix uniformly, leading to higher hydrogen concentrations near pipeline walls. However, this phenomenon is considered unlikely in high-pressure networks with rapid flow rates.

2.2. Potential customers and their needs for safe use of hydrogen

2.2.1. Domestic customers

In 2023, 73% of GB households used natural gas for heating, which accounted for 44% of the country's annual gas demand [19].

Domestic consumption of hydrogen faces two key requirements. First, according to an HSE investigation conducted in 2015, appliances used in domestic settings can operate safely only when the hydrogen content in the gas stream remains below 23% by volume [20]. This means that pure hydrogen consumption in households would require the complete replacement of all gas appliances. Second, because domestic natural gas consumption is

metered by volume rather than by energy content, the hydrogen share in the gas stream must remain constant throughout the day.

2.2.2. Industrial customers

In 2023, industry accounted for 29.6% of Great Britain's total gas consumption, and many gas-intensive sectors are aiming to transition to hydrogen [19].

Industrial hydrogen use can be divided into two subgroups:

1. Hydrogen as a feedstock for chemical processes:

- Steel production: Carbon-neutral steel can be produced by reducing iron ore with hydrogen to create direct reduced iron (DRI), which is then melted in an electric arc furnace[21].
- Ammonia production: Ammonia synthesis requires hydrogen and nitrogen to react under high temperatures. Traditionally, the hydrogen is produced on-site from natural gas[22].

2. Hydrogen for generating high-temperature heat:

- Ceramics manufacturing: Requires furnaces operating at 930–1,480 °C [23].
- Brick manufacturing: Also requires furnaces operating at 930–1,480 °C [24].

2.2.3. Power Stations

In 2023, 26% of Great Britain's natural gas consumption was used for electricity generation [19]. The adaptation of combined-cycle gas turbines (CCGTs) to operate with natural gas–hydrogen blends remain uncertain. At present, CCGTs can only run safely with hydrogen concentrations up to 1% by volume. A new feasibility study in Great Britain is investigating the potential for safe operation with blends containing 2% hydrogen by volume [25]. In contrast, CCGTs designed to operate on 100% hydrogen appear more promising, with companies such as GE and RWE actively developing hydrogen-ready turbines [26].

Therefore, it is likely that CCGTs would rely on natural gas until upgraded to use 100% hydrogen.

2.3. Operation of a high-pressure gas network with hydrogen

2.3.1. hydrogen and compressor stations

One of the main operational challenges in hydrogen transmission is compression**.** Since hydrogen has a molecular weight only one-sixteenth that of methane, centrifugal compressors require much higher impeller speeds and additional compression stages when compressing pure hydrogen [27]. As a result, reciprocating compressors are generally more effective for compressing pure hydrogen [27]. This issue is less pronounced when hydrogen is injected at lower concentrations (up to 20% by volume of the total gas mixture) [28]. All compressors in the GB high-pressure gas network are centrifugal, and their operation with hydrogen is currently being investigated by National Gas in the *FutureGrid* project[29].

There are publications that have focused on the impact of blended hydrogen and natural gas on the operational metrics of compressors. Zabrzeski et al. [30] studied the phenomena by focusing on changes in the metrics of pipelines connected to the compressor station. The article highlighted that injecting hydrogen into a natural gas stream decreases friction between mixed gas and pipeline, resulting in smaller pressure drops along the pipeline. This phenomenon causes compressor stations to use less energy.

Dong et al. [31] and Xiong et al [32] simulations of centrifugal compressor units and investigated the impact of % of volumetric hydrogen in the gas mix on the compression ratio. The two articles independently reached similar conclusions. Furthermore, Dong et al. found that that by increasing the % volumetric hydrogen from null to 10%, the compressor ratio decreases from 1.45 to 1.25. Xiong et al found that by increasing the % volumetric hydrogen in the mix from null to 20% the compression ratio decreases from 1.6 to 1.4.

Bainier & Kurz [33] used a commercial software to simulate the operation of centrifugal compressor in a looped gas network, when hydrogen is blended with natural gas in the stream. In this methodology, a predefined compressor operating map is used to estimate energy consumption of compressor unit. The authors highlight that with the increase of volumetric hydrogen from null to 10%, the shaft power required for operation increases by 7%. They also highlight that replacing natural gas with 100% hydrogen increases the required shaft power by 215%. centrifugal compressor operation is more energy-intensive with an increase in hydrogen content in the gas mix.

Increasing hydrogen concentration beyond 20% leads to an exponential increase in centrifugal compressor energy demand. This is a significant finding, as it strengthens the case for limiting hydrogen injection to up to 20% volumetric.

Compressor operation can also change the network's hydrogen content. Zhou et al. [34]demonstrated that sudden compressor shutdowns lead to a sudden decrease of up to a quarter of the hydrogen content in parts of the gas network downstream of the compressor station. Witek & Uilhoorn [35] observed the same phenomenon and reported that compressor shutdown and start-up causes sudden changes in the gas composition, making it difficult to calculate the right linepack levels of a network with injected hydrogen.

The GB high-pressure gas network has 24 centrifugal compressor stations. Therefore, three main questions are raised about the operation of these compressors with blends of hydrogen and natural gas:

1. How much power is consumed for compression when hydrogen is injected into the network up to 20% volumetric of the stream?
2. How much power is required for compressing and transmitting pure hydrogen with the same infrastructure as today?
3. How does the operation of compressor stations affect the hydrogen content downstream of compression when hydrogen is injected up to 20% volumetric of the steam?

2.3.2. Hydrogen and network linepack

Linepack, the gas network's capacity to store gas, is a crucial feature that shields the network from unexpected demand surges within a day. For the GB gas network, linepack is one of the frequently utilised attributes. The extent of annual linepack utilisation in GB is highlighted by Rowley and Wilson [30] and documented by National Gas [36]. The low energy density of hydrogen causes changes to this attribute. Furthermore, hydrogen has a heating value per unit volume of a third of natural gas at standard conditions. Wang et al. [37] demonstrated that as the percentage of hydrogen in the network increases, the pressure in the network needs to increase to keep the same level of linepack in energy terms. Wesselink et al.[38] highlight that in a gas network with hydrogen injections, an increase in linepack levels will induce more HE in the pipeline, and linepack levels need to be optimised to keep HE to a minimum. Wu et al. [39] and Jiang et al. [40] examined how linepack levels will change due to fluctuations in renewable-

generated hydrogen injected into the gas network. However, the academic literature needs to demonstrate the extent of this effect.

Since linepack is a highly utilised attribute in the GB gas network, it is vital to answer two questions regarding the impact of hydrogen transmission on linepack:

1. How does hydrogen injection into the network change the linepack levels?
2. How does pure hydrogen transportation affect linepack levels in the network?

2.3.3. Hydrogen mixture in a natural gas network

In gas networks, the relatively high pressures and flow rates result in turbulent flow regimes. When hydrogen is injected, it mixes with natural gas and does not diffuse independently[41].

The high-pressure gas network contains numerous supply terminals, with gas entering from different directions and mixing as it flows toward demand points. When hydrogen is injected at multiple locations, it blends with the surrounding gas streams rather than diffusing separately. As these streams merge, the volumetric percentage of hydrogen in the resulting flow may differ from that of the initial streams, meaning that hydrogen content can vary spatially across the network..

In addition, the flow rates of gas streams fluctuate over time. Consequently, if hydrogen injection volumes remain unadjusted, the hydrogen content in the network will also vary temporally.

In this thesis, mixture of hydrogen and natural gas is described as homogeneous when there is small variations in composition of gas in different locations of gas network and simultaneously, in different timesteps within a single day of gas network operation. Conversely, a inhomogeneous mixture refers to noticeable compositional variations of gas across in different locations of network and/or in different timesteps within a single day of operation. Similar terminology is also used by Fernandes et al. [42]

When hydrogen and natural gas mix, the gas heating value will change with the volumetric ratio of hydrogen present. As the heating value of mixed gas changes, the volumetric consumption of gas will also change. Volumetric gas demand changes will affect the gas network's operational metrics (i.e., pressure and linepack levels, and the energy consumption of the compressor stations).

Only a few papers have studied the regime of hydrogen and natural gas mix in pipelines in real gas networks. Fernandes et al.[42] and Khabbazi et al.[43] investigate the hydrogen and natural gas mixture at the injection point using computational flow analysis in the Italian gas network. The first paper focusing on a mixture along the pipe is by Guandalini et al. [28], where hydrogen is injected mid-way along a single pipeline. This single pipeline model mimics how hydrogen is injected mid-way along the natural gas pipeline. Zhang et al. investigate how hydrogen mixes in a 20-node representation of the Belgian gas network using four hydrogen injection points. The most expanded study is by Ekhtiari et al. [44] using a 23-node representation of the Irish high-pressure gas network. The findings of all these studies point out that hydrogen and natural gas do not mix homogeneously in networks; however, the results depend on the structure of the gas network, and the results for Irish and Belgian gas networks do not identify specific challenges that the GB gas network is likely to face with this issue.

Certain papers have attempted to mitigate the inhomogeneous mixture of hydrogen and natural gas in pipelines by optimising hydrogen injection rates during the day. For example, Saedi et al. [45] developed an optimisation model that finds the optimal gas flow for maintaining consistent hydrogen content in parts of the Australian gas network.

The GB high-pressure gas network is structured differently from the Irish, Belgian, and Australian gas networks. Therefore, two main questions arise:

1. How do modes of hydrogen injection affect natural gas and hydrogen mixing regimes in the network?
2. Which parts of the network will receive more hydrogen, and which parts will be deprived of hydrogen?

2.3.4. Hydrogen deblending

The gas industry is investigating deblending as a potential solution to variations in hydrogen–natural gas concentrations in the high-pressure network. Deblending technologies are installed between the transmission system and end-users, separating a specific gas from the mixture and delivering it directly to the customer.

For domestic end-users, deblending can help ensure compliance with hydrogen concentration requirements. When hydrogen content exceeds 20% by volume, the technology can extract the excess hydrogen from the stream. Conversely, when hydrogen concentration falls

below 20% by volume, the system can reduce the natural gas fraction to maintain the threshold. In this way, deblending stabilises hydrogen levels in the domestic supply, regardless of temporal fluctuations or geographical location.

For power stations, where the adoption of hydrogen–natural gas blends remains uncertain, deblending offers a key advantage by enabling the separation of hydrogen and ensuring delivery of natural gas only.

Industrial customers can also benefit. Sectors that use hydrogen as a chemical feedstock—such as steel and ammonia production—could connect to the grid through deblending sites, which would separate and supply hydrogen from the mixture. Conversely, industries that rely on high-temperature heat could use deblending to regulate the hydrogen concentration in their supply, ensuring it remains consistent.

The gas industry is therefore investigating deblending as a potential solution for varying hydrogen and natural gas concentrations in the high-pressure gas network. Deblending refers to technologies installed between high-pressure gas networks and gas customers. These technologies separate a specific gas from the mix of gases in the high-pressure network and deliver that specific gas to the customer. More than 22 technologies are available for deblending, as stated in a report by NREL [46]. A handful of reports focus on the economic analysis of deblending technologies. For example, the report by National Grid Gas [47] evaluates the existing and mature deblending technologies by calculating the CAPEX and OPEX. The paper also evaluates the sensitivity of each technology, CAPEX and OPEX, to various technical factors. Both reports by NREL and National Gas agree that there are three of these technologies that are commercially viable at the time of writing:

1. Cryogenic separation: The mix-gas enters a separation chamber and is cooled in stages to -179° C, condenses natural gas and separates hydrogen from the mix-gas.
2. Pressure swing adsorption (PSA): The mix-gas is introduced to an adsorber unit, which is a solid-porous material that traps non-hydrogen gases on its surface at high pressures.
3. Membrane separation: The mix-gas passes through a set of hollow fibrous tubes that permeate hydrogen while keeping natural gas in the mix-gas.

These technologies must be further tailored for high-pressure gas networks because they all have specific limitations. Furthermore, PSA technology is only suitable for gas streams with hydrogen concentrations above 50%, and membrane technologies are unsuitable for producing

hydrogen purities above 89%. In addition, the hydrogen that goes through these processes must be repressurised. Furthermore, the residue gas in both cryogenic separation and PSA technologies requires multiple compression stages to be released back into the gas network. The hydrogen produced through permeation using membrane separation loses pressure and needs compression to be used by consumers.

These complications have led National Gas to design two specific setups for deblending in the GB high-pressure gas network:

Cryogenics: As seen in Figure *2.1*The cryogenic setup proposed by National Gas., the mix-gas first passes through a pretreatment process where impurities such as solids or water particles are removed, then goes through a three-stage cryogenic separation process. Afterwards, hydrogen with 98% purity is released from the top of the distillation tower, and the residue gas is released from the bottom of the tower and goes through four stages of compression before being released back into the high-pressure gas network.

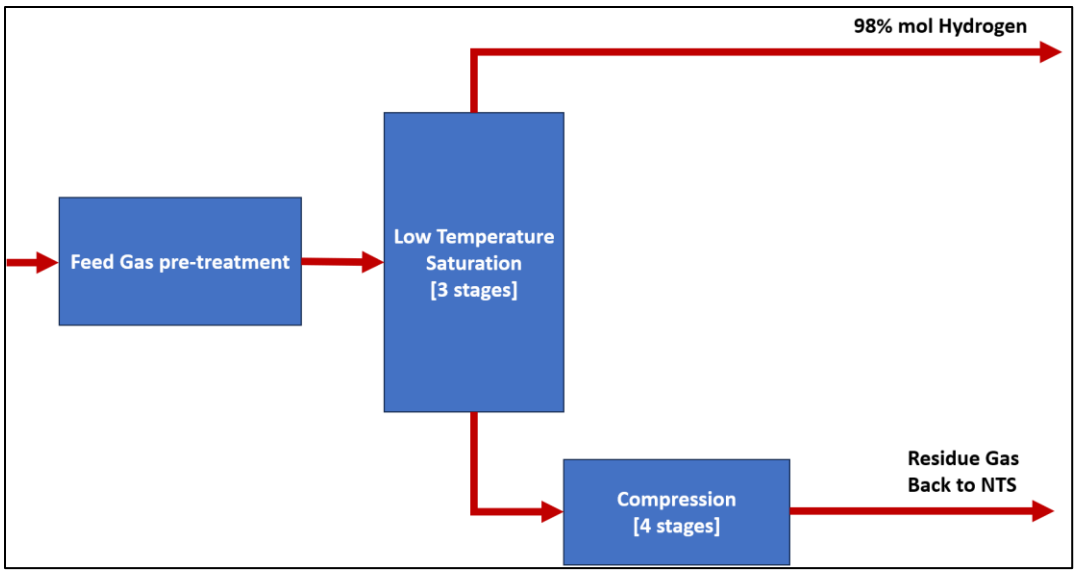

Figure 2.1. The cryogenic setup proposed by National Gas.

PSA plus membrane separation setup: As seen in Figure *2.2*, combining membrane separation and PSA makes it possible to operate the setup with all ranges of hydrogen in the mix-gas. The mix-gas first goes through a purification process where solid particles and water vapours are removed from the stream. It then goes through a twin-membrane separation process, where hydrogen of 90% purity is permeated out of the stream. The residue from the membrane process is directly released back to the NTS.

Hydrogen then goes through a three-stage compression process and is introduced into a PSA process. The PSA produces 98% pure hydrogen, ready to be delivered to the customer. The residue from the PSA process goes through a four-stage compression process before being released into the high-pressure gas network.

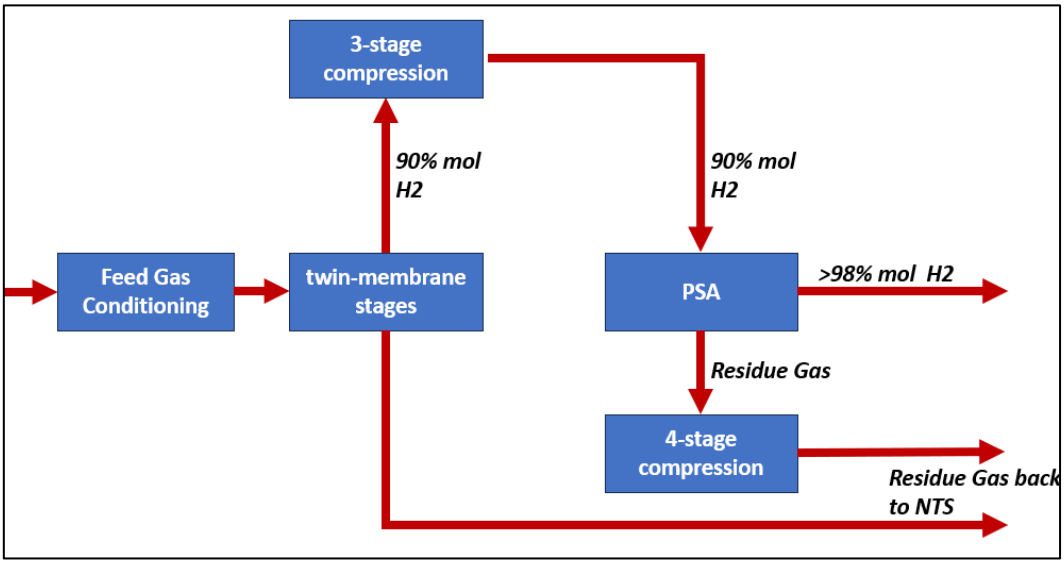

Figure 2.2. Membrane plus PSA setup proposed by National Gas.

A recent report by DNV [48] focused on deblending's impact on the GB high-pressure gas network. The report found that high levels of deblending change the composition of mixed gas in the network. Furthermore, separating pure hydrogen from the network deprives the downstream pipes of hydrogen , and the rest of the consumers may not receive hydrogen . A report by Frontier Economics [49] establishes that deblending costs depend on whether it is used for methane or hydrogen recovery, highlighting that deblending only for hydrogen recovery may be expensive.

The report by National Gas [47] highlights that the energy consumption of the deblending technologies is sensitive to two main factors: first, the hydrogen concentration in the feed-in gas stream; and second, the volume of gas required as feed gas to meet the end customer's demand. Concerning these factors, the questions raised in this thesis are as follows:

1. Which type of deblending technology is feasible for the GB high-pressure gas network?
2. Is it feasible to use deblending technologies only for industries demanding pure hydrogen?
3. What is the overall energy consumption in the high-pressure gas network with several deblending facilities?

2.4. Review of modelling techniques

2.4.1. Modelling within-day linepack variations

Calculating the linepack level in the gas network is a complex challenge, as it involves solving the continuity equation.

Some academic papers have used numerical analyses that do not solve the flow equations. Instead, they have used representative data. For example, Arvesten et al. [50] studied means of evaluating the price of linepack under uncertainty. Another example is the work by Tran et al.[51], who developed a numerical model to estimate optimal linepack patterns for a GB high-pressure gas network according to customisable parameters.

Some academic sources lean towards solving the continuity equation in steady-state conditions. In such state, the linepack level is contingent upon natural gas pressure levels, and obtaining an accurate estimate of pressure levels in every segment of each pipe in the network is a formidable task. Furthermore, the steady-state form of the continuity equation, with its light computational burden, is a valuable tool for situations that demand quick estimates. A recent example is a journal paper by Ettouney and El-Rifai [52], which showcases the authors' innovative approach to developing a new numerical method to calculate linepack levels of a sample gas network.

Although steady-state representation of the gas network is useful for studying gas networks in a snapshot, these methods do not analyse the network's behaviour over time. Numerous academic papers have used a modified version of steady-state analysis, also called a quasi-steady-state method, to overcome this challenge. This method defines the time-varying behaviour of flow and pressure using multiple steady-state analyses, each corresponding to a single time step of the time horizon.

Keyaerts et al.[53] applied the quasi-steady-state method to model a real-world gas network and examined the effects of under-pricing linepack utilisation on gas network operations. Chaudry et al.[54] developed a combined gas and electricity network model (CGEN) of GB using a similar quasi-steady-state analysis, demonstrating the practicality of these methods. Qadrdan et al. [55–58] utilised variations of CGEN to analyse the impact of RES on the GB gas network, further highlighting the relevance of these studies. More recently, Mi et al.[59] and Schwele et al. [60] developed integrated energy network models to study the extent to which linepack can

provide flexibility to the electricity network, showing the potential impact of linepack research on the broader energy sector.

The modified version of steady-state analysis fails to capture the pressure variations in the pipe's length, and the relationship between flow and pressure over time. Therefore, many academic papers have used unsteady-state analysis, which attempts to iterate flow and pressure behaviour by solving expansions of continuity equations and ignoring the changes in gas momentum. For example, Chaudry et al. 2008 used an unsteady-state representation of the gas network model [61]. Clegg & Mancarella developed an integrated model of gas and electricity networks using the unsteady-state formulation to study flexibility; variations of their model have been used in three studies to study the role of linepack in providing flexibility for electricity networks[62], the impact of power-to-gas on gas networks[63] and the resilience of GB energy networks to extreme weather events[64]. Zou et al. [65] developed an unsteady-state model of a gas network to study the impact of compressor optimisation on network linepack levels. More recently, Hyett et al. [66]developed a model of an Israeli gas network model using unsteady-state analysis to study the impact of supply and demand variations on the network's linepack levels.

Changes in momentum are difficult to ignore when a fast event occurs in the network. Examples of fast events are pipe bursts or sudden compressor failures that lead to sudden pressure and flow variations. To analyse these events, some academic papers have used fast-transient analysis. Dos Santos et al. [67] and Sunday et al. [68] developed fully transient models, including the momentum equation for studying the impact of leaks on gas flow and detecting leaks along pipelines in gas networks.

The amount of hydrogen injection varies throughout the day, as does the demand for natural gas from the high-pressure network. These variations will cause variations in within-day linepack levels. However, these variations are not rapid, making fast-transient analysis unnecessary. Therefore, this thesis uses a momentumless analysis to simulate flows in the gas network.

2.4.2. Modelling compressor stations

Compressor stations maintain gas at high-pressure levels in high-pressure gas networks. In gas networks such as GB's, the combination of compressor stations used during the day dictates the flow direction in the network, and various combinations may be used to achieve various flow directions.

Each compressor station in Great Britain houses multiple compression units, driven either electrically or by gas. All compressors in the network use centrifugal processes. Centrifugal compression is inherently three-dimensional, and analysing flow behaviour requires a rotating frame of reference [69,70].

When modelling the entirety of high-pressure gas network, such detailed modelling of compressor stations is unnecessary. Instead, the gas industry typically represents compressor stations using operational maps. These maps, empirically created and updated by operators for each unit, depict the relationship between gas flow and pressure within a compressor. Because operational maps are commercially sensitive, they are not publicly available, and academic studies using them are rare—for example, the work of Woldeyohannes and Majid [71].

When such data is not available, a theoretical formula could estimate energy consumption based on gas compression and gas flow passing through the compressor. Most academic papers on gas network simulations use this formula to simulate compressor stations. The integrated gas and electricity network models by Chaudry et al. [54,61], Clegg & Mancarella [62,63,72], Qadrdan et al. [55–58] and Ameli et al.[73] represent the GB gas network compressor stations using this approach.

Given that operational maps of compressors in GB were not available at the time of writing, the theoretical energy-flow-pressure formula was used in this thesis to simulate the compressor stations in the GB high-pressure gas network.

2.4.3. Modelling hydrogen and natural gas mixing

To model the mixture of hydrogen and natural gas in a pipeline, two sets of equations are required. The first set is referred to as transport equations, which describe how the molar fraction of gases change after mixing, as a set of partial differential equations in time and space [74]. The second set is the equation of state (EoS), which links the physical properties of the mixture to the molecular composition of its constituent gases.

While the advective transport equation is unique, several EoS formulations have been developed by the industry. Each EoS incorporates binary interaction coefficients (BICs) to represent interactions between different gases. Because BICs vary across formulations, the choice of EoS is critical.

The selection of an EoS should be based on three factors: (1) whether the developers made the EoS for the pressures and temperatures relevant to the study; (2) whether all gases in the study are compatible with the EoS ; and (3) whether sufficient computational resources are available to implement the method with accuracy.

Recent academic studies have applied a variety of EoS: Guandalini [68,69] and Ekhtiari et al. [44] used the Papay correlation; Chaczykowski et al. [75] applied GERG-400; Witek et al. [36] employed GERG-2008; Zhang et al.[36] [76] used the Soave–Redlich–Kwong formulation; and Zhou [34] applied the Benedict–Webb–Rubin (BWR) model.

The thesis has adopted a modified Benedict–Webb–Rubin–Starling (BWRS) formulation to solve the advective transport equations. The manual suggests that BWRS is particularly suitable for simulating hydrogen–natural gas mixtures in high-pressure networks, where pressures range between 40–90 bar(g) and temperatures remain near 10 °C. Although BWRS is among the most computationally demanding formulations, it offers the highest accuracy for the conditions studied.

2.4.4. Modelling deblending stations' energy consumption

Modelling of Cryogenic, PSA or membrane separation is widely conducted using commercial software. Academic articles simulating Cryogenic separation [77–80] , for PSA [81] and for membranes [82]. n these studies, the authors modelled the structure of chemical plants containing cryogenic separation units and analysed their behaviour within the overall plant system. [84] Synergi Gas, for example, models deblending using a steady-state module. The software also calculates the amount of feed gas required to meet the demand for gas with a specified hydrogen composition. Furthermore, Synergi Gas simulates the impact of withdrawing gas with a given hydrogen composition on the gas network by modelling the effects of deblending on pressure, linepack levels, and gas composition throughout the network.

The feed flow rate and the hydrogen content of the feed gas were then used to estimate the energy consumption of the deblending stations. Furthermore, by comparing these two parameters with the energy consumption of deblending sites studied by National Gas[47], the energy consumption of the deblending sites in the case studies was estimated.

2.5. Modelling Tools

Researchers in academia often develop custom codes and implement numerical methods to solve the partial differential equations (PDEs) governing fluid flow. This approach offers a high degree of customization, allowing researchers to tailor every aspect of the model to their specific research question. However, this approach presents significant challenges, particularly for modelling complex systems like gas networks. Developing an unsteady-state model for a gas network requires advanced mathematical expertise, exceeding the scope of an engineering project. Furthermore, achieving the necessary granularity to accurately represent a large, complex network like the Great Britain (GB) gas network with a custom-built, unsteady-state model is computationally demanding and technically difficult.

Commercially available software packages offer a viable alternative. These packages provide reliable modelling solutions and readily enable high-granularity simulations. At the time of writing, two such packages were considered: SIMONE [83], Synergi Gas[84]. [87]While both offer comparable modelling accuracy, Synergi Gas was selected due to its availability of affordable academic licensing.

Synergi gas software models: 1) The physical assets that build the GB gas network, i.e. pipelines, compressor stations, demand and supply nodes. 2) Unsteady-state behaviour of the network, enabling the study of the within-day behaviour of the network. 3) Operation and energy consumption of compressor stations. 4) hydrogen and natural gas mixture in the gas network. 5) operation of de-blending stations.

2.6. Data Tools

All data used in thesis were cleaned and organised using Power Query tool in Microsoft Excel[85].

2.7. Graphics Tools

All the graphics in the thesis were created using Origin software developed by OriginLab[86].

2.8. Summary

The conducted literature review highlighted several questions to be answered about the operation of GB high-pressure gas network with hydrogen.

First group of questions concern the impact of hydrogen on operation compressor stations. Furthermore, it is still not clear how much energy will be consumed when hydrogen is injected into the GB network up to 20% volumetric. It is crucial to know how much energy will be consumed when the gas network transmits pure hydrogen. And there needs to be clarification on the impact of the operation of compressor stations on the hydrogen content of the network, when hydrogen is injected up to 20% volumetric.

Second group of questions concern the impact of hydrogen injection on linepack levels in the gas network. Furthermore, the impact of hydrogen injection and pure hydrogen transmission on linepack levels should be demonstrated specifically for GB high-pressure gas network.

Third group of questions concern how hydrogen mix with natural gas in the network upon injection. Furthermore, impact of modes of hydrogen injection on rates of natural gas and hydrogen mixing should be investigated. Should hydrogen and natural gas do not mix consistently across the network, which regions of the network will receive more hydrogen than others?

And the last group of questions concern the feasibility of operating deblending technology in GB high-pressure gas network. Furthermore, the most suitable type of deblending technology for GB should be identified. And the overall energy consumption of operating deblending technologies should be estimated.

The literature review also highlights the reasons supporting choice of the modelling methods and tools.

To accurately estimate the linepack levels in the gas network in within day, the continuity equation has been solved in unsteady state. As compressor operational maps are unavailable, compressor stations have been modelled using theoretical compression formula. To accurately simulate the interaction between hydrogen and natural gas in the network, a modified version of Benedict Webb Rubens and Starling equation has been used. And finally, to simulate the deblending technology, a steady-state module has been used that accurately simulates the gas feed volume required for operation, as well as the hydrogen content of gas at the feed.

Synergi Gas has been selected as the appropriate software, and simulation tool, as it conducts all of above and assist in filling the gaps found in literature.

Chapter Three. Methodology, development, calibration and validation of the model

The model of the high-pressure gas network was developed using Synergi Gas software. The data used for modelling were processed in Excel Power Query, and the graphics were generated using Origin software. Chapter Three explains in detail the process used to develop the model, as depicted in Figure 3.1.

Synergi Gas is a piece of commercial software that simulates physical assets such as pipelines, compressor stations, and deblending stations. It connects these assets according to user-provided coordinates to create a network. The software can conduct both steady-state and unsteady-state analyses to simulate the behaviour of gas flow in the network and generate profiles for pressure, linepack, compressor energy consumption, and deblending feed-in gas volumes.

Two sets of data were used to create two case studies: the Winter Case and the Summer Case. The Winter Case and the Summer Case represent typical within-day network operations under existing conditions; the Winter Case depicts a typical winter day operation in 2019, and the Summer Case depicts a typical summer day operation in 2022. These two case studies were required to represent the real operational behaviour of the gas network. To ensure this, the gas demand and supply data for the network were carefully selected from a representative day. Furthermore, the model settings were calibrated so that the outputs fell within the seasonal range.

The calibrated case studies were then used to create four additional case studies, which simulate the behaviour of the gas network in the future.

In this chapter, first, the methodology used by Synergi Gas to perform modelling is explained. Second, the input data build and the Winter and Summer cases are introduced. Here, input data refer to both the data describing the physical assets of the model and the gas demand and supply levels of both the Winter and Summer cases. The chapter then explains the calibration process, by which the optimal compressor combination and optimal operating settings for each compressor are chosen. The validation of the results of the calibration process is then presented by comparing linepack levels with real seasonal data. Finally, the remaining case studies created are briefly explained. The chapter refrains from explaining Excel Power Query and Origin, as these are outside the scope.

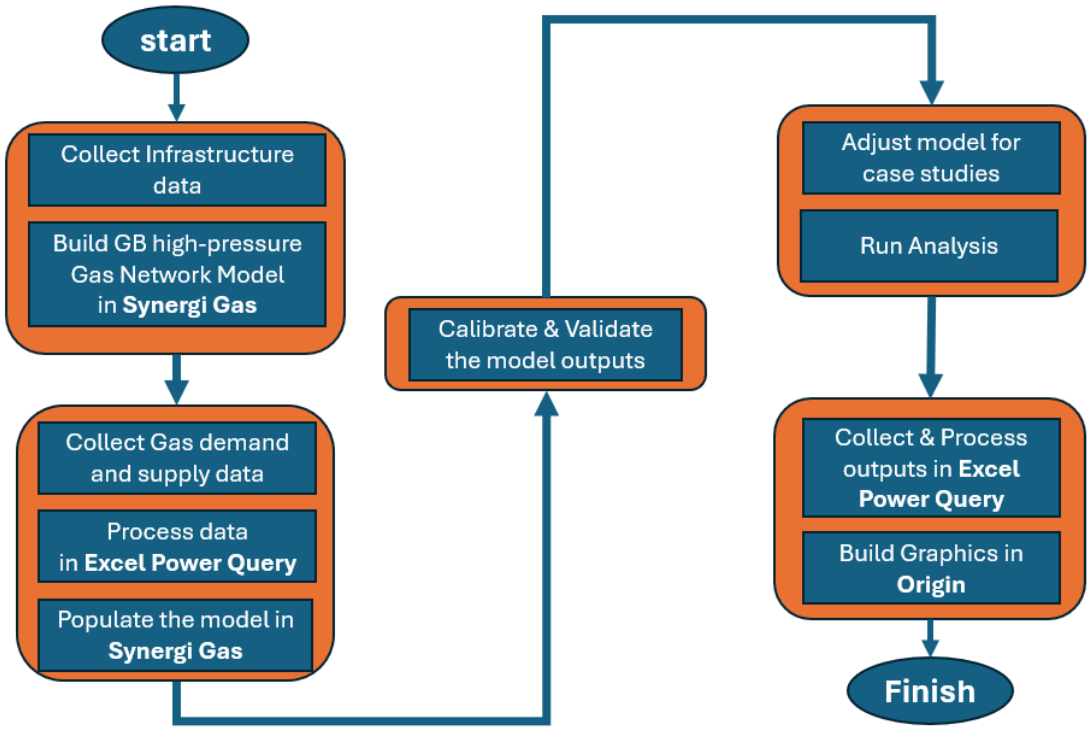

Figure 3.1. Schematic describing the Model development process.

3.1. Methodology

3.1. 1. Steady-state model of flow in pipeline

In the steady-state model, the flow along the pipeline is a known attribute, since both demand and supply are inputs to the model. In addition, the St Fergus supply point has a known pressure. Using these inputs, the model calculates the pressure drop across the pipelines.

3.1.1.1. The general flow equation

The general flow equation for the steady flow of gas in a pipe is derived from Bernoulli's equation. For steady-state flow, the mass flow is constant along the pipe. Assuming the pipe has a constant cross-sectional area A:

$$\rho_1 \, w_1 A = \rho_2 w_2 A \qquad (3.1)$$

This means that the density decreases when gas velocity increases, and the gas's kinetic energy increases. Since the velocity varies along the pipe, it is vital to consider a small element of length when calculating the frictional resistance and to integrate over the pipe length to obtain the total head loss due to friction. Figure 3.2 shows a schematic of a pipe segment with steady-state flow of gas.

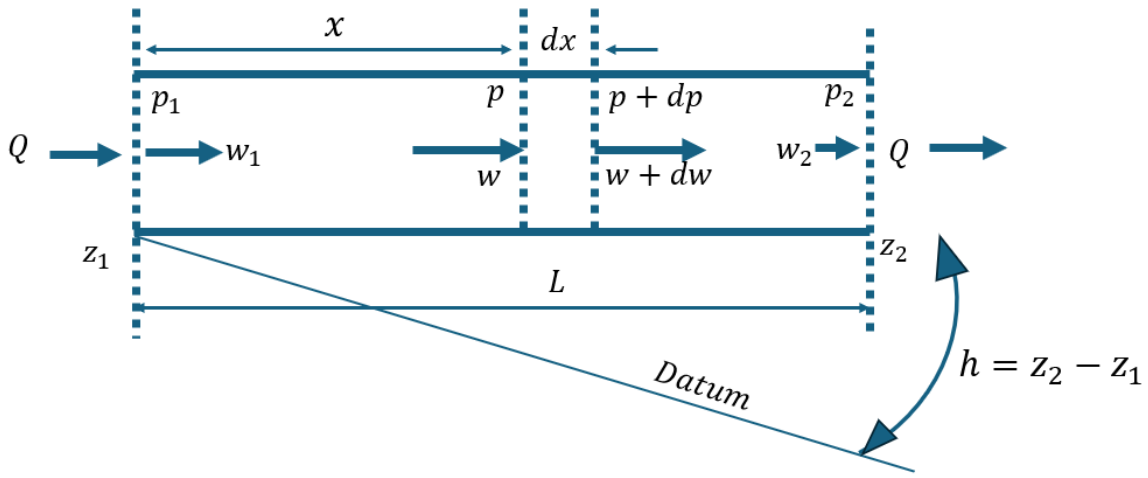

Figure 3.2. Pipe schematic

For the two ends of the pipe element, the Bernoulli equation is re-written as:

$$\frac{\mathrm{p}}{\rho \mathrm{g}} + \frac{\mathrm{w}^2}{2\mathrm{g}} + \mathrm{z} = \frac{\mathrm{p} + \mathrm{dp}}{\rho \mathrm{g}} + \frac{(\mathrm{w} + \mathrm{dw})^2}{2\mathrm{g}} + (\mathrm{z} + \mathrm{dz}) + \mathrm{d}h_f \tag{3.2}$$

Since $(\frac{\mathrm{dw}^2}{2g})$ and $(\frac{2wdw}{2g})$ have small values, they are dropped. By balancing the two sides of equation 2.2, it is re-written as:

$$-\frac{\mathrm{dp}}{\rho \mathrm{g}} = \mathrm{d}h_f + \mathrm{dz} \tag{3.3}$$

Head loss due to friction across the elements is given by Darcy's equation:

$$\mathrm{d}h_f = \frac{4f}{D}\frac{w^2}{2g}dx \tag{3.4}$$

where f is the dimensionless friction factor and D is the internal diameter of the pipe.

$$-\frac{dp}{\rho g} = \frac{4f}{D}\frac{w^2}{2g}dx + dz \tag{3.5}$$

Hence

$$-dp = \frac{2f\rho w^2}{D}dx + \rho g dz \tag{3.6}$$

From the continuity equation:

$$\rho w = \rho_1 \, w_1 \tag{3.7}$$

Therefore

$$w = \frac{\rho_1}{\rho} w_1 \tag{3.8}$$

The loss of energy due to friction is converted into thermal energy which is dissipated through the walls of the pipe to the surroundings. The temperature T of the gas remains approximately constant, and the flow is isothermal. Therefore:

$$\frac{p}{\rho} = \frac{p_1}{\rho_1} \tag{3.9}$$

Therefore:

$$\rho = \frac{p}{p_1}\rho_1 \tag{3.10}$$

And:

$$-\mathrm{dp} = \frac{2\mathrm{f}}{\mathrm{D}}\rho_1 w_1^2 \frac{\mathrm{p}_1}{\mathrm{p}}\mathrm{dx} + \frac{\mathrm{p}}{\mathrm{p}_1}\rho_1 \mathrm{g dz} \tag{3.11}$$

From the ideal gas equation of state:

$$\mathrm{p}_1 = \rho_1 \mathrm{ZRT} \tag{3.13}$$

Hence:

$$-\mathrm{p}\,\mathrm{dp} = \frac{2\mathrm{f}}{\mathrm{D}}\rho_1^2 w_1^2 \mathrm{ZRT}\,\mathrm{dx} + \frac{\mathrm{p}^2}{\mathrm{ZRT}}\mathrm{g}\,\mathrm{dz} \tag{3.14}$$

In the elevation term $\frac{p^2}{ZRT} g\, dz$, the value p can be taken as the average pressure along the pipe.

$$\rho_1{}^2 w_1^2 = \rho_n^2 w_n^2 = \rho_n^2 \frac{Q_n^2}{A^2} = \frac{\rho_n^2 Q_n^2}{(\pi D^2/4)^2} \tag{3.15}$$

Where the subscript n refers to quantities at standard conditions of pressure 0.1 MPa and temperature 288K. Hence:

$$-\mathrm{pdp} = \frac{32\mathrm{f}\rho_\mathrm{n}^2 \mathrm{Q}_\mathrm{n}^2}{\pi^2 \mathrm{D}^5}\mathrm{ZRTdx} + \frac{\mathrm{p}_\mathrm{av}^2}{\mathrm{ZRT}}\mathrm{gdz} \tag{3.16}$$

The gas constant R is related to the constant for air. Consider the equation of state for the gas and for air at the same pressure and temperature, the compressibility factor Z being unity for these conditions.

For any gas:

$$p_n = \rho_n R T_n \tag{3.17}$$

For air:

$$p_n = (\rho_{air})_n R_{air} T_n \tag{3.18}$$

$$\frac{\rho_n}{(\rho_{air})_n} = \frac{R_{air}}{R} = S \tag{3.19}$$

Hence:

$$R = \frac{R_{air}}{S} \tag{3.20}$$

where S is the specific gravity of the gas. Thus:

$$\rho_n = \frac{p_n}{RT_n} = \frac{Sp_n}{R_{air}T_n} \tag{3.21}$$

Substituting in equation the equations above for R and p we get:

$$-pdp = \frac{32}{\pi^2} f \left(\frac{Sp_n}{R_{air}T_n}\right)^2 \frac{Q_n^2}{D^5} \frac{ZR_{air}}{S} Tdx + \frac{p_{av}^2 S}{ZR_{air}T} gdz \tag{3.22}$$

i.e.

$$-pdp = \frac{32}{\pi^2} \frac{fSZT}{R_{air}D^5} Q_n^2 \left(\frac{p_n}{T_n}\right)^2 dx + \frac{p_{av}^2 S}{ZR_{air}T} gdz \tag{3.23}$$

By integrating equation 2.23 from $x = 0$, $p = p_1$, to $x = L$, $p = p_2$ we get:

$$-\left(\frac{p_2^2 - p_1^2}{2}\right) = \frac{32}{\pi^2} \frac{fSZT}{R_{air}D^5} Q_n^2 \left(\frac{p_n}{T_n}\right)^2 L + \frac{p_{av}^2 S}{ZR_{air}T} gh \tag{3.24}$$

Hence:

$$p_1^2 - p_2^2 = \frac{64}{\pi^2 R_{air}} \frac{fSLZT}{D^5} \left(\frac{p_n}{T_n}\right)^2 Q_n^2 + \frac{2p_{av}^2 S}{ZR_{air}T} gh \tag{3.25}$$

Hence, the frow Qn is given by:

$$Q_n = \sqrt{\left(\frac{\pi^2 R_{air}}{64}\right)} \times \frac{T_n}{p_n} \sqrt{\frac{\left\{(p_1^2 - p_2^2) - \frac{2p_{av}^2 Sgh}{ZR_{air}T}\right\} D^5}{fSLTZ}} \tag{3.26}$$

Equation 4.8 is the general flow equation for steady-state gas flow.

If the pipe is horizontal, the elevation term ($\frac{2p_{av}^2 Sgh}{ZR_{air}T}$) is zero and equation 4.8 reduces to:

$$Q_n = C\frac{T_n}{p_n}\sqrt{\frac{(p_1^2 - p_2^2)D^5}{fSLTZ}} \tag{3.27}$$

where:

$$C = \sqrt{\frac{\pi^2 R_{air}}{64}} = \text{constant} \tag{3.28}$$

3.1.1.2. AGA fully turbulent friction factor for steady-state:

The friction factor is estimated using AGA formulation for fully turbulent flow of gas, in high-pressures:

$$f = \left[-2\log\left(\frac{\varepsilon/d}{3.7}\right)\right]^{-2} \tag{3.29}$$

where ϵ is the roughness of pipe, assumed to be 0.067mm [87].

3.1.2. Unsteady state model of flow of gas in pipe

In the unsteady-state flow model, the demand and supply levels are inputs to the model. The initial pressure levels, which are the pressures at $t = 0$, are also inputs to the model. The model then calculates the pressure variations over time and the pressure depression along the pipeline.

Furthermore, the linepack within the network is determined using the initial pressure levels and the variations in supply and demand observed during the simulation.

The governing equations used in this section are taken directly from the Synergi Gas 4.9.4 Manual [84].

3.1.2.1. Unsteady-State flow along a pipe

The equations for the conservation of mass and momentum along a single straight pipe, neglecting the altitude of the pipe, are:

$$\frac{\partial}{\partial \mathrm{x}}(\rho \mathrm{v}) + \frac{\partial \mathrm{p}}{\partial \mathrm{t}} = 0 \tag{3.30}$$

$$\rho \frac{dv}{dt} = -\frac{\partial p}{\partial x} + F \tag{3.31}$$

Equation 2.30 describes the absolute derivative in a moving control boundary as the partial derivative of both time ($\frac{\partial}{\partial t}$) and motion of the control boundary ($v\frac{\partial}{\partial x}$):

$$\frac{d}{dt} = \frac{\partial}{\partial t} + v\frac{\partial}{\partial x} \tag{3.32}$$

where ρ, v and p are the density, velocity and pressure of the gas, respectively, x is the distance along the pipe and t is the time.

The mass flow rate Q along the pipe is given by:

$$Q = \rho A v \tag{3.33}$$

where A is the cross-sectional area of the pipe. The frictional force, F, is given by:

$$F = -\frac{f|q|^{a-1}q}{2|p|} \tag{3.34}$$

where q is the standard volumetric flowrate along the pipe, f is the friction factor of the pipe and a is the gas flow exponent.

The standard volume is the volume that a given mass of gas would occupy at standard conditions. The standard volume flow rate is therefore related to the mass flow rate by:

$$q = \frac{Q}{\rho_s} \tag{3.35}$$

where ρ_s is the density at standard conditions.

For a fixed mass of gas:

$$\frac{pV}{Z\theta} = \text{constant} \tag{3.36}$$

where V is the volume of the gas, θ is the temperature and Z is the compressibility. From this, a relationship between pressure and density is obtained:

$$p = \frac{\rho}{\rho_s}\frac{Z\theta}{Z_S\theta_S}p_s \tag{3.37}$$

where θ_S and p_s are the standard temperature and pressure, and Z_S is the compressibility at the standard conditions.

Considering the long-term variation in pressure, the effect of the momentum on the gas will be small and the frictional forces are expected to dominate.

Thus, the term representing momentum $\rho\frac{dv}{dt}$ in equation 2.30 is neglected. The conservation equations are thus transformed:

$$\frac{\partial}{\partial x}(p|p|) + k_F|q|^{a-1}q = 0 \tag{3.38}$$

$$\frac{1}{A}\frac{\partial q}{\partial x} + \frac{Z_s\theta_s}{p_s}\frac{\partial}{\partial t}\left(\frac{p}{Z\theta}\right) = 0 \tag{3.39}$$

Assuming that the temperature of the gas is constant over time, equation 2.39 is simplified:

$$\frac{1}{A}\frac{\partial q}{\partial x} + \frac{Z_s\theta_s}{p_s\theta}\frac{\partial}{\partial t}\left(\frac{p}{Z}\right) = 0 \tag{3.40}$$

3.1.2.2. Linepack

Linepack in the pipeline at time t is simulated as in equation 2.42:

$$L_t = L_0 + \int_0^t (q - q(0))\,dt \tag{3.41}$$

where L_0 is the pipeline linepack at the beginning of the simulation, which is calculated using steady-state conditions. This is also referred to as the starting linepack:

$$L_0 = \frac{p_m A\, l}{p_s Z R \theta_S} \tag{3.42}$$

where A is the cross-sectional area of the pipe and l is the length of the pipe and p_m is the average pressure of the pipeline.

3.1.3. Compressor Station model

The compressor energy consumption is calculated based on gas flow in the compressor, and suction and discharge pressures of the compressor. The model is used for both steady and unsteady-state simulations.

$$\mathrm{W} = \frac{\mathrm{P_b}, q, \mathrm{n^e}}{\eta\,(\mathrm{n}-1)}\left[\left(\frac{p_2}{p_1}\right)^{\frac{\mathrm{n}-1}{\mathrm{n}}} - 1\right] \qquad (3.43)$$

$\mathrm{P_b}$ is set to be 1 bar-g.

3.1.4. Component tracing model

In the non-ideal gas mixture, the species composition and thermodynamic properties are coupled. At each time step, the mole fractions from the previous step are used to evaluate the compressibility factor Z, partial molar volumes, and thermodynamic factors using the equation of state. These quantities are then employed in the Maxwell–Stefan formulation to determine the diffusive fluxes, which are substituted into the species conservation equation to update the mole fractions.

Ultimately, the molar compositions of natural gas and hydrogen are determined both temporally and spatially.

3.1.4.1. Equation of State

Two different gas streams were defined, 100% hydrogen and GB natural gas. The 100% hydrogen only contains molecular hydrogen, and the GB natural gas was defined by five main components, as shown in Table 3.1:

Table 3.1. Assumed components of natural gas

Component	Molecular Percentage %
Methane	93
Ethane	3
Propane	2.1
Nitrogen	1.6
Carbon dioxide	0.3

Synergi Gas recommends the Starling modification of Benedict-Webb-Rubin (BWRS) to simulate the composition of mixed gas in each node during the simulation. The BWRS equation of state is presented in equation 2.45:

$$p = \rho_\mathrm{m}\mathrm{R}\theta + \left(B_0\mathrm{R}\theta - A_0 - \frac{C_0}{\theta^2} + \frac{D_0}{\theta^3} + \frac{E_0}{\theta^4}\right)\rho_\mathrm{m}^2 + \left(b\mathrm{R}\theta - a - \frac{\beta}{\theta}\right)\rho_\mathrm{m}^3 + \alpha\left(a + \frac{d}{\theta}\right)\rho_\mathrm{m}^6 + \frac{c\rho_\mathrm{m}^2}{\theta^2}(1 + \gamma\rho_\mathrm{m}^2)\exp\left(-\gamma\rho_\mathrm{m}^2\right) \qquad (2.45)$$

where the 10 coefficients can be evaluated from equations 2.46 to 2.56:

$$A_0 = \sum_i^u \sum_j^u m_i m_j A_{0i}^{\frac{1}{2}} A_{0j}^{\frac{1}{2}} (1 - k_{ij}) \tag{2.46}$$

$$B_0 = \sum_i^u m_i B_{0i} \tag{2.47}$$

$$C_0 = \sum_i^u \sum_j^u m_i m_j C_{0i}^{\frac{1}{2}} C_{0j}^{\frac{1}{2}} \left(1 - k_{ij}\right)^3 \tag{2.48}$$

$$D_0 = \sum_i^u \sum_j^u m_i m_j D_{0i}^{\frac{1}{2}} D_{0j}^{\frac{1}{2}} \left(1 - k_{ij}\right)^4 \tag{2.49}$$

$$E_0 = \sum_i^u \sum_j^u m_i m_j E_{0i}^{\frac{1}{2}} E_{0j}^{\frac{1}{2}} \left(1 - k_{ij}\right)^5 \tag{2.50}$$

$$\alpha = \left[\sum_i^u m_i \, \alpha_i^{\frac{1}{3}}\right]^3 \tag{2.51}$$

$$\gamma = \left[\sum_i^u m_i \, \gamma_i^{\frac{1}{3}}\right]^3 \tag{2.52}$$

$$a = \left[\sum_i^u m_i \, a_i^{\frac{1}{3}}\right]^3 \tag{2.53}$$

$$b = \left[\sum_i^u m_i \, b_i^{\frac{1}{3}}\right]^3 \tag{2.54}$$

$$c = \left[\sum_i^u m_i \, bc_i^{\frac{1}{3}}\right]^3 \tag{2.55}$$

$$\beta = \left[\sum_i^u m_i \, \beta_i^{\frac{1}{3}}\right]^3 \tag{2.56}$$

m_i and m_j are the mole fraction of the components i and j in the mixture, respectively. Furthermore, k_{ij} is the interaction coefficient of the components i and j in the mixture. The k_{ij} values for the components are listed in Table 3.2. These values are as provided in Synergi manual, and can also be found in work by Lielmezs, J. [88]:

Table 3.2. The interaction coefficient k_{ij} between different gases used in this study.

	Methane	**Ethane**	**Propane**	**Hydrogen**	**Nitrogen**	**Carbon-dioxide**
Methane	0	0.01	0.023	0	0.025	0.05
Ethane		0	0.0031	0	0.07	0.048
Propane			0	0	0.1	0.045
Hydrogen				0	0	0
Nitrogen					0	0

3.1.4.2. Transport Equations

Species transport equation states that:

$$\frac{\partial(c\, m_i)}{\partial t} + \frac{\partial}{\partial x}\,(C\, m_i v\, +\, J_i) = 0 \qquad (3.44)$$

Where c is the molar concentration:

$$c\, =\, \frac{p}{(Z(p,\theta,m)R\,\theta)} \qquad (3.45)$$

Where $Z(p,\theta,m)$ is driven from the EoS.

J is calculated using the Maxwell–Stefan diffusive flux equation:

$$-\sum_{j\neq i}\frac{(m_j J_i -\, m_i J_j)}{(C\,\mathfrak{D}_{ij})} = \sum_{j=1}^{N-1}\Gamma_{ij}\frac{\partial m_i}{\partial x}\, +\frac{\bar{V}_i -\, \bar{V}}{R\,\theta}\frac{\partial p}{\partial x},\quad i\, =\, 1,\dots,N\, -\, 1 \qquad (3.46)$$

With constraints of :

$$\sum_i m_i = 1,\quad \sum_i J_i = 0. \qquad (3.47)$$

.

3.1.5. Hydrogen Injection model

In this study, a hydrogen concentration limit of 20% by volume is adopted for the model, in line with existing safety evidence. National Gas in Great Britain has conducted physical tests on all types of assets used in the high-pressure network, and the results, published in the *FutureGrid Phase 1 Closure Report* [25] confirm that the presence of hydrogen up to 20% by volume in the network is safe

To implement this ratio, each injection site is modelled as follows. At each injection site three gas streams are considered:

1)The hydrogen injection stream q_i^h (unknown).

2) The incoming stream q_i^c.

3) The outgoing stream q_i^o .

This configuration is illustrated in Figure 3.3.

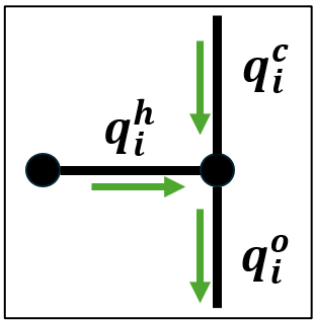

Figure 3.3. Schematic describing hydrogen injection nodes and pipes.

At each node of the network, the gas flow balance equation applies, dictating that the volumetric flow of gas entering and leaving a node must be equal. At a hydrogen injection node, the relationship between the outgoing stream $\mathrm{q_i^o}$, the incoming stream $\mathrm{q_i^c}$ and the hydrogen injection stream $\mathrm{q_i^h}$ is therefore defined as:

$$\mathrm{q_i^o = q_i^h + \ q_i^c} \qquad (3.48)$$

At the injection node, it was ensured that the hydrogen injection stream $\mathrm{q_i^h}$ constitutes to only 20% volumetric of the outgoing stream $\mathrm{q_i^o}$:

$$\frac{\mathrm{q_i^h}}{\mathrm{q_i^h + \ q_i^c}} = 20\% \qquad (3.49)$$

Therefore, the volume of hydrogen injection stream $\mathrm{q_i^h}$ was set to ¼ of the amount of the incoming gas stream q_i^c at all time steps:

$$q_i^h = \frac{1}{4} q_i^c \tag{3.50}$$

Note that this does not factor hydrogen that is already in the incoming stream.

3.1.6. Deblending station model

Deblending refers to technologies that separate a specific gas from the mix of gases in the high-pressure network and deliver that specific gas to the customer. These technologies are installed between the NTS and a customer, either a power station, industrial site or an LDZ network.

Every deblending station has an Inlet gas stream q_d^i, product gas steam q_d^p and rejected gas stream q_d^r (unknown). The flows in and out of a deblending station is depicted in Figure 3.4.

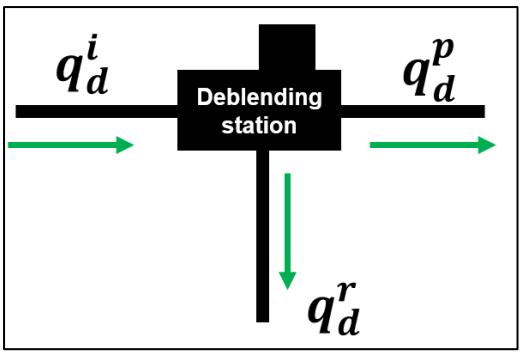

Figure 3.4. Schematic of a deblending site in Synergi Gas Software

q_d^i has a gas composition: X% hydrogen and Y% natural gas, where:

$$X_d^i + Y_d^i = 100 \tag{3.51}$$

q_d^p has a gas composition of N% hydrogen and M% natural gas, where:

$$N_d^p + M_d^p = 100 \tag{3.52}$$

The total mass balance dictates:

$$q_d^i = q_d^p + q_d^r \tag{3.53}$$

therefore, the mass balance for hydrogen becomes:

$$\frac{X_d^i}{100} q_d^i = \frac{N_d^p}{100} q_d^p + \frac{H_d^r}{100} q_d^r \tag{3.54}$$

where H_d^r is the percentage of hydrogen in the reject gas.

Also, the mass balance for natural gas becomes:

$$\frac{Y_d^i}{100} q_d^i = \frac{M_d^p}{100} q_d^p + \frac{100 - H_d^r}{100} q_d^r \tag{3.55}$$

Minimum feed requirement for hydrogen is that:

$$q_d^i \geq (\frac{N_d^p}{X_d^i}) q_d^p \tag{3.56}$$

and the minimum requirement for methane is that:

$$q_d^i \geq (\frac{q_d^p}{Y_d^i}) M_d^p \tag{3.57}$$

To meet both requirements, the inlet stream must be:

$$q_d^i = q_d^p \, max\left(\frac{N_d^p}{X_d^i}, \frac{M_d^p}{Y_d^i}\right) \tag{3.58}$$

and therefore, the reject stream must be:

$$q_d^r = q_d^i - q_d^p = q_d^p \left(\max\left(\frac{N_d^p}{X_d^i}, \frac{M_d^p}{Y_d^i}\right) - 1\right) \tag{3.59}$$

The hydrogen balance in the reject steam is:

$$\frac{H_d^r}{100}\left(q_d^i - q_d^p\right) = \frac{X_d^i}{100}\, q_d^i - \frac{N_d^p}{100}\, q_d^p \tag{3.60}$$

therefore, the hydrogen percentage in reject steam is:

$$H_d^r = \frac{X_d^i \, q_d^i - N_d^p \, q_d^p}{q_d^i - q_d^p} \tag{3.61}$$

And natural gas composition in the rejected stream is:

$$G_d^r = 100 - H_d^r = \frac{Y_d^i \, q_d^i - M_d^p \, q_d^p}{q_d^i - q_d^p} \tag{3.62}$$

3.2. Inputs

3.2.1. Physical features of the GB high-pressure gas network

The model of the gas network was developed using data taken from National Gas, which are confidential. However, simplified versions of these data are publicly available. [8,89] The structure of the gas network is defined by demand and supply nodes, pipelines, and compressor stations.

3.2.1.1. Nodes

The model includes a total of 284 nodes, consisting of nine supply nodes, 13 nodes representing demand from industries directly connected to the high-pressure gas network, 34 nodes representing demand from gas-fired power stations, and 78 nodes representing demand from lower-pressure gas networks such as Local Distribution Zones (LDZs) connected to the high-

pressure network. The remaining nodes are junction points where pipelines connect, but there is no demand or supply [8] .

In addition, each node has an initial pressure level, which enables the iterative process of the simulation to start. The initial pressure at each node is determined during the calibration process

3.2.1.2. Pipelines

Each pipeline is defined by its length, inner diameter, maximum and minimum operational pressures, and the two nodes it connects. The data are confidential; however, a simplified version can be found in the Gas Ten Year Statement [8]

3.2.1.3. Compressor Stations

Each compressor station is defined by its maximum available capacity (MW), maximum outlet pressure (bar-g), minimum inlet pressure (bar-g), and overall efficiency. The maximum available capacity (MW) is confidential and cannot be disclosed. Alternative data for the remaining attributes can be found in the *Gas Ten Year Statement* and *Compressor Supporting Documents* [8,89] and these are defined in Table 3.3.

In addition, each compressor station has a control scheme that defines whether the compressor station regulates its inlet or outlet pressure. It also has a set pressure, which is monitored through the control scheme. Both the control scheme and the set pressure must be determined during the calibration process.

Table 3.3 Compressor stations in the NTS map.

Reference Number on map	**Compressor**	**Max Outlet Pressure [bar-g]**
1	**St Fergus**	**68.5**
2	**Aberdeen**	**85**
3	**Kirriemuir**	**85**
4	**Avonbridge**	**85**
5	**Moffat**	**85**
6	**Wooler**	**75**
7	**Carnforth**	**75**

8	**Nether Kellet**	**70**
9	**Warrington**	**70**
10	**Alrewas**	**70**
11	**Churchover**	**75**
12	**Wormington**	**75**
13	**Felindre**	**94**
14	**Aylesbury**	**75**
15	**Lockerley**	**75**
16	**Bishop Auckland**	**75**
17	**Hatton**	**75**
18	**Peterborough**	**70**
19	**Wisbech**	**75**
20	**Huntingdon**	**75**
21	**King's Lynn**	**75**
22	**Cambridge**	**75**
23	**Diss**	**75**
24	**Chelmsford**	**70**

NOTE: Efficiency of compressor stations were assumed 0.8; Minimum Inlet pressure of all compressor stations was assumed 40 bar-g.

3.2.1.4. Geographical representation of gas network

The GB gas network is manually drawn in the Geographic Information System (GIS) interface of the Synergi Gas software. The map does not represent the asset coordinates accurately, nor does it accurately represent the scale of the assets. It serves solely as a visual aid for the reader.

The network is divided into 12 zones and six regions to facilitate studies on operational metrics. Figure 3.5 shows a map of the developed model of the high-pressure gas network, and Table 3.4 summarises the model inputs and outputs.

Table 3.4 Summary of model inputs, their source and outputs.

Inputs to model	Source of data	Outputs from model

Supply Node	1. Gas supply rate (GW) 2. Pressure level at initial condition (t=0) 3. Hourly Disaggregation Profiles 4. Constant rate for projecting supply in future years.	.1 Comes from National Gas Data Centre.[90] .2 is Derived through calibration process. .3 comes from National Gas Data Centre[90] .4 comes from Gas Ten Year Statement workbook. [8]	a. Pressure level (bar-g) b. % of each gas composition
Demand Node	1. Gas demand rate (GW) 2. Pressure level at initial condition (t=0) 3. Hourly Disaggregation Profiles 4. Constant rate for projecting demand in future years.	.1 comes from National Gas Data Centre.[90] .2 is Derived through calibration process. .3 comes from National Gas Data Centre[90] .4 comes from Gas Ten Year Statement workbook. [8]	a. Pressure level (bar-g) b. % of each gas composition
Pipeline	1. Length (km) 2. Diameter (m) 3. Efficiency factor 4. Roughness (m)	1—4 are Confidential. Alternative data source is Gas Ten Year Statement.[8]	a. Linepack (GWh)
Compressor Station	Installed power (MW) Minimum inlet pressure limit (bar-g) Maximum outlet pressure limit (bar-g Set pressure (either on the inlet or outlet)	1 is Confidential with no alternative source. For 2 and 3, alternative data source is gas Ten Year Statement.[8] 4 is derived through calibration process.	a. Energy consumption (MWh) b. Inlet and outlet pressure levels

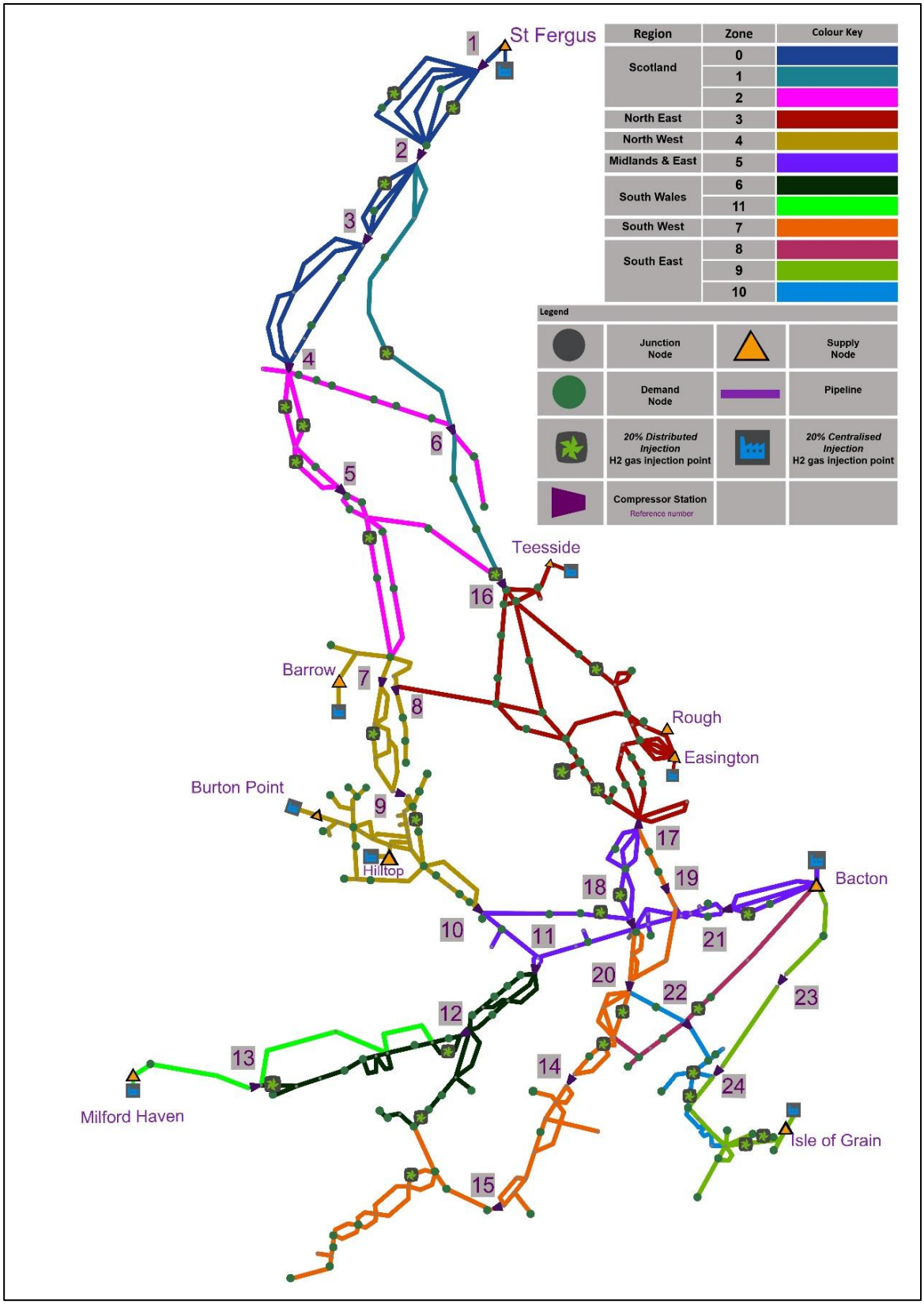

Figure 3.5 . Schematic of the NTS model

In Synergi Gas 4.9.4, supply and demand levels are defined in energy terms. The model calculates the pressure at each node in the network, the linepack within the pipelines, compressor energy consumption, and gas composition at each node at each time step. The Synergi Gas 4.9.4 software performs transient simulations with component tracing analysis simultaneously. Demand and supply values were obtained from the National Gas database [91].

3.2.2. Supply and Demand

3.2.2.1. Supply and Demand of Winter Case

The winter season considered in developing the gas network model extends from October 2018 to March 2019 inclusive. This represents the last winter season before the COVID-19 pandemic and is characterised by moderate gas consumption for heating and electricity generation. The UK Continental Shelf (UKCS) is the primary source of natural gas supply, and a significant portion of GB gas enters the network through the St Fergus supply point in Scotland.

Figure 3.6 (a) illustrates the gas supply during the winter season using box-and-whisker diagrams. During winter, natural gas is supplied mainly from the UK Continental Shelf. The mean supply from the continental shelf is 198 million cubic metres per day (Mm³/d). Liquefied Natural Gas (LNG) is the second most important source of natural gas; however, the season's mean LNG supply is less than one-tenth of the mean gas supply from the shelf.

Figure 3.6 (b) illustrates winter gas consumption by offtake type using box-and-whisker diagrams. As shown in Figure 3.6 (b), gas is mainly delivered to LDZ networks, where it is ultimately used for heating. The mean gas demand from LDZs is 122 Mm³/d. However, gas use for power generation via combined-cycle gas turbines (CCGTs) is also significant, with consumption of 114 Mm³/d. Industrial sites use only a small proportion of the total gas, and almost no gas is injected into storage sites or exported.

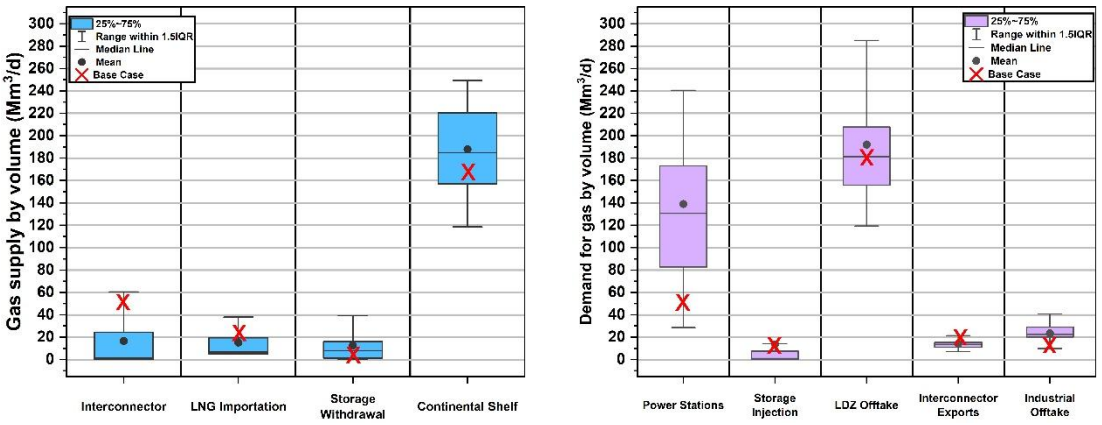

(a) **(b)**

Figure 3.6. Supply and demand in Winter Season 2018–2019.[90]

The winter day of 25 November 2018 was selected for modelling because the supply and demand of gas on this day follow the same trend as those of the 2018–2019 winter season. In Figure 3.6 (a) and (b), symbol on each boxplot indicates the gas supply and demand levels on 25 November 2018. On this day, St Fergus in Scotland served as the leading gas supplier to the network, followed by Easington in the northeast. Consequently, gas flowed from the north of the network towards the south and from the east towards the west.

The demand at each node in the Winter Case is input data and can be found in Appendix A, Table A.1.

3.2.2.2. Supply and Demand in the Summer Case

The summer season selected for developing the gas network model extends from May 2022 to October 2022. Due to the outbreak of the conflict in Ukraine, mainland Europe lost one of its major sources of gas supply. This led mainland Europe to replace the lost supply with gas from Great Britain (GB). Because GB has an extensive LNG re-gasification infrastructure, LNG purchased by mainland Europe was shipped to GB, re-gasified, and injected into the high-pressure gas network before being transferred to mainland Europe via the Bacton Interconnector.

The summer of 2022 was exceptionally important because it demonstrated the GB gas network's capability to cope with changing gas-flow directions. Furthermore, during this season, gas in the southern regions of the network flowed from west to east to deliver gas from the Milford Haven LNG terminal to the Bacton Interconnector.

Figure 3.7 (a) illustrates the summer-season supply by source using box-and-whisker diagrams. The UK Continental Shelf (UKCS) remained the most significant gas supplier, with a seasonal mean of 164 million cubic metres per day (Mm^3/d). However, a significant portion of gas was supplied via LNG sites, resulting in a seasonal mean of 44 Mm^3/d, which is double that of the winter season.

Figure 3.7 (b) illustrates summer-season gas consumption by offtake type using box-and-whisker diagrams. As shown in Figure 3.7 (b), gas was mainly exported to the EU via the interconnectors at Bacton during the summer season. The seasonal mean export level was 85 Mm^3/d. The second-largest consumers were the power stations, with a mean of 60 Mm^3/d, and the third-largest consumers were the LDZ offtakes, with a mean of 52 Mm^3/d.

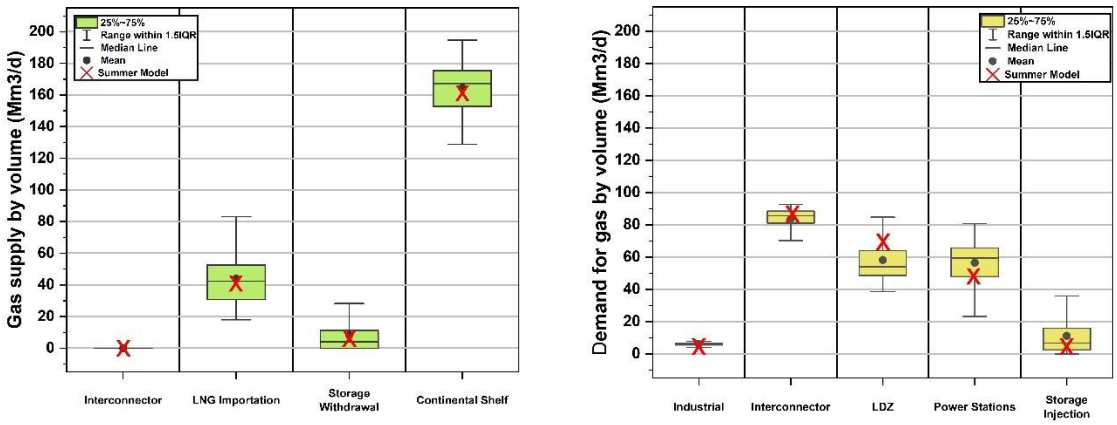

(a) **(b)**

Figure 3.7. Supply and demand of summer season 2022

The summer day selected for modelling is 25 August 2022, which reflects the trends of the summer season of 2022. In Figure 3.7 (a) and (b), the 'X' symbol on each boxplot indicates the supply and demand values on 25 August 2022. On this day, St Fergus and Easington were the leading gas suppliers to the network, followed by a relatively large volume of gas from Milford Haven. Consequently, gas in the southern regions of the network flowed from west to east, demonstrating an alternative operational mode of the gas network.

The demand data for the Summer Case are input data and can be found in Appendix A, Table A.2.

3.2.2.3. Hourly Disaggregation Profiles

As the demand and supply data are available at a daily resolution, they must be disaggregated into hourly time steps to capture the hourly dynamics of the gas network. The hourly profile was derived from data available on the National Gas Portal, which presents hourly variations in gas demand by sector. A representative profile was selected for each sector and applied accordingly. The points between hourly time steps were interpolated using a ramp function.

The distribution profiles are input data and can be found in Appendix A, Table A.3. which demonstrates the hourly values of the profile as well as the hourly disaggregation profiles.

3.3. Calibration and validation of the model

Calibration refers to the process by which the final configurations of the compressor stations in the model were chosen. The aim of this process was to ensure that the operational attributes of the network accurately represent real conditions.

These attributes include compressor energy consumption, pressure levels, and linepack levels, with linepack being the most important. Linepack is a function of pressure levels in pipelines, and pipeline pressure is affected by compressor operation, making linepack an indirect representation of compressor behaviour as well. Moreover, changes in the hourly linepack level of the network are a function of changes in the network's gas supply and demand. Therefore, linepack serves as a parameter that represents all the model outputs.

By comparing the resulting linepack with the observed linepack, it was demonstrated that all the model attributes represent real operational behaviour, thereby validating the model results. In other words, the calibration results were validated.

The hourly linepack levels of the network are publicly available in the National Gas database [93]. These levels are reported both as aggregated network linepack and disaggregated by twelve geographical zones of the network.

3.3.1. Calibration Steps

The high-pressure gas network has been calibrated through the process shown in Figure 3.8. This process consisted of the following steps:

1. Set the initial pressure at each node
2. Select the compressors to be included
3. Adjust the set pressure of each compressor station. The compressor station fixes either the inlet or outlet pressure to the defined set pressure.
4. Specify whether the set pressure is fixed at the inlet or outlet of the compressor.
5. Run the transient simulation.
6. Check whether the pressure levels at each node are within the operational range. The minimum operational pressure is 40 bar-g across all pipelines, while the maximum operational pressure differs between linepack zones. These data are obtained from National Gas but are not publicly available.
    a. If pressures are not within range, return to Step 3.
    b. If pressures are within range, continue to Step 7.
7. Check whether the flow direction in the network is acceptable. The flow direction should correspond to one of the scenarios described in National Gas documentation [89].
8. Check whether the resulting linepack levels fall within the seasonal linepack range. The seasonal linepack range is constructed using real data obtained from the National Gas public database [90]

a. If linepack levels are not in range, return to step 3.

b. If linepack levels are within range, the model is considered calibrated.

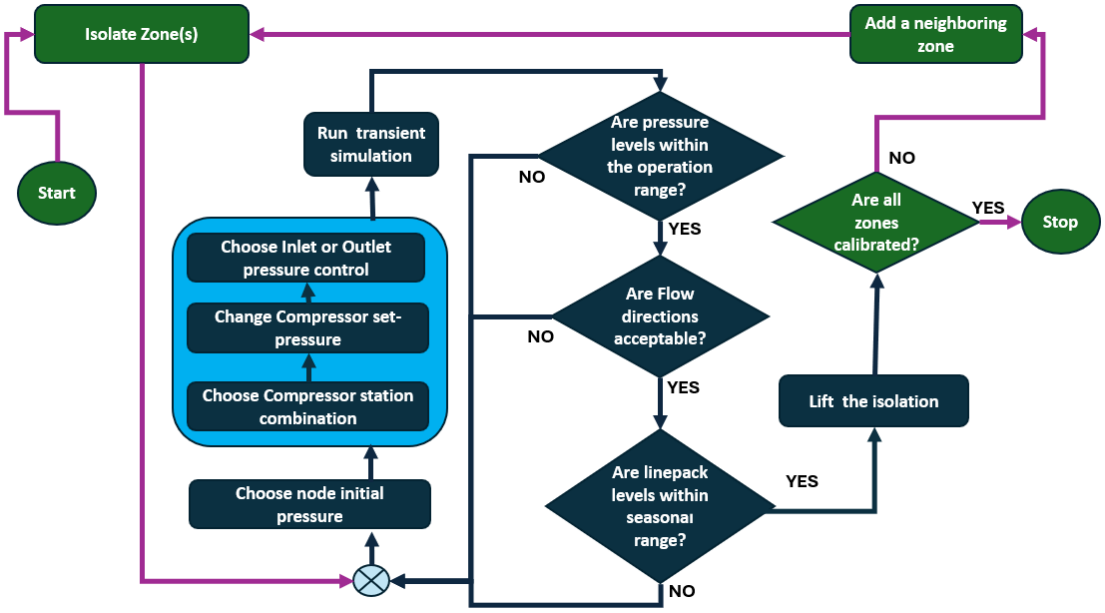

Figure 3.8. Flowchart describing the calibration process.

3.4. Results of the calibration

3.4.1. Calibrated Compressor Stations Setup

Different combinations of gas compressors, set-pressure levels, and control modes were tested to reproduce this gas flow regime. The final combination of compressors used for the Summer Case is shown in Table 3.5. The flow direction across the network.

Table 3.5. List of compressors used for the Summer Case

Region	Name	Purpose	Set Pressure
Northeast	Hatton	Directing flow of gas from Easington to Midlands and East of England.	55 bar-g @ inlet
Northwest	Carnforth	Directing flow from Scotland to Northwest England.	55 bar-g @ inlet
West Midlands	Churchover	Directing the flow of gas from South Wales to the Midlands.	50 bar-g @ inlet
East-Midlands	King's Lynn-	Directing the flow of gas to the Bacton interconnector.	50 bar-g @ inlet

	reversed direction		
Scotland	Avonbridge	Directing gas flow from the South of Scotland towards the North of England.	55 bar-g @ inlet
	Aberdeen	Directing the flow of gas from the North of Scotland to the South of Scotland.	55 bar-g @ inlet
	St Fergus	Boosting pressure of gas immediately after release from St Fergus supply point.	45 bar-g @ inlet

Through the calibration process, various combinations of gas compressors, set-pressure levels, and control modes were tested to reproduce this gas flow regime. The final combination of compressors used for the Winter Case is shown in Table 3.6 .

Table 3.6. List of compressor stations used for the Winter Case.

Region	**Name**	**Task**	**Set Pressure**
Northeast	Hatton	Directing gas flow from Easington to the Midlands and East of England.	55 bar-g @ inlet
Northwest	Carnforth	Directing the flow of gas from Scotland to Northwest England.	50 bar-g @ inlet
	Nether Kellet	Boosting pressures for extremities in Northwest England.	70 bar-g @ outlet
Southeast	Diss	Directing flow from Bacton to Southeast England. Boosting pressure levels in extremities of Southeast England.	65 bar-g @ outlet

Midlands and East	Kings Lynn	Directing the flow of gas from the Bacton supply point to the Midlands. Preventing over-pressurisation in pipelines connected to Bacton supply point.	58 bar-g @ inlet
Scotland	Avonbridge	Boosting the flow of gas coming from Aberdeen. Preventing over-pressurising nodes between Avonbridge and Wooler.	70 bar-g @ outlet
	Aberdeen	Directing the flow of gas from the North of Scotland to the South of Scotland Preventing over-pressurisation between Aberdeen and St Fergus.	55 bar-g @ inlet
	St Fergus	Directing the flow of gas from gas suppliers into the network.	45 bar-g @ inlet
	Wooler	Boosting pressure of gas in East Scotland Preventing de-pressurisation between Wooler and Bishop Auckland.	70 bar-g @ outlet

Figure 3.9 (a) and (b) illustrate the operation of the compressors in the Winter and Summer Cases. The x-axis represents the total energy consumption of each compressor station during the simulation, while the y-axis represents the average utilisation of each compressor station. The average utilisation is defined as the ratio of average energy consumed to the total energy capacity for each compressor station. The points are colour-mapped, with the colour corresponding to the total flow of gas passing through each compressor station. This colour map is represented by the secondary y-axis on the right-hand side.

The total energy consumption of the compressor stations in the Winter Case was 3,718 MWh. In the Summer Case, this decreased to 2,210 MWh.

The power consumption of compressors in Scotland was considerably higher in the Winter Case compared with the Summer Case. There are two main reasons for this. First, the flow levels that the Scottish compressors handle are higher in winter than in summer. Furthermore, in the Winter Case, St Fergus and Aberdeen each compress a volume of gas approximately 1.4 times that of the Summer Case. Second, in the Winter Case, St Fergus has an average compression ratio of 1.40, and Aberdeen 1.41. In the Summer Case, the St Fergus compression ratio reduces to 1.33, while that of Aberdeen decreases to 1.24.

In the Summer Case, the compressors located in the Midlands and East—Hatton and King's Lynn—handle a large gas flow. Despite this, their energy consumption and average utilisation are relatively lower than in the Winter Case. The reason for this is that both compressors operate with a lower compression ratio in summer. In the Winter Case, Hatton has a compression ratio of 1.23, and King's Lynn 1.16. In the Summer Case, however, Hatton has a compression ratio of 1.14, and King's Lynn 1.15.

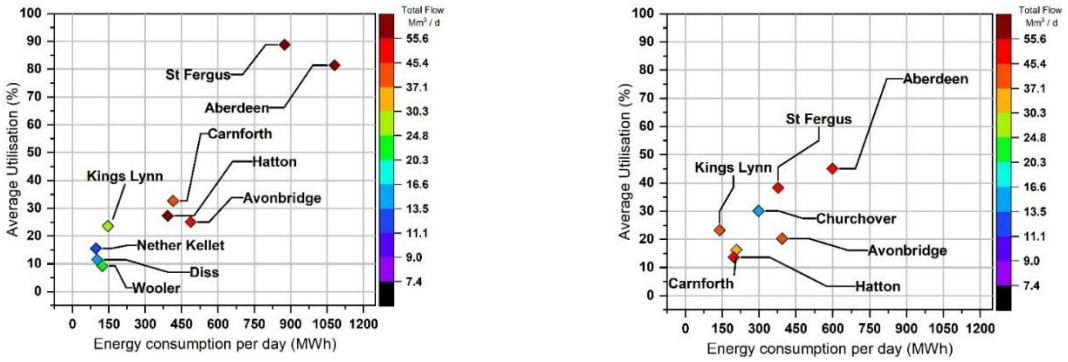

(a) **(b)**

Figure 3.9. Compressor energy consumption and utilisation (a) in the Winter Case and (b) in the Summer Case.

3.4.2. Network flow direction

The direction of gas flow in the network is heavily influenced by the configuration of compressor stations used in the model. The direction of flow should follow a typical pattern for winter and summer, as outlined by National Gas [89].

Figure 3.10 shows the direction of flow in (a) the Winter Day Case and (b) the Summer Day Case. In the Winter Day Case, gas mainly flows from St Fergus in Scotland southwards towards northern

England and the Midlands. Another stream of gas flows from the LNG supplied via Milford Haven towards the Bacton transport interconnector, which then transports gas to the European continent.

In the Summer Day Case, the flow from St Fergus towards northern England also exists; however, the volumes are lower than in the Winter Case. In southern England, the flow direction is reversed relative to the Winter Day Case. Furthermore, large quantities of gas are imported from the European continent via Bacton, flowing westwards towards South Wales and the South West

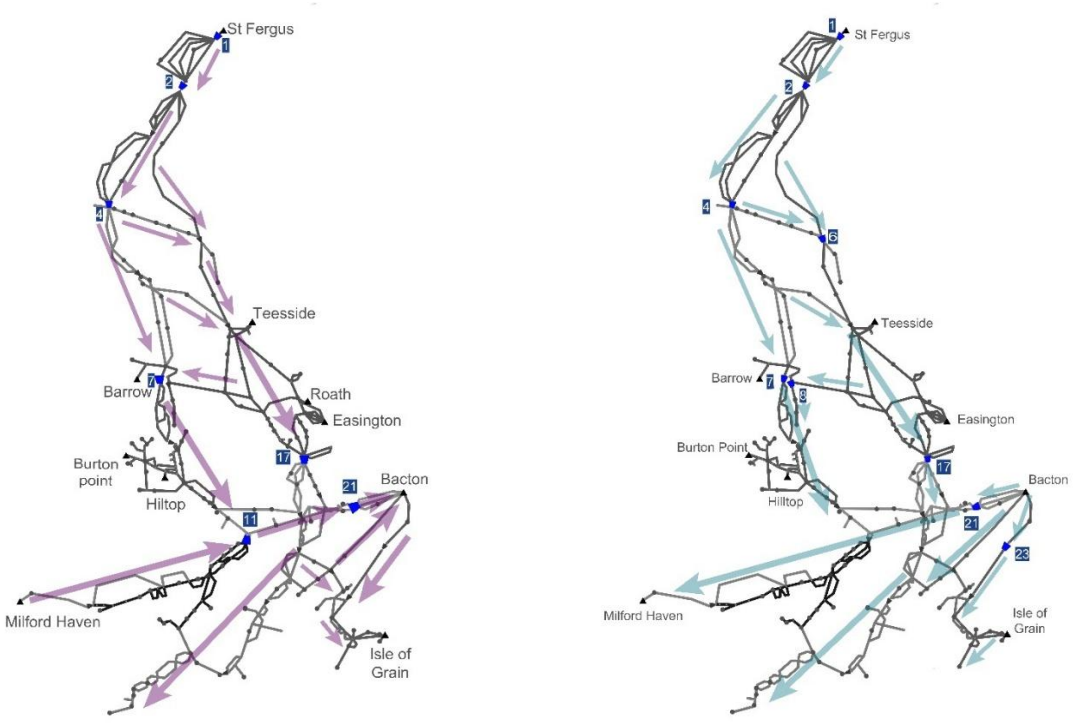

(a) **(b)**

Figure 3.10. Flow directions in (a) the Winter Case and (b) in the Summer Case.

3.4.3. Pressure levels

Initial pressure levels, although a starting point for the simulation, are results of the calibration process and has been determined through an iterative process. Therefore, they are presented in the main body of the chapter. The initial pressure levels chosen for nodes in winter case is as in Table 3.7, and that for the Summer case in Table 3.8.

Table 3.7. Initial pressure levels in Winter Case

Zone 0 -Scotland							
Name	**Pressure**	**Name**	**Pressure**	**Name**	**Pressure**	**Name**	**Pressure**

Aberdeen	51	Avonbridge	70	Balgray	55	Blackness	55
Burnhervie	52	Careston	55	Crieff	55	Drum	55
Gowkhall	55	Kinknockie	53	Kirriemuir	55	Kirriemuir	72
Shell Backhaul	55	St Fergus	54				
Zone 1 -Scotland							
Name	**Pressure**	**Name**	**Pressure**	**Name**	**Pressure**	**Name**	**Pressure**
Armadale	55	Avonbridge	70	Broxburn	55	Coldstream	55
Elvanfoot	55	Saltwick	55	Glenmavis	55	Grangemouth	55
Humbleton	55	Hume	55	Keld	55	Langholm	55
Lockerbie	55	Longtown	55	Lupton	55	Melkinthorpe	55
Moffat	55	Moffat	61	Nether Hwclgh	55	Soutra	55
Towlaw	55	Wetheral	55				
Zone 2 - Scotland							
Name	**Pressure**	**Name**	**Pressure**	**Name**	**Pressure**	**Name**	**Pressure**
Aberdeen	55	Aberdeen	55	Bishop Auckland	61	Corbridge	55
Guyzance	55	Lochside	55	Wooler	55	Wooler	70
Zone 3- North East							
Name	**Pressure**	**Name**	**Pressure**	**Name**	**Pressure**	**Name**	**Pressure**
Aldbrough	61	Asselby	58	Baldersby	60	Beeford	61
Beltoft	57	Bishop Auckland	55	Blyborough	56	Brigg	56
BurleyBank	58	Coryton &&	58	Cowpen Bewley	55	Elton	55
Ganstead	61	Gooleglass	58	Hornsea	61	ICIBILLINGHAM	55
Immingham 1906.1	58	Keadby	57	LtBurdon	55	Pannal	58
Paull && Saltned	61	Pickering	55	Rawcliffe	58	Saltend	70
Saltned	59	Scunthorpe	57	Sproatley	61	Stallingbor1	58
Supply Easington	62	Susworth Trent E.	57	Susworth Trent W.	57	Tees Phil BOC &&	55
Teesside	55	Thornton Curt	58	Thrintoft	59	Towton	58
Walesby	56	West Burton	58				
Zone 4- North West							
Name	**Pressure**	**Name**	**Pressure**	**Name**	**Pressure**	**Name**	**Pressure**
Alrewas	55	Alrewas Comp	56	Aspley	56	Audley	57
Austrey	55	Birch Heath	57	Blackburn M &&	75	Bridgefarm	57
Bridgewater &&	57	Burscough	62	BurtonPoint	57	Carnforth	50
Carnforth	65	Carrington	60	Churchover Comp	54	Deeside PS	57
Drointon	56	Eccleston	57	Elworth	57	Entry Node	55
EX Blackrod && blkburn	75	EX Maelor	56	EX Shellstar	54	Ferney Knoll	61

Hawarden	57	HaysChem	57	Helsby	54	Hilltop	57
Holford	58	Holmes Chapel	58	ICIRuncorn && Rocksavage	52	Malpas	57
Mawdesley	62	MickleTrafd	57	Milwich	56	Nether Kellet	54
Nether Kellet	50	No115	57	No119	57	Pennington	55
Pickmere	58	Samlesbury	75	Sellafield	55	Shocklach	57
Shustoke	55	Stublach	58	Stublach	58	Supply Barrow	55
Supply BurtonPoint	57	Treales	63	Warburton	60	Warmingham	57
Warnington	60	Warnington	60	WestonPoint	52	Wheelock	57

Zone 5 - Midlands

Name	**Pressure**	**Name**	**Pressure**	**Name**	**Pressure**	**Name**	**Pressure**
Alrewas Comp	55	Blaby	56	Brisley	56	Caldecott	56
Churchover	55	Corby	56	Cottam	60	Hatton	55
Hatton	70	Kings Lynn	58	Kings Lynn	63	KingsLynn	60
Market Harboro'	55	Palmpaper &&	61	PeterborEye	57	Peterborough	57
Peterborough	57	Peterborough	57	Peterborough Tee	57	Saddle Bow	60
Staythorpe &&	59	Supply Bacton	58	Tur Langton	56	West Winch	61
Wisbech Nene E.	59	Wisbech Nene W.	59				

Zone 6 - South Wales

Name	**Pressure**	**Name**	**Pressure**	**Name**	**Pressure**	**Name**	**Pressure**
Aberdulais	76	Avonmouth	48	BaglanBay	76	Churchover Comp	54
Cirencester	50	Clifrew	76	Dowlais	76	DyffrynClyd	76
Easton Grey	51	Evesham	53	EX Seabank	48	Fiddington	76
Gilwern	76	Honeybourne	54	Leamington	54	LittletnDrew	50
Llanvetherine	76	LowerQuinton	53	Newbold Pacey	54	Ross	76
Rugby	54	Sapperton	52	Seabank	48	StratfrdAvon	54
Tirley Pri	76	Treadow	76	Wormington	53	Wormington	76

Zone 7 - South West

Name	**Pressure**	**Name**	**Pressure**	**Name**	**Pressure**	**Name**	**Pressure**
Aylesbury	56	Aylesbury	56	Aylesbeare	46	Barnington	47
Barton Stacey	53	Braishfield	52	Centrax O/T	45	Centrax Tee	45
Chalgrove	56	Coffinswell	45	Didcot	56	East Ilsley	55
EX Choakford	45	Gosberton	59	Hardwick	57	Horndon	62
Huntingdon	52	Huntingdon	70	Ilchester	47	Ispden	56
Kenn (South)	45	Kirkstead	60	Langage	45	Lockerley	52
Lockerley	52	Lutton	54	Mappowder	49	Marchwood	52
Michelmersh	52	Nutfield	56	Ottery St. Mary	46	Pucklechurch	49

Slapton	57	Spalding	55	Steppingley	58	Sutton Bridge	59
Sutton Bridge	59	Theddlethorpe	55	Tydd St. Giles	59	Tydd St. Giles	59
Willington	59	Winkfield	56				
Zone 8 - South East							
Name	**Pressure**	**Name**	**Pressure**	**Name**	**Pressure**	**Name**	**Pressure**
Cambridge Comp Tee	55	EX Peters Green	55	Great Wilberham	55	No198	55
Roudham Heath	56	Royston	55	Whitwell	56		
Zone 9 - South East							
Name	**Pressure**	**Name**	**Pressure**	**Name**	**Pressure**	**Name**	**Pressure**
Diss Comp Tee	55	Diss Comp Tee	65	EX Tatsfield	61	Farmingham	62
Grain	63	Gravesend Thames Sth	62	GTYarmouth	58	Marchwood	62
Medway	63	Roxwell	50	Roxwell	65	Shorne	62
Stanford Le Hope	62	Supply Isle of Grain	63	Yelverton	58		
Zone 10 - South East							
Name	**Pressure**	**Name**	**Pressure**	**Name**	**Pressure**	**Name**	**Pressure**
Epping Green	66	Lt Barford	59	Matching Green	66	Rye House	66
Stapleford	64	Tilbury Thames Nth	62				
Zone 11 - South Wales							
Name	**Pressure**	**Name**	**Pressure**	**Name**	**Pressure**	**Name**	**Pressure**
Blackbridge	78	Felindre	76	Felindre	76	Supply Herbrandston	78
Three Cocks	76						

Table 3.8. Initial pressure levels in Summer Case.

Zone 0							
Name	Pressure	Name	Pressure	Name	Pressure	Name	Pressure
StFergus	40	Kinknockie	55	ShellBackhaul	55	Drum	55
Aberdeen	55	Crieff	55	Blackness	55	Burnhervie	55
Balgray	55	Aberdeen	55	Careston	55		
Zone1							
Name	Pressure	Name	Pressure	Name	Pressure	Name	Pressure
Grangemouth	55	Coldstream	55	Wetheral	55	Keld	55
Moffat	55	Hume	55	Saltwick	55	Elvanfoot	55
Glenmavis	55	MelkInthorpe	55	Soutra	55	Lupton	50
Broxburn	55	Towlaw	55	Langholm	55	Lockerbie	55

NetherHwclgh	55	Longtown	55	Armadale	55	Humbleton	55
Peterhead	55						
Zone2							
Name	Pressure	Name	Pressure	Name	Pressure	Name	Pressure
Aberdeen	55	Corbridge	55	Lochside	55	Wooler	70
Guyzance	55	Wooler	70				
Zone 3							
Name	**Pressure**	**Name**	**Pressure**	**Name**	**Pressure**	**Name**	**Pressure**
Immingham	50	Thrintoft	50	Susworth Trent E.	50	Tees Phil BOC	50
Asselby	50	ThorntonCurt	50	Gooleglass	50	Pickering	50
Stallingbor	50	ICIBillnghm	50	Baldersby	50	Keadby	50
Saltned	50	Walesby	50	WestBurton	50	Pannal	50
Easington	50	Paull & Saltned	50	Auckland	50	Blyborough	50
Coryton	50	Bishop Auckland	62	LtBurdon	50	Teesside NSMP	50
Elton	50	Towton	50	Aldbrough	50	Cowpen Bewley	50
Saltend	50	Murrow	50	Ganstead	50	Sproatley	50
Hornsea	50	Brigg	50	Beeford	50	Teesside	50
BurleyBank	50	Scunthorpe	50	Easington	50	Rawcliffe	50
Susworth Trent W.	50						
Zone 4							
Name	**Pressure**	**Name**	**Pressure**	**Name**	**Pressure**	**Name**	**Pressure**
Shellstar	55	Deeside	55	Birch Heath	55	Rocksavage	55
Pennington	50	Hawarden	55	Bridgewater	55	Ferney Knoll	55
Helsby	55	Blackburn M	50	Elworth	55	MickleTrafd	55
HaysChem	55	Wheelock	55	Churchover	60	BurtonPoint	55
Holford	55	Stublach	55	Milwich	55	Carrington	55
Pickmere	55	Shocklach	55	Alrewas	55	Virtual Demand	55
Drointon	55	Eccleston	55	Warnington	60	Aspley	55
Maelor	55	Warnington	60	Shustoke	55	HolmesChapel	55
Mawdesley	55	Alrewas	55	Audley	55	Warmingham	55
Sellafield	50	Austrey	55	Burscough	55	Blackrod	50
WestonPoint	55	Samlesbury	50	Hilltop	55	Malpas	55
Nether Kellet	50	Holford	55	Treales	55	Carnforth	55
Sublach	55	Winnington	55	Bridgefarm	55	Barrow	50
zone 5							

Name	Pressure	Name	Pressure	Name	Pressure	Name	Pressure
Palmpaper	55	Hatton	55	Peterborough	55	BactonBBL	68
Bacton	68	Churchover	60	Wisbech Nene W.	55	Staythorpe	55
Wisbech Nene	55	Hatton	55	Blaby	55	Mkt Harborogh	55
Peterborough	55	Peterborough Tee	55	Palmpaper	55	Peterbor Eye	55
Caldecott	55	KingsLynn	55	WestWinch	55	Saddle Bow	55
Brisley	68	Kings Lynn	50	Corby	55	Bacton	68
zone 6							
Name	**Pressure**	**Name**	**Pressure**	**Name**	**Pressure**	**Name**	**Pressure**
Aberdulais	55	Leamington	55	Ross	55	Llanvetherine	55
Churchover	60	Stratfrd Avon	55	Littletn Drew	55	Tirley Pri	55
EastonGrey	55	Avonmouth	55	Dyffryn Clyd	55	Wormington	65
Clifrew	55	Gilwer	55	Pucklechurch	55	LowerQuinton	55
Zone 7							
Name	**Pressure**	**Name**	**Pressure**	**Name**	**Pressure**	**Name**	**Pressure**
Centrax O/T	60	Kirkstead	60	Tydd St. Giles	55	Barton Stacey	60
Lockerley	50	Gosberton	55	Michelmersh	60	EX Choakford	60
Marchwood	60	Huntingdon	50	Willington	65	East Ilsley	60
Lockerley	50	Nutfield	60	Ottery St. Mary	60	Horndon	68
Winkfield	60	Ilchester	60	Braishfield	60	Barnington	60
Kenn	60	Chalgrove	60	IPsden	60	Mappowder	60
Hardwick	65	Theddlethorpe	50	Aylesbeare	60	Aylesbury	55
Sutton Bridge	55	Humbley	65	Coffinswell	60	Langage	60
Huntingdon	50	Sutton Bridge	55	Spalding	55	Steppingley	65
Zone 8							
Name	**Pressure**	**Name**	**Pressure**	**Name**	**Pressure**	**Name**	**Pressure**
Gt Wilbraham	68	Whitwell	-	Roudham Heath	68	Royston	65
Peters Grn	-	Cambridge Comp Tee	60		-		-
Zone 9							
Name	**Pressure**	**Name**	**Pressure**	**Name**	**Pressure**	**Name**	**Pressure**
Kemsley	68	Stanford Le Hope	-	Shorne	68	Gravesend Thames	68
Roxwell	-	Yelverton	68		-		-
Zone 10							
Name	**Pressure**	**Name**	**Pressure**	**Name**	**Pressure**	**Name**	**Pressure**

Farningham	68	Tatsfield	-	Grain	68	Sellige	68
Marchwood	-	GT Yarmouth	68	Medway	-	Isle Grain	68
Zone 11							
Three Cocks	55	Felindre	65	Blackbridge	55	Milford Haven	55
Milford H	55						

Figure 3.11 (a) and (b) illustrate the pressure levels at extremities and supply points in the Winter and Summer Cases. The x-axis indicates the minimum pressure at each node during the simulation, and the y-axis indicates the maximum pressure at each node during the simulation. Each axis includes a data rug that depicts the range within which the maximum and minimum pressure levels are distributed. The points on the graphs are colour-mapped, with the colour representing the daily gas flow at each node. This colour map is displayed by the secondary y-axis on the right-hand side.

In the Winter Case, the minimum pressure levels range from 40 bar-g to 65 bar-g, while the maximum pressure levels range from 40 bar-g to 77.5 bar-g. In the Summer Case, the minimum pressure levels range from 40 bar-g to 60 bar-g, and the maximum pressure levels range from 40 bar-g to 72.5 bar-g. Both ranges are shorter than those in the Winter Case.

In the Winter Case, the gas demand levels at the extremities are significantly higher than those in the Summer Case. Three of the extremities have demands between 2 and 3.2 Mm^3/d, one has a demand of 6 Mm^3/d, and two others have demands between 8 and 12.7 Mm^3/d. In the Summer Case, all the extremities have demand levels below 2 Mm^3/d.

Despite the high demand for interconnector exports to the continent, domestic demand for gas is low in summer. This causes the pressure levels in the Summer Case to be less dispersed than in the Winter Case. The standard deviation of all pressure levels in the Winter Case is 8.9 bar-g, while that of the Summer Case is 5.9 bar-g, further supporting this observation.

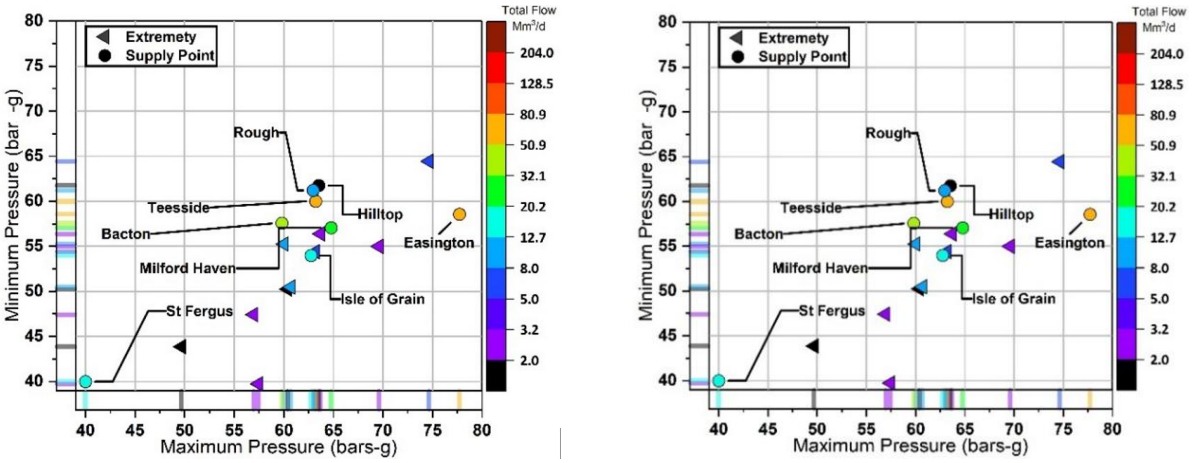

Figure 3.11. Pressure levels at the supply points (a) in the Winter Case and (b) in the Summer Case.

Figure 3.12 and Figure 3.13 illustrate the maximum and minimum pressure levels observed in each zone of the network in relation to the minimum and maximum operational pressures in the corresponding regions. Figure 3.12 presents the results of the Summer Case and Figure 3.13 presents those of the Winter Case.

Furthermore, Figure 3.12 and Figure 3.13 show that both case studies have pressure levels within the allowable operational range. Extended versions of Figures 3.12 and 3.13 are provided in Appendix B.

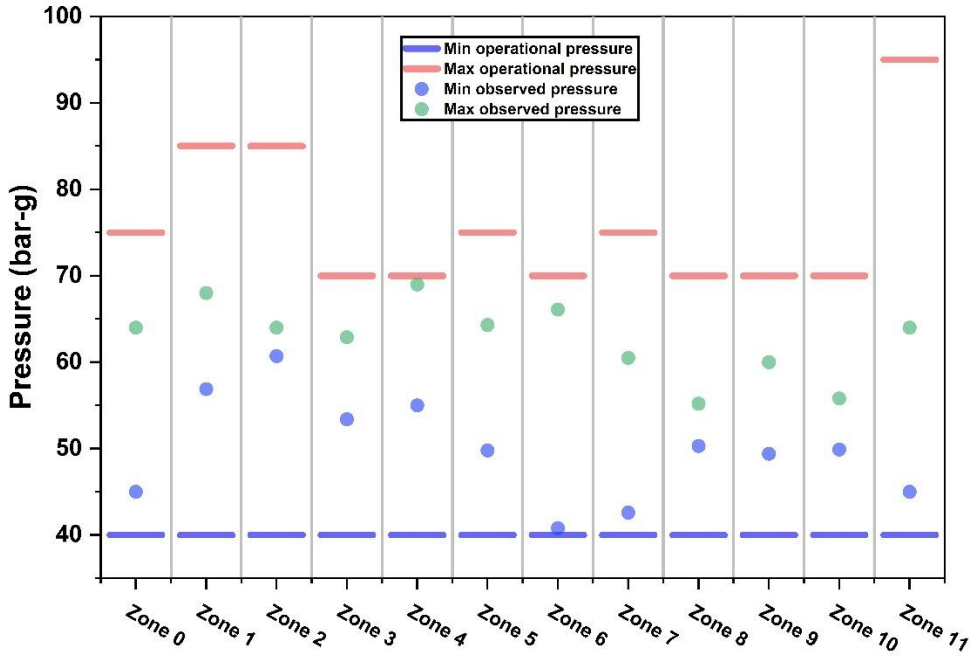

Figure 3.12. Maximum and minimum allowable operational pressure at each zone vs. minimum and maximum observed pressure levels at each zone. Winter Case.

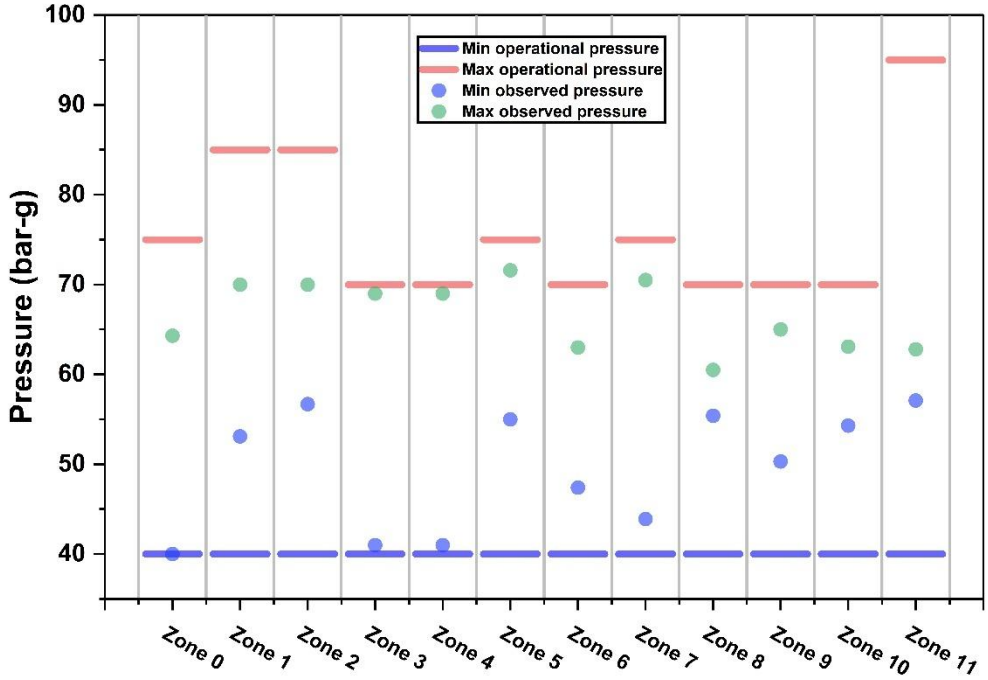

Figure 3.13. Maximum and minimum allowable operational pressure at each zone vs. minimum and maximum observed pressure levels at each zone. Summer Case.

3.4.4. Operational Linepack vs. Seasonal Range

As explained in Section 3.3, in the final step of the calibration process, the resulting linepack is compared with the seasonal linepack range. The seasonal linepack range is obtained from the National Gas public database [1]. The resulting linepack, which is a function of pressure levels in the pipelines that vary with compressor operation, represents all the model attributes. Therefore, should the resulting linepack fall within the seasonal linepack range, it can be inferred that all the other attributes are also within the seasonal operational range.

Figure 3.14 depicts the hourly linepack of the entire model in relation to the seasonal linepack range. Figure 3.14(a) shows that, in the Winter Case, both the start-of-day and end-of-day linepack are 346.9 Mm^3, with a linepack swing—the difference between the maximum and minimum linepack over the day—of 16.6 Mm^3. Figure 3.14 (b) shows that, in the Summer Case, both the start-of-day and end-of-day linepack are 335.7 Mm^3, and the linepack swing is 14.1 Mm^3.

Three metrics were used to quantify the calibration quality of each case. The first is the proportion of the resulting hourly linepack that falls within the seasonal range. The second is the maximum deviation of the hourly linepack from the median of the seasonal range, and the third is the minimum deviation from that median. In both models, 100% of the hourly linepack population falls within the seasonal range. In the Winter Case, the maximum deviation from the seasonal median is 2.1%, and the minimum deviation is 0%. In the Summer Case, the maximum deviation is 2.6%, and the minimum deviation is 0%.

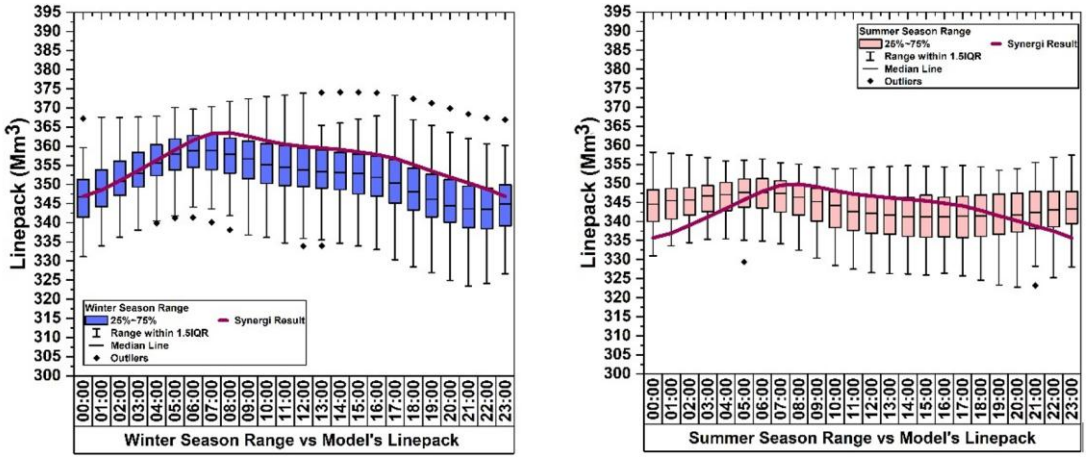

(a) **(b)**

Figure 3.14. Total linepack vs season's range (a) in the Winter Case and (b) in the Summer Case.

The calibration status of the Winter and Summer Cases was evaluated for every Linepack Zone. Figure 3.15 and Figure 3.16 present the calibration status of each zone in the Winter and

Summer Cases. Figure 3.15 indicates that, out of the 12 zones in the Winter Case, nine have all hourly linepack values within the expected seasonal range. Among the zones within range, the maximum deviation from the median varies between 2.4% and 8.0%, while the minimum deviation ranges from 0% to 2.5%.

According to Figure 3.15, there are three zones with out-of-range results: Zone 2 in Scotland, Zone 4 in north-west England, and Zone 11 in South Wales. In Zone 2, none of the linepack results fall within the range, with a maximum deviation from the median of 10.1% and a minimum deviation of 7.5%. In Zone 4, only 12.5% of results are within the seasonal range, with a maximum deviation of 21% and a minimum deviation of 17%. Finally, in Zone 11, none of the results fall within the range, with a maximum deviation of 27% and a minimum deviation of 25%.

Figure 3.16 illustrates that, in the Summer Case, 10 out of 12 zones have hourly linepack values within the expected seasonal range. In the zones where all linepack figures are within range, the maximum deviation from the median varies between 2.4% and 9%, while the minimum deviation ranges from 2.4% to 7.5%. However, two zones—Zone 4 in north-west England and Zone 11 in South Wales—have results that fall outside the range. In Zone 4, none of the results are within range, with a maximum deviation of 15% and a minimum deviation of 13%. Similarly, in Zone 11, none of the results are within range, with a maximum deviation of 19.5% and a minimum deviation of 17%.

Figure 3.15 and Figure 3.16 reveal deviations in Zones 2, 4, and 11 from the seasonal range. It is noteworthy that this deviation persists in both models, despite differences in compressor configurations, gas supply and demand values, and flow regimes.

The absence of gas regulator stations in the high-pressure gas network model is likely the primary cause of this deviation. Gas regulator stations are facilities that reduce gas pressure in the pipeline by physically expanding gas molecules. Incorporating regulator stations would enable higher pressure levels to be maintained in zones upstream of the regulator, while lower pressures could be achieved downstream.

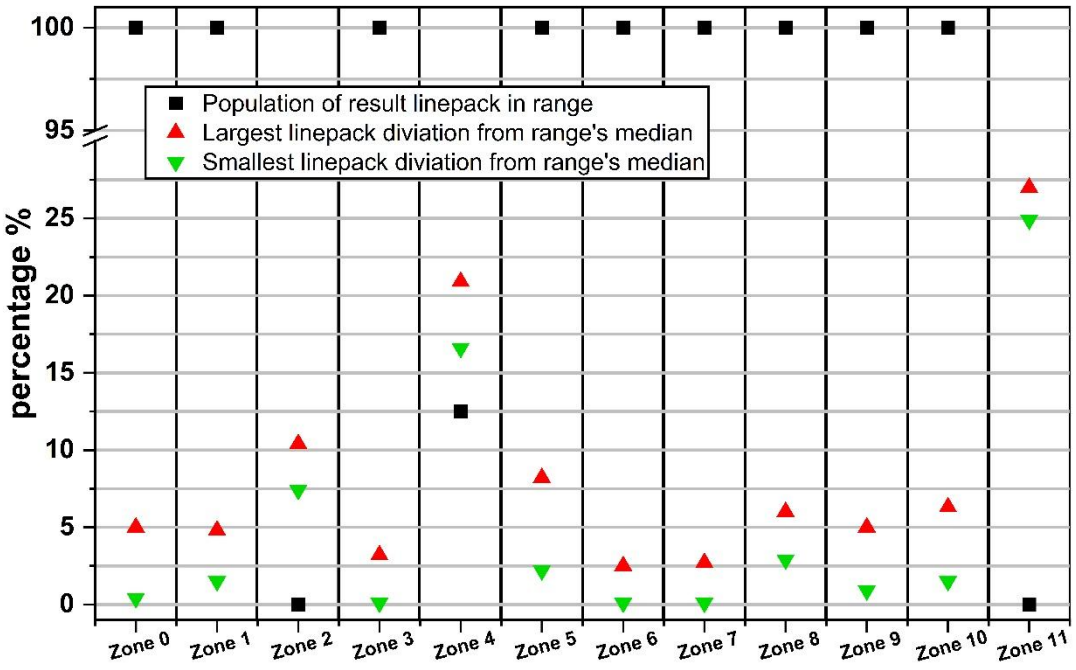

Figure 3.15 Linepack in every linepack zone of the Winter Case.

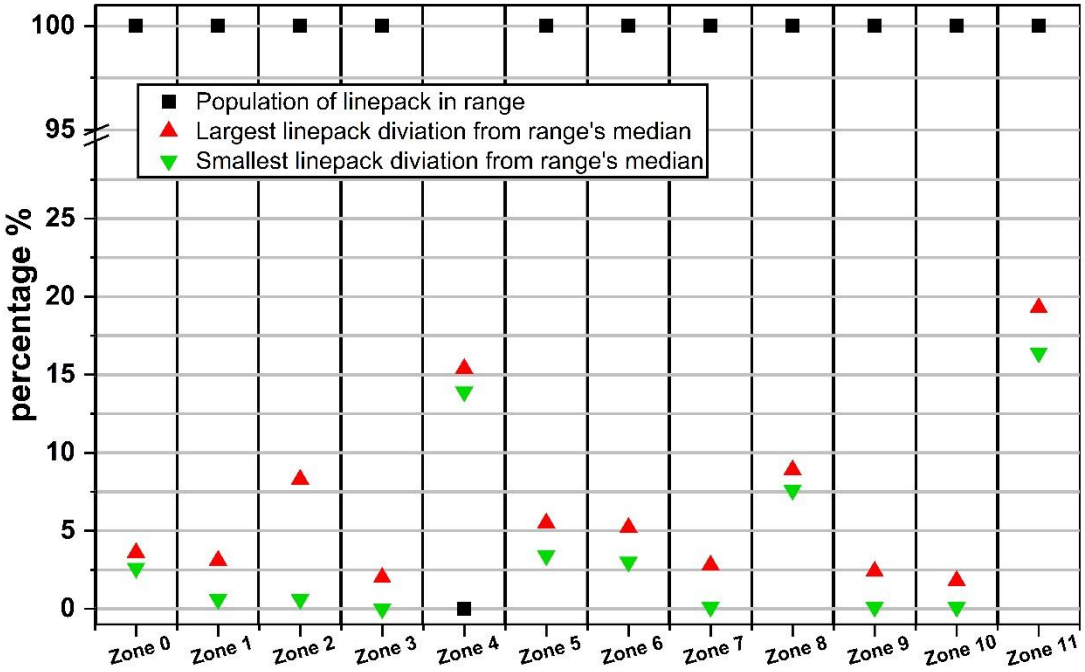

Figure 3.16 Linepack in every linepack zone of the Summer Case.

3.5. Case Studies

After Calibration of the Summer and Winter models, four other case studies were created with either the summer or winter model as reference. This means that demand and supply levels in nodes were projected using a conversion factor. All case studies are summarised in Table 3.9 below.

Table 3.9. Description of models

Name of Model	Description	Reference Model	Year	Supply & Demand Conversion Factor
Winter Model	Used as a reference case for all the other models depicting events during the winter season.	-	2018	-
Summer Model	Used as a reference case for all the other models depicting events during the summer season.	-	2022	-
20%Centralised Injection	Injecting 20% volumetric hydrogen from natural gas supply terminals into the gas network.	Winter Model	2035	0.58
20% Distributed Injection	Injecting 20% volumetric of wind-generated hydrogen from 28 busbars scattered across the GB.	Winter Model	2035	0.58
100% H_2	Transporting only hydrogen across GB via the high-pressure gas network.	Winter Model	2050	0.58
Deblending in winter	Deblending of hydrogen and natural gas in the high-pressure gas network. This hydrogen is injected via 28 busbars scattered across GB.	Winter Model	2035	0.58
Deblending in summer	Deblending of hydrogen and natural gas in the high-pressure gas network. This hydrogen is injected via 28 busbars scattered across GB.	Summer Model	2035	0.50

3.6. Discussion

The hypothesis underpinning this work was that a simplified gas network model, incorporating a selected set of compressor stations, could reproduce the operational characteristics of the GB high-pressure gas network under both typical summer and winter conditions. It was expected that simulated pressures, flow directions, and linepack levels would fall within the ranges observed in real-world operation.

The results confirmed this hypothesis. All simulated pressure levels remained within the operational limits defined by National Gas, indicating that the simulated conditions closely approximated safe and realistic operation. The gas-flow directions followed the typical seasonal patterns, demonstrating that the chosen combination of compressor stations successfully approximated real operation. Most importantly, the simulated hourly linepack levels were compared against the seasonal linepack range obtained from National Gas's public database. Since linepack is a function of pipeline pressure and variations in hourly flows, and compressor operation directly affects pressures, it served as an indirect validation of compressor station performance. Both the aggregated model linepack and the zonal assessments demonstrated strong alignment with seasonal ranges, confirming that the model captured realistic network behaviour

At the aggregated level, both the Summer Case and the Winter Case showed linepack levels within the seasonal range, and all node pressures were within operational limits. This demonstrates that the model, with the selected compressor stations, is effective in reproducing the operation of the NTS for both a typical summer and a typical winter day. At the zonal level, nine out of the twelve defined Linepack Zones were calibrated successfully, with linepack results closely matching the observed seasonal ranges.

However, limitations were observed in three zones: Zone 2 (Scotland), Zone 4 (north-west England), and Zone 11 (South Wales). These zones did not calibrate against the seasonal ranges. The most likely explanation is the absence of regulator stations in the model. Regulator stations play a key role in creating large pressure differences between adjacent regions, and their omission—due to the lack of publicly available operational data—prevented full calibration in these areas. Including regulator stations in future modelling is likely to address this issue and enhance overall accuracy.

The impact of this work is threefold. First, it demonstrates that even with a simplified compressor configuration, the model can replicate realistic NTS operation across seasons,

providing a validated and practical framework when detailed operational data are unavailable. Second, it highlights the critical role of regulator stations in zonal calibration, thereby identifying a clear direction for future research and model improvement. Third, and most importantly, by demonstrating that both the Winter Case and the Summer Case reproduce results close to reality, the validity of the subsequent case studies is assured, since they build on a model already proven to reflect real operational conditions. Collectively, these findings contribute to the development of more accurate and useful tools for gas-network analysis, supporting operational planning, resilience assessment, and strategic decision-making.

3.7. Summary

This chapter has demonstrated the development, calibration, and validation processes of the Winter Day and Summer Day case studies.

In describing the development of the case studies, a detailed description of the GB high-pressure gas network model was provided. Furthermore, all the data required to build the model were presented. The calibration process was then outlined step by step to help readers understand the procedure and the parameters considered. Finally, during validation, the results obtained from the case studies were compared with real operational data. Linepack values were confirmed to be within the seasonal range, pressure levels within the operational range, and flow directions consistent with typical seasonal patterns.

Chapter Four. Operational implications of transporting hydrogen via the GB high-pressure gas network

This chapter presents four case studies and aims to answer two research questions:

1. How would the rising volume of hydrogen in the gas network affect operational attributes of the high-pressure gas network, such as pressure levels, linepack and compressor energy consumption in a typical winter day operation?
2. Assuming that the hydrogen supply will be geographically dispersed across Britain, how does the location of hydrogen injection affect the volumetric percentage of hydrogen in each region?

This chapter applies transient analysis coupled with gas-component tracing analysis to address these research questions. Four case studies were conducted. The first represents the existing natural gas network in Great Britain on a typical winter day in 2018. The second models the gas network in 2035 with 20% volumetric hydrogen injection from eight gas entry points using the steam methane reforming (SMR) process. The third represents the gas network in 2035 with 20% volumetric hydrogen injection from 28 injection points co-located with wind farms dispersed across GB. Finally, the fourth case study represents the operation of the same gas network with 100% hydrogen in the year 2050.

4.1. Description of case studies

Four case studies were conducted to demonstrate the operation of the high-pressure gas network on a winter's day in 2018, 2035 and 2050. *Table 4.1* shows the main aspects of each case study.

Table 4.1. Description of case studies

Case	Year	Duration	Supply (Mm^3/d)

Study		Of Simulation	Natural Gas	Wind-generated hydrogen	SMR-generated hydrogen
Winter Day	2018	24 hours (10-minute time steps)	465 (Fixed hourly rate)	—	—
20% Centralised Injection	2035	24 hours (10-minute time steps)	132 (Fixed hourly rate)	—	35 (Fixed hourly rate)
20% Distributed Injection	2035	24 hours (10-minute time steps)	132 (Fixed hourly rate)	35 (Variable hourly rate)	—
100% H_2	2050	24 hours (10-minute time steps)	—	—	565 (Fixed hourly rate)

Figure 4.1 presents the gas supply and demand in the four case studies. In the figure, demand and supply are shown by region. Supply by region refers to the total gas volume supplied to the network through supply points located in that region, while demand by region represents the total gas volume required by nodes located in that region

Figure 4.1. indicates that the quantities of demand and supply across regions do not match. Consequently, some regions are net importers of natural gas, whereas others are net exporters. This imbalance demonstrates the necessity of a gas network to connect the regions.

In the Winter Case, most of the gas is supplied from Scotland and the Northeast region. In contrast, in the other case studies, the Southeast region provides most of the gas. This distribution aligns with National Gas's projections..

The energy demand in the 20% Centralised and 20% Distributed Injection cases is 58% of that in the Winter Model. This reduction reflects National Gas's [3] projected gas demand for 2035 and 2050. The two cases in which hydrogen is injected into natural gas have identical gas supply and demand levels. The energy demand in the 100% H_2 case is also equivalent to that in the 20% Centralised and Distributed Injection cases; however, because hydrogen has a lower energy density, the volumetric flow rate in the 100% H_2 case increases significantly compared with both 20% injection cases.

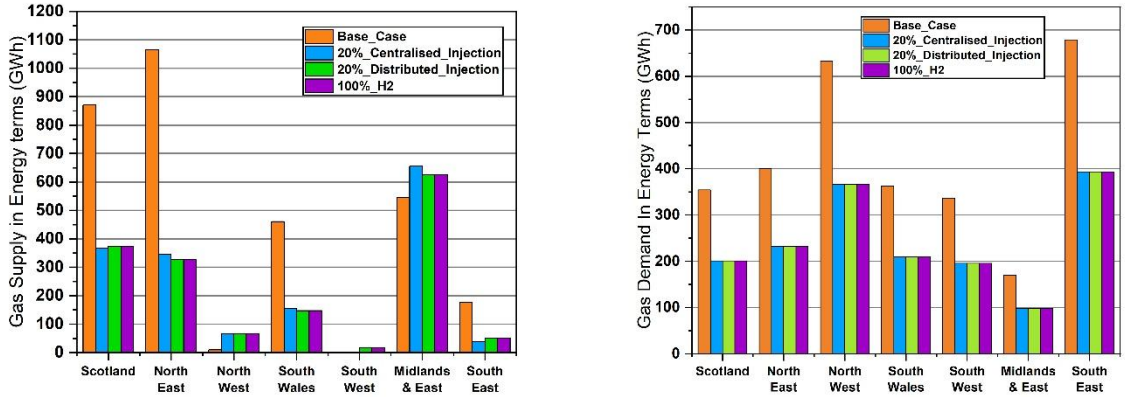

(a) **(b)**

Figure 4.1. Daily gas flows in energy terms, (a) supply (b) demand.

4.1.1. Case 1: Winter Model

The Winter Model represents a typical winter day in 2018 when the network transports natural gas. Gas demand and supply follow a typical winter day's profile, as shown in Figure 4.2.

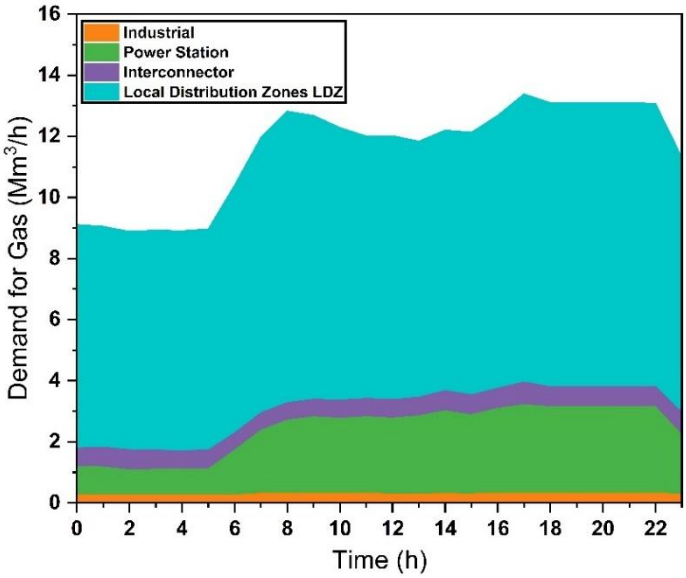

Figure 4.2.Demand for gas by sector in the Winter Model.

In 2018, the St Fergus supply terminal supplied most of the gas to the NTS. Therefore, in the Winter Model, compressor stations in Scotland and North England were set to support gas flow from Scotland to the South of England via the Northeast region [92].

The pressure levels in the network should always remain within a range to satisfy commercial and safety requirements. The upper bound of this range varies in each region depending on the maximum operating pressures of the pipelines, which is between 70–90 bar-g [93]. The minimum of this range depends on the compressor's minimum inlet pressure, which is 40 bar-g [92]. The compressors used in the Winter Model are described in Table 4.2.

4.1.2. Case 2: 20% Centralised injection

The 20% Centralised Injection Case Study investigated the effects of injecting hydrogen into the grid on a typical winter day in 2035. Hydrogen was injected from the same points as the natural gas supply terminals. The hydrogen injected into the grid was assumed to be produced via the steam methane reforming (SMR) process, commonly referred to as blue hydrogen. It was also assumed that the CO_2 produced from the SMR plants would be captured and sequestered. At each injection point, a 20% volumetric share of hydrogen was injected into the natural gas stream. Because the natural gas supply was assumed to remain constant over each hourly interval, the hydrogen injection was also constant within that period. The total volume of hydrogen injected was 35 Mm³/d

In the 20% Centralised Injection, supply from St Fergus in Scotland declined, and Bacton in the south of England became the leading gas terminal. This resulted in a reversal of the predominant gas-flow direction, from southwards to northwards. The compressors were configured to move gas away from the south-east towards neighbouring regions. Table 4.2 summarises the compressors used.

Table 4.2. Compressor detail in the Winter Model study.

Compressors	Purpose	Set Pressure
St Fergus	• Boosting pressures at St Fergus Terminal	• 40bar-g @ Inlet
Aberdeen	• Directing flow from St Fergus towards Scotland and the North of England • Keeping pressures below 65bar-g between St Fergus and Aberdeen	• 55bar-g @ Outlet
Nether Kellet	• Supporting pressures at network extremities, Blackrod and Blackburn	• 75bar-g @ Outlet

Hatton	• Supporting gas flowing from the Northeast to the South of England	• 75bar-g @ Outlet
King's Lynn	• Supporting gas flowing from Bacton terminal towards the Midlands • Keeping Bacton pressures below 75bar-g	• 75bar-g @ Outlet
Huntingdon	• Supporting gas flowing from the Midlands towards the South West	• 75bar-g@ Outlet

Table 4.3. Description of compressors in 20% Centralised Injection Case Study.

Compressors	Purpose	Set pressure
St Fergus	• Same as the Winter Model	40@ Inlet pressure
Aberdeen	• Same as the Winter Model	55@ Inlet pressure
Diss	• Supporting flow of gas from Bacton.	55@ Inlet pressure
Alrewas	• Used to direct flows from the Midlands towards the Northwest.	55@ Inlet
King's Lynn	• Same as the Winter Model	55 @Inlet
Huntingdon	• Same as the Winter Model	55 @Inlet

4.1.3. Case 3: 20% distributed injection

The 20% Distributed Injection Case Study investigates the effects of injecting hydrogen from wind generation sites across Great Britain (GB) on a typical winter day in 2035, with 28 hydrogen injection points placed at locations adjacent to wind power generation sites. The location of these sites were determined using the Future Energy Scenarios regional data produced by National Grid ESO [3]. The location of each injection point is shown in Figure 4.3. Like the Centralised Injection Case, the hourly injection rate corresponds to 20% of the volumetric gas-stream flow rate. At each injection node, the gas composition remains constant at 20% hydrogen and 80% natural gas.

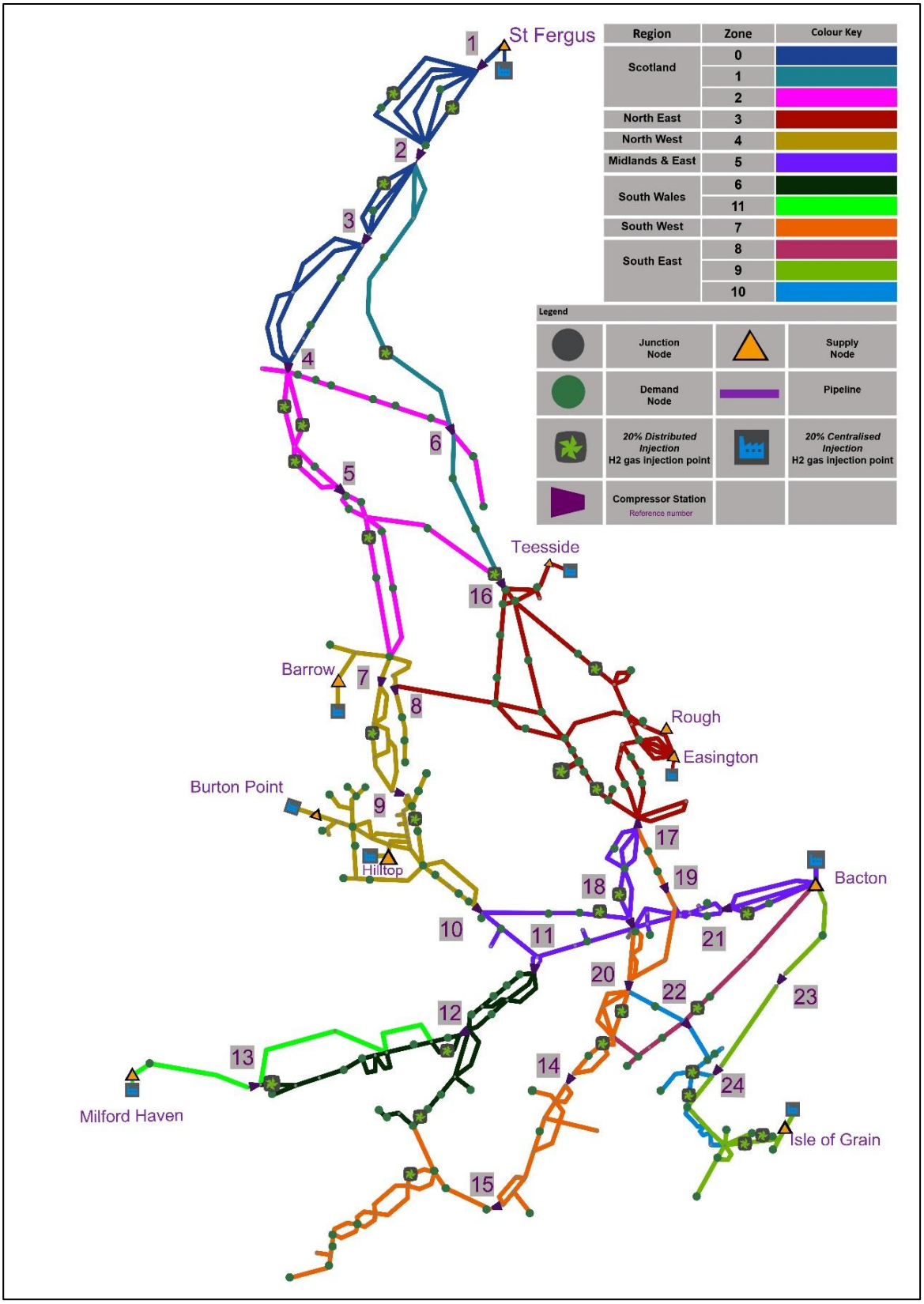

Figure 4.3.Map of high-pressure gas network model with markings for location of 20% Distributed Injection and 20% Centralised Injection.

Figure 4.4 shows how much hydrogen was injected in every region of the gas network in each case study. In 20% Centralised Injection, regions hosting large volume of natural gas supply, also host relatively large volume of hydrogen. In 20% Distributed Injection, the number of injection points is proportional to number of wind generation points.

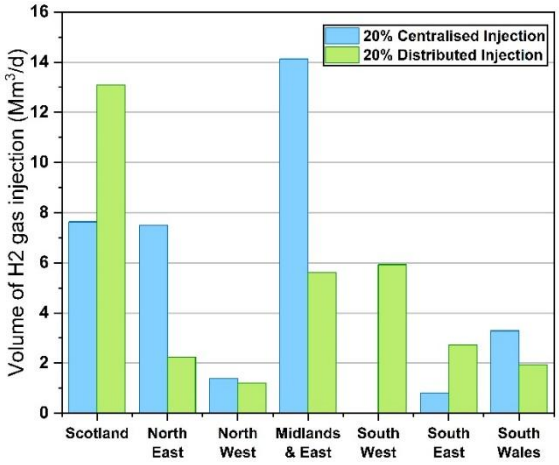

Figure 4.4. The volume of hydrogen injected into each region.

4.1.4. Case 4: 100% H_2

The 100% H_2 case represents a typical winter day in 2050 when the network only transports hydrogen. In total, 40 Mm^3 of the injected hydrogen is wind-generated, and 351.7 Mm^3 is blue hydrogen generated by methane reformation with CCS. The compressor settings are the same as in the 20% Distributed and 20% Centralised Injection cases because the gas flow direction is the same. In the 100% H_2 case, the compressor energy consumption is not limited to the existing compressor capacity. This was done to measure the extra energy required to compress pure hydrogen.

4.2. Results and discussion

4.2.1. Operation of the gas network with hydrogen

The results are divided into two sections: operation of the gas network and hydrogen composition across the network. The high-pressure gas network operation is investigated in three aspects: pressure levels, linepack levels and compressor energy consumption.

4.2.1.1. Pressure levels

Figure 4.5. plots the maximum pressures of supply points and extremities against their minimum pressures experienced during the 24-hour simulation. Here, extremities are the nodes at the far ends of the high-pressure network at a considerable distance from the supply points. The axes in Figure 4.5 have a data rug that shows how aggregated or dispersed the pressure levels are. The pressure points are colour-mapped, and their colour corresponds to the daily gas flow in each node.

In the Winter Model, St Fergus supply pressure is always at 40 bar-g. In the North East, Teesside has a range of 63–70 bar-g (7 bar-g range), and Easington 62–68 bar-g (6 bar-g range). In the Midlands & East, Bacton ranges from 58–65.3 bar-g (7.3 bar-g range). In the South East, Isle of Grain pressure varies from 55–57.5 bar-g (2.5 bar-g change). Finally, in South Wales, Milford Haven pressure varies between 50–52 bar-g (2 bar-g range).

In the 20% Centralised Injection, St Fergus pressure is always at 40 bar-g. In the North East, Teesside pressure varies between 66–67 bar-g (1 bar-g range). Easington varies between 63 –66 bar-g (3 bar-g range). In the Midlands & East, Bacton varies between 58.6–60 bar-g (1.4 bar-g range). In the South East, Isle of Grain varies between 62.5–67.5 bar-g (5 bar-g range). In South Wales, Milford Haven varies between 55–57.5 bar-g (2.5 bar-g range).

In the 20% Distributed Injection, St Fergus pressure is always at 40 bar-g. In the North East, Teesside pressure varies between 67.5–70 bar-g (2.5 bar-g range), and Easington between 65–67.5 bar-g (2.5 bar-g range). In the Midlands & East, Bacton has a pressure difference between 57.5–69 bar-g (11.5 bar-g range). In the South East, Isle of Grain pressure level varies between 65–69 bar-g (4 bar-g range). In South Wales, Milford Haven pressure level varies between 57.5–60 bar-g (2.5 bar-g range).

In the 100% H_2 case, St Fergus is always at 40 bar-g. In the North East, Teesside varies between 64–70.2 bar-g (6.2 bar-g range). Easington varies between 61.4–68 bar-g (7.4

bar-g range). In the South East, Isle of Grain has a pressure range between 56.5–68 bar-g (11.5 bar-g range). Finally, in South Wales, at Milford Haven, the pressure varies between 50 and 52 bar-g (2 bar-g range).

Figure 4.5 (a) shows that pressures in the Winter case are distributed with maximums ranging between 40–71.5 bar-g and minimums between 40–69.5 bar-g. Figure 4.3 (b) shows that in the 20% Centralised Injection case, the maximum pressures range between 40–68 bar-g, and the minimum pressures between 40–67.5 bar-g. Figure 4.3 (c) shows that the 20% Distributed Injection case also has a similar pressure range, with maximums between 40–70 bar-g and minimums between 40–68 bar-g. Figure 4.3 (d) shows that the 100% H_2 case has a similar pressure range, with maximums between 40–71 bar-g and minimums between 40–65 bar-g.

As the supply points have a constant flow rate, the variations in pressure levels at these points reflect variations in the region at which they are located. Here, St Fergus supply point is an exception to the rule, As the supply point is co-located with St Fergus compressor station, the pressure level at the supply point is controlled at 40bar-g by the compressor.

The rest of the supply points all have variable pressure levels, in all the case studies. Indicating that pressure levels are varying during the day in the regions. However, in both the Winter Case and 100% H_2 case, these variations are larger than the injection cases. Since the volumetric flow rate in the gas network is much larger in the Winter case and 100% H_2 case than in the injection cases, the larger flow rate causes larger variations in the pressure levels in the two case studies.

The pressure ranges include pressure levels of both supply nodes and extremities. Looking at the minimum and maximum pressure ranges, all the pressure levels are within the operational range. Introduction of hydrogen does not cause the network to violate these ranges.

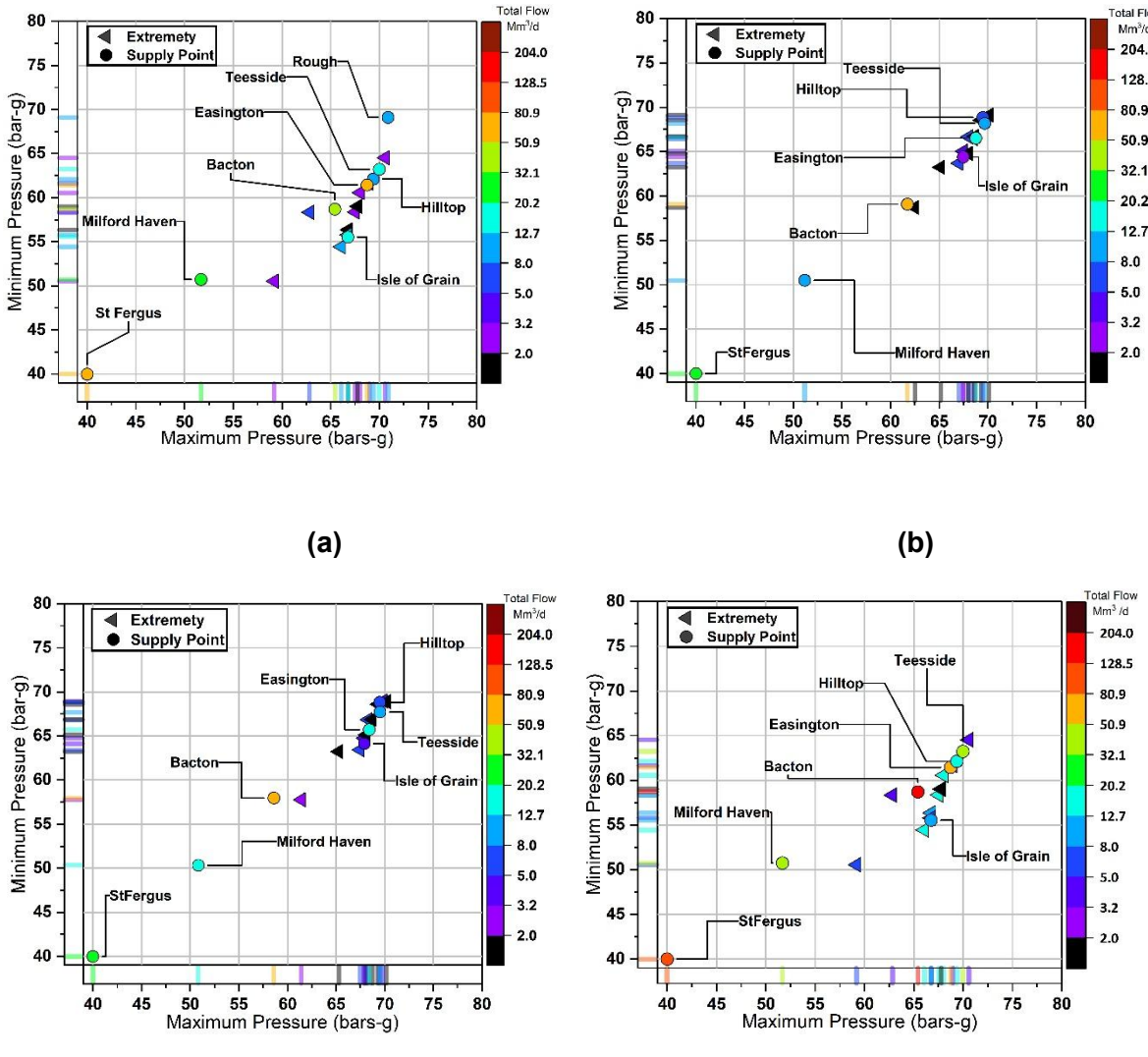

Figure 4.5. Comparison of maximum and minimum pressures of the extremities and supply points (a) in Winter Model, (b) in 20% Centralised Injection Case, (c) in 20% Distributed Injection Case and (d) in 100% H_2 Case.

The pressure dispersion differs across the four case studies. The Winter Model and 100% H_2 Case show more dispersed pressure levels than both the 20% Centralised and 20% Distributed Injection cases, as shown in Figure 4.5. To quantify this dispersion, the standard deviation of all pressure levels across all time steps was calculated and compared. The Winter Model and 100% H_2 Case each have a standard deviation of 5.67 bar-g, while the 20% Distributed and Centralised Injection cases have lower dispersions of 4.83 bar-g and 4.34 bar-g, respectively. This suggests that hydrogen blending—either centralised or distributed—leads to slightly more stable pressure conditions compared to the Winter and 100% H_2 cases.

The variation in pressure dispersion across nodes is related to the level of gas flow rates experienced during the 24-hour simulation. The colour-mapping of nodes in Figure 4.5 indicates that nodes with higher pressure variability generally correspond to higher volumetric flow rates. In the Winter Model and 100% H_2 Case, most nodes experience higher flowrates, with fewer than two extremities recording daily flow rates below 2 Mm³/d. In comparison, both injection cases contain seven such low-flow extremities, indicating lower regional throughput and pressure variation.

A similar pattern is observed at the supply points. The Winter Model includes two supply points with flow rates above 50.9 Mm³/d**,** and the 100% H_2 Case includes two supply points with flow rates above 128.5 Mm³/d**,** whereas the injection cases operate at lower flow levels. This comparison supports the relationship between flow magnitude and pressure variability.

This behaviour can be explained by the lower volumetric energy density of hydrogen. To meet the same energy demand, larger gas volumes are required, which leads to higher flow rates and corresponding pressure losses along the pipelines.

However, energy demand also differs between the case studies. The Winter Model represents 2018 demand, whereas the injection cases correspond to 2035 demand levels. As a result, the overall pressure drops in these cases remain comparable despite the differences in gas composition. Nevertheless, the minimum pressures recorded at each node in the 100% H_2 Case are lower than those in the injection cases, under the same assumed energy demand. This indicates that increasing hydrogen content, rather than energy demand alone, contributes to greater pressure variation.

Overall, the comparison shows that hydrogen injection—whether centralised or distributed—results in slightly smaller pressure variations than the Winter and 100% H_2 cases. Despite these differences, all cases remain within operational limits, and the network extremities do not experience notable pressure drops. Therefore, additional compression or pipeline reinforcement does not appear necessary, suggesting that the existing network can accommodate hydrogen injection without major modification.

4.2.1.2. Linepack levels

Figure 4.6 demonstrates the total network linepack for every simulation hour. Figure 4.6(a) shows linepack in energy terms and Figure 4.6(b) in volumetric terms.

As shown in Figure 4.6(a) the volumetric starting linepack of the Winter case, 20% Centralised Injection and 20% Distributed Injection cases are extremely similar, ranging between 346.9–

350Mm3. However, the volumetric starting linepack of 100% H_2 case is much lower than other cases, at 312Mm3.

Comparing the volumetric starting linepack of the Winter case with the 100% H_2 case, despite the rise in volumetric flows in the 100% H_2 case, the starting linepack has reduced. This demonstrates that demand and supply levels do not correlate with the starting level of the linepack in the network.

As seen in Figure 4.6(b), the starting linepack in energy terms is distinct from the volumetric starting linepack levels. The Winter case has a starting linepack level of 3865.2 GWh. Also, the 20% Centralised Injection and 20% Distributed Injection cases have similar starting linepack levels in energy terms, 3369 and 3431 GWh. The 100% H_2 case has the lowest starting linepack in energy terms, 997.3 GWh.

Figure 4.6(a) also shows that fluctuations of volumetric linepack levels in the 100% H_2 case are more significant than in the other cases. For example, from the hours 0 to 6, the volumetric linepack increased from 310.0 Mm^3 to 339.8 Mm3, a 29.8 Mm3 increase. In the NG 2018 case, the linepack rose from 346.9 to 366.3 Mm^3 during the same period, a 19.4 Mm^3 increase. Also, between the hours 14 to 23, the volumetric linepack in 100% H_2 case drop from 332.9 to 309.9 Mm^3, a 23 Mm^3 drop. In the same period, the NG 2018 case linepack dropped from 352.9 to 344.1 Mm^3, a 8.8 Mm^3 drop.

The initial linepack, the quantity of linepack at the beginning of the day, is determined by the network pressure. Changes in linepack during the day depend on the imbalance between gas supply and demand. Since hydrogen has approximately one-third the volumetric energy density of natural gas, an equivalent energy imbalance corresponds to a larger volumetric imbalance. This results in more pronounced fluctuations in linepack over the course of the day

Linepack plays a crucial role in gas network operations. It enables the network to meet demand when supply from entry points is insufficient. Furthermore, higher linepack levels allow for greater fluctuations in gas demand, a characteristic also known as gas network flexibility.

The results indicate that in a case study with 100% H_2, linepack drops significantly, which would, in turn, considerably reduce the network's flexibility in meeting unprecedented demand. However, the research also shows that the injection of hydrogen into the existing gas grid does not significantly affect overall linepack levels.

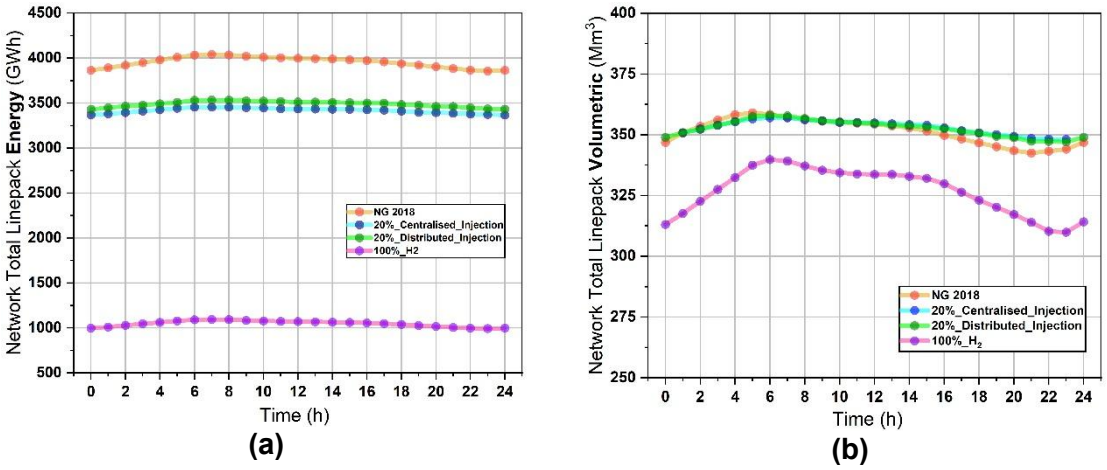

Figure 4.6. Linepack levels in four case studies during 24 hours of simulation (a) in energy terms (GWh) and (b) in volumetric terms Mm^3.

Linepack in different regions

Figure 4.7shows the regional linepack across all case studies. Looking at the regional linepack, all regions follow a similar trend. The Winter Case has the highest linepack level, followed by the 20% Centralised and 20% Distributed Injection cases, which have levels of linepack between 0.83–0.94 of the Base case. And finally, 100% H_2 case with linepack levels between 0.23–0.29 of the Base Case.

South Wales and Midlands & East are the only regions with a linepack level higher in the 20% Distributed Injection compared with 20% Centralised Injection. Amongst the two, South Wales has a higher linepack level in the 20% Distributed Injection, up to 23% higher than the 20% Centralised Injection case. This is due to the large number of hydrogen injection points in the region in the 20% distributed injection case.

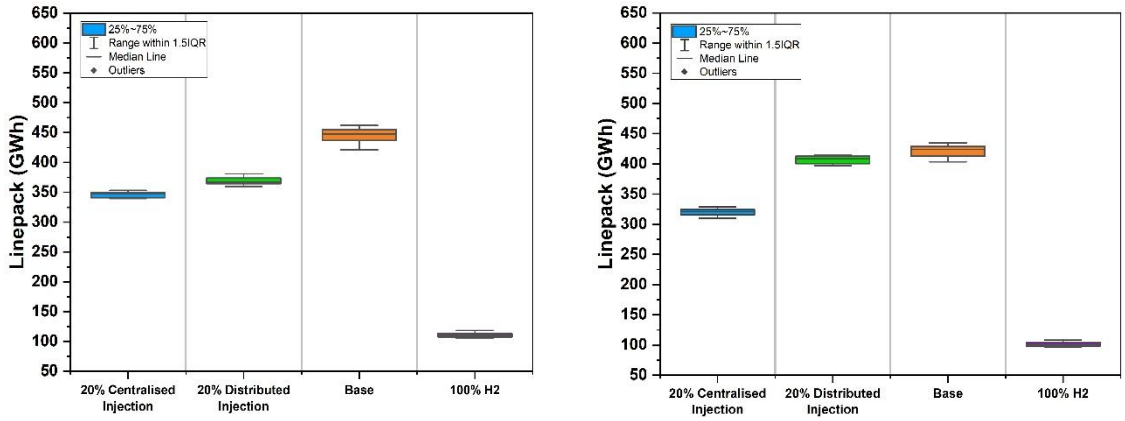

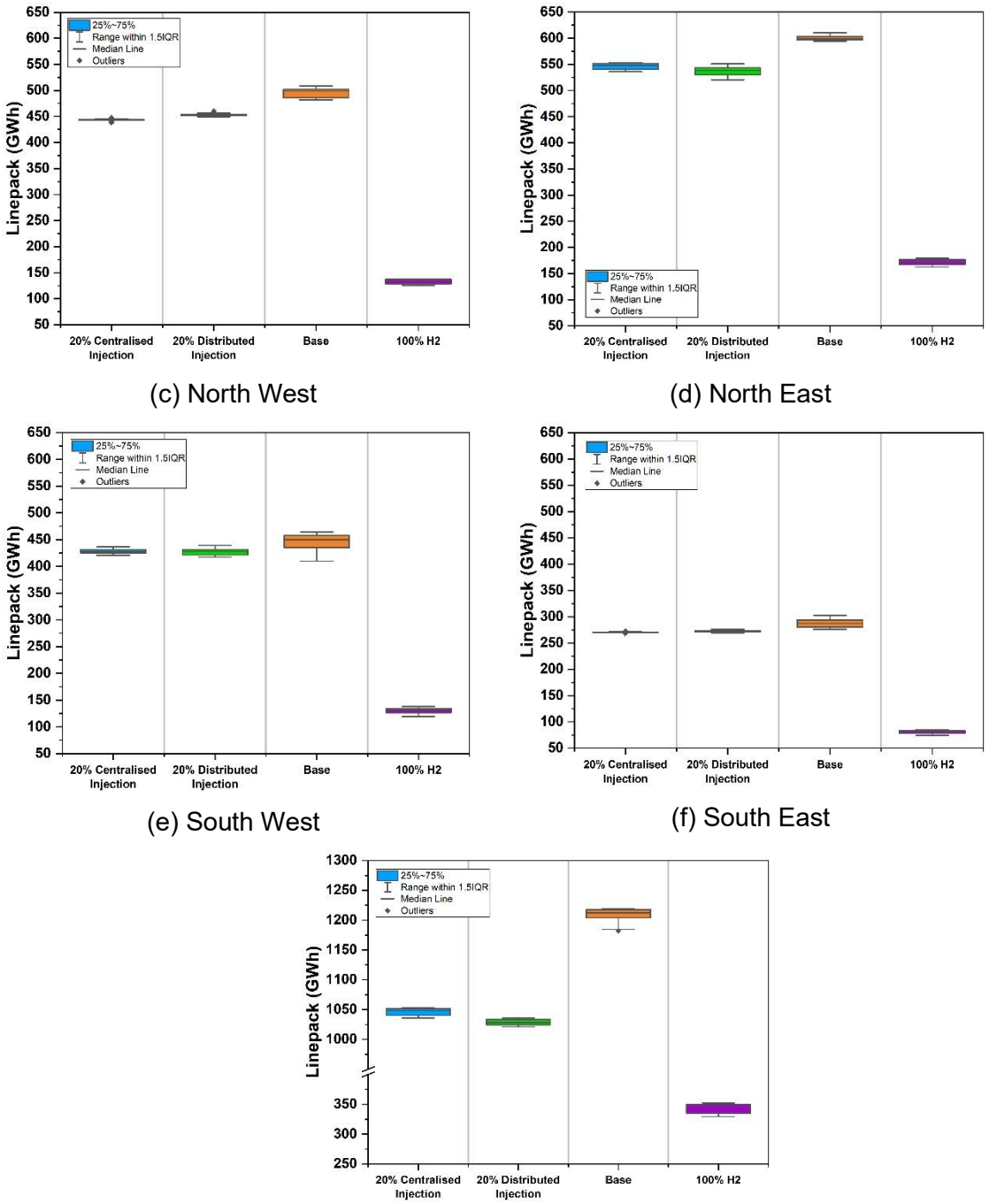

(c) North West

(d) North East

(e) South West

(f) South East

(g) Scotland

Figure 4.7. Regional linepack in GWh.

4.2.1.3. Compressor Operation

Figure 4.8. Compressor energy consumption and average utilisation (a) in the Winter Case and (b) in 20% Centralised Injection (c) 20% Distributed Injection and (d) in 100% H2 case.

Compressor stations in the model are characterised by their maximum energy capacity and maximum outlet pressure limit. All compressors operate with a minimum inlet pressure of 40 bar-g.

The figure demonstrates three attributes that vary with introduction of hydrogen: 1) The X-axis presents the percentage of average utilisation of each compressor. 2)The Y-axis shows the total energy consumption of each compressor for 24 hours. 3) The colourmap shows the total volume of gas compressed by each compressor for 24 hours.

The compressor energy consumption depends on the volume of compressed gas and the compression ratio achieved. With increasing hydrogen content of the gas mixture in the network, the energy density of the gas mixture decreases, meaning that a larger gas volume must be transported to deliver the same amount of energy. Consequently, higher volumetric flow rates are expected to be handled by the compressor stations. As a result, the energy consumption of compressor stations varies in response to changes in the hydrogen concentration within the network.

To better understand the operation of compressor stations, the results have been described and discussed by region. For every region, first the energy consumed by compressor was reported along with the total volume of gas it compressed. Then, the average utilisation of compressors was discussed. And finally, the reported results were analysed.

Scotland

In the Winter Case, compressor stations in Scotland exhibit the highest combined energy consumption, exceeding 2,562 MWh during the day. Four compressor stations are active in this case study: Aberdeen (1,085 MWh for compressing 74 Mm^3), Avonbridge (481 MWh for compressing 47 Mm^3), St Fergus (875 MWh for compressing 77.1 Mm^3), and Wooler (121 MWh for compressing 22.4 Mm^3).

In the 20% Centralised Injection case study, total energy consumption in Scotland decreases significantly to 612 MWh, with only two active compressor stations: Aberdeen (494 MWh for 35 Mm^3) and St Fergus (119 MWh for compressing 29 Mm^3).

In the 20% Distributed Injection case study, the total energy consumption remains similar at 598 MWh, again with two active stations: Aberdeen (462 MWh for compressing 31.5 Mm^3) and St Fergus (137 MWh for compressing 29.4 Mm^3).

In the 100% H_2 case study, energy consumption increases substantially to 2,502 MWh, although only two compressor stations are operational. Aberdeen (1,085 MWh for compressing 110 Mm^3), and St Fergus (1,418 MWh for compressing 105 Mm^3).

Regarding utilisation, in the Winter Case, St Fergus, Aberdeen, and Avonbridge exhibit high average utilisation levels of 87%, 81%, and 50%, respectively. Wooler, however, shows a low utilisation of only 9.5%. In the 20% Centralised Injection case study, the utilisation of Aberdeen and St Fergus is low, at 35% and 10%, respectively. These values remain the same in the 20% Distributed Injection case. In the 100% H_2 case, St Fergus operates at full capacity (100% utilisation), while Aberdeen shows a utilisation of 75%.

The Winter Case represents the gas network as it operated in 2018, when Scotland experienced a high gas flow rate, primarily due to the St Fergus supply point connected to the UK Continental Shelf. The other case studies reflect conditions projected for 2035 and 2050, when the Continental Shelf is expected to play a less prominent role.

Midlands & East

In all cases, the Midlands & East region has a single compressor station: Kings Lynn. In the Winter Case, Kings Lynn has an energy consumption of 145.4 MWh for compressing 29 Mm^3 of gas. In the 20% Centralised Injection case, energy consumption increases to 529 MWh for compressing 69 Mm^3 of gas. In the 20% Distributed Injection case, Kings Lynn shows a similar energy consumption of 517 MWh for compressing 64 Mm^3 of gas. And finally, In the 100% H_2 case, energy consumption spikes to 1,722 MWh for compressing 192.2 Mm^3 of gas.

In the Winter Case, Kings Lynn operates at a utilisation level of 25%. In the 20% Centralised Injection case study, utilisation increases to 85%, and in the 20% Distributed Injection case, it rises to 84%. In the 100% H_2 case, utilisation increases drastically to 262.5%, significantly exceeding the currently installed compression capacity.

In the 2035 and 2050 case studies, as the UK Continental Shelf in Scotland becomes less dominant, the Midlands & East region emerges as the primary source of gas supply to the rest of the network. The region hosts the Bacton supply point, which imports gas from continental Europe. Consequently, Kings Lynn, being the compressor station located near Bacton, is heavily utilised.

North East

The North East region has only one compressor station: Hatton, which consumes 392 MWh of energy to compress 57.4 Mm^3 of gas. In all other case studies, no compressor station operates in this region.

In the Winter Case, Hatton operates at an average utilisation of 28%. During the Winter Case, a significant volume of gas must be transferred from the North East to neighbouring regions. The Hatton compressor facilitates this by generating a pressure difference between

the North East and the Midlands & East regions. In the other case study, however, the Midlands & East region becomes the primary gas supplier, making the operation of Hatton unnecessary.

North West

In the Winter Case, the region has a total energy consumption of 510.6 MWh. Two compressor stations are active: Nether Kellet, with 96.5 MWh for compressing 11 Mm^3 of gas, and Carnforth, with 414 MWh for compressing 38 Mm^3.

In the other case studies, the only active compressor station in the region is Alrewas. In the 20% Centralised Injection case study, Alrewas consumes 283.7 MWh of energy to compress 30.7 Mm^3 of gas. In the 20% Distributed Injection case study, energy consumption at Alrewas is 189.9 MWh for 27.1 Mm^3. In the 100% H_2 case, Alrewas consumes 640.5 MWh to compress 65.3 Mm^3 of gas.

In the Winter Case, Carnforth operates at an average utilisation of 30%, and Nether Kellet at 15%. In the 20% Centralised Injection case study, Alrewas shows a utilisation of 48%. In the 20% Distributed Injection case study, its utilisation is 32%. In the 100% H_2 case, utilisation at Alrewas rises to 104%, exceeding the installed compression capacity.

In the Winter Case, the high gas flow from Scotland necessitates the operation of Carnforth and Nether Kellet to facilitate transmission. In the other case studies, Alrewas creates a pressure difference that supports the flow of gas from the Midlands & East to the North West.

South East

The only active compressor in the South East region is Diss. In the Winter Case, Diss consumes 102.5 MWh to compress 15.2 Mm^3 of gas. In the 20% Centralised Injection case study, energy consumption is 95.8 MWh for 14.1 Mm^3 of gas. In the 20% Distributed Injection case study, Diss consumes 79.3 MWh for 11.9 Mm^3. In the 100% H_2 case, energy consumption increases to 281 MWh for 41 Mm^3 of gas.

In terms of utilisation, Diss operates at 11% in the Winter Case. This increases slightly to 15% in the 20% Centralised Injection case, and to 12% in the 20% Distributed Injection case. In the 100% H_2 case, Diss shows a utilisation of 48%.

The Diss compressor creates a pressure difference that facilitates gas flow from the Midlands & East to the South East. Despite the increased supply from the Bacton entry point in the Midlands & East in the injection cases, flow through the Diss compressor decreases. This is due to the South East having two parallel pipeline branches, with Diss located on only

one of them. As a result, the increased flow from the Midlands & East does not directly translate into higher flow levels through the Diss compressor.

South West

In the Winter Case, no compressor station is active in the South West region. In both the 20% Centralised Injection and 20% Distributed Injection cases, the Huntington compressor is operational. In the 20% Centralised Injection case, Huntington consumes 284.4 MWh to compress 57.4 Mm³ of gas. In the 20% Distributed Injection case, it consumes 210 MWh to compress 52.1 Mm³.

In the 100% H_2 case, two compressor stations are active: Huntington and Lockerley. Huntington consumes 930 MWh to compress 155 Mm³ of gas, while Lockerley consumes 152 MWh for 29.2 Mm³.

In terms of utilisation, the Huntington compressor operates at 50% in the 20% Centralised Injection case and 40% in the 20% Distributed Injection case. In the 100% H_2 case, its utilisation rises significantly to 150%, exceeding the current installed compression capacity. Lockerley, which is only active in the 100% H_2 case study, operates at an average utilisation of 36%.

South Wales

In the 100% H_2 case, compression in South Wales is required to support gas flow from the Milford Haven supply point to the rest of the region. In this case, the Felindre compressor consumes 120.4 MWh of energy to compress 32.8 Mm³ of gas.

In the 100% H_2 case, the Felindre compressor operates at an average utilisation of 12.5%. In all other cases, the South Wales network maintains adequate pressure levels without the need for compression.

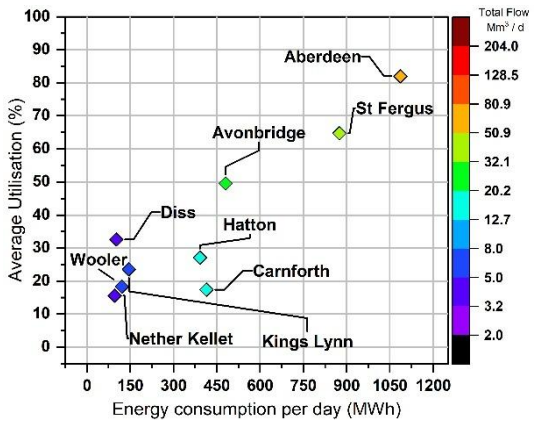

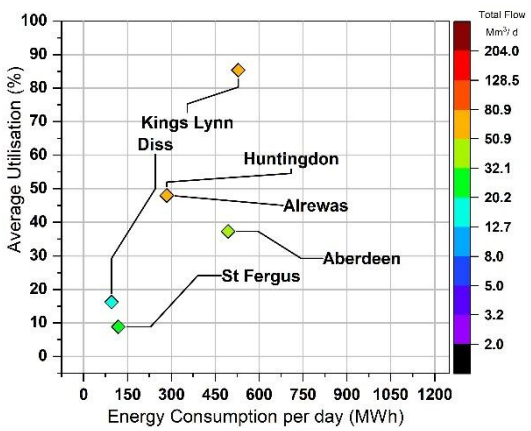

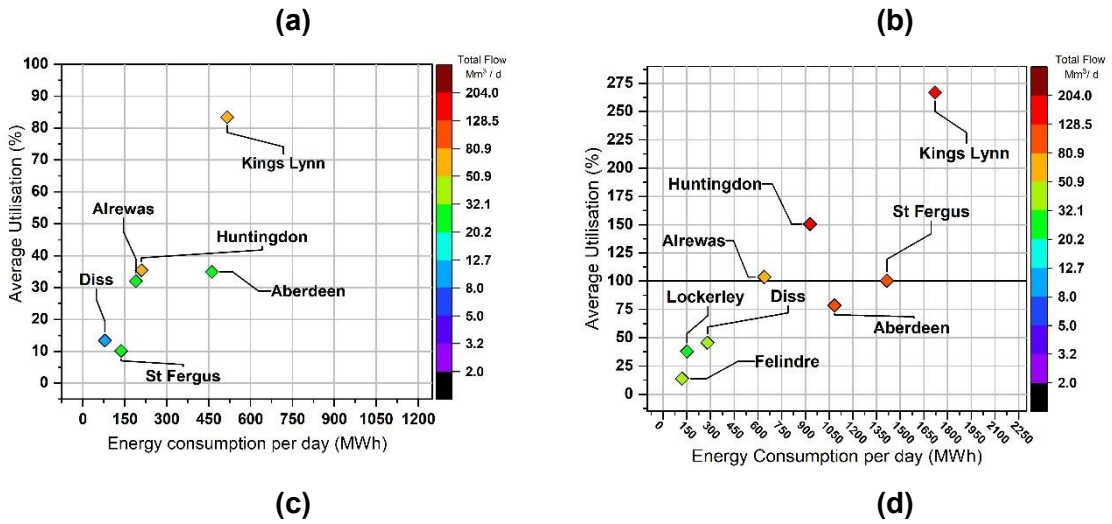

Figure 4.8. Compressor energy consumption and average utilisation (a) in the Winter Case and (b) in 20% Centralised Injection (c) 20% Distributed Injection and (d) in 100% H_2 case.

Total compressor-station energy consumption varies significantly across the four case studies due to changes in where gas enters the system, flow directions, and gas composition. The Winter Case exhibits the highest overall energy use, driven by substantial north–south transmission from the St Fergus supply point and the corresponding need for multiple stations—particularly in Scotland and the North West—to maintain pressure across the network. In contrast, both the 20% Centralised Injection and 20% Distributed Injection case studies show a much lower need for compression overall. This reflects the diminishing role of the UK Continental Shelf by 2035 and the increased reliance on supply from the Midlands & East region, where Bacton becomes the principal entry point; as a result, only a limited number of compressors operate, and at comparatively low utilisation levels.

In the 100% H_2 case, total energy consumption rises sharply, exceeding or approaching Winter Case levels in several regions despite fewer active stations. This increase stems from hydrogen's lower density and the consequent need for higher compression to sustain adequate transmission pressures, particularly in Scotland, the Midlands & East, the North West, and the South West. In addition, regions such as South Wales—which require no compression in the other scenarios—need compressor operation in order to support hydrogen flows from Milford Haven. Overall, while partial hydrogen blending greatly lowers the total amount of compression required, a fully hydrogen-based transmission network leads to much higher energy use and would require more compression capability than is currently installed.

4.2.2. Hydrogen content at different nodes of the gas network

4.2.2.1. Hydrogen content at the national level

Figure 4.9 is a population diagram demonstrating the Hydrogen content of all network nodes in both 20% Centralised and Distributed Injection cases at time step t=8 h; the horizontal axis shows the percentage of the nodes with the same range of volumetric percentage of hydrogen. This graph excludes the nodes where Hydrogen is injected into the gas network. Time step t=8 was chosen because the peak demand of the network occurs at this time step. This figure demonstrates that 20% Centralised Injection is more successful in keeping hydrogen in the network below 25% volumetric compared to the 20% Distributed Injection case. Moreover, in 20% Centralised Injection, 90% of nodes have a hydrogen content between 20–25 %. In the 20% Distributed Injection case, the hydrogen content varies from 0 to 60% volumetric range. The largest group of nodes have a hydrogen content between 10–15% volumetric; however, this group only comprises 25% of all nodes.

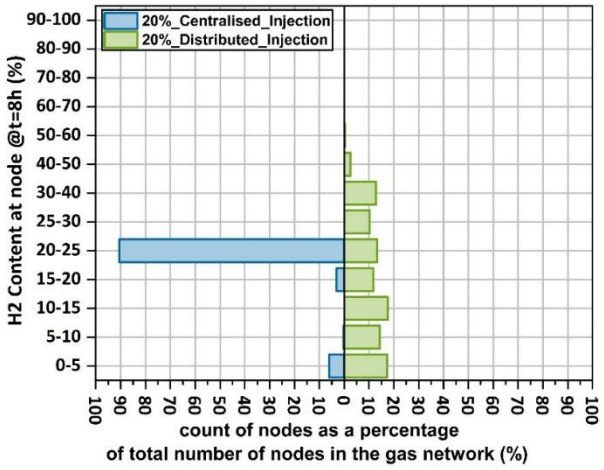

Figure 4.9.Population diagram of volumetric percentage (%) of hzdrogen at nodes of the gas network.

4.2.2.2. Hydrogen content of every region of GB

Figure 4.10 demonstrates that under 20% Centralised Injection, the hydrogen content in most nodes is consistent throughout the 24 hours and close to 20% volumetric, with few nodes with zero hydrogen content.

Figure 4.10 demonstrates the hydrogen content under the 20% Distributed Injection case. The hydrogen content during the 24 hours of simulation is different from the previous case. In addition, the y-axis on the right-hand side measures the standard deviation of hydrogen content in every region.

As the figures depict, 20% Centralised Injection has a non-varying hydrogen content, while 20% Distributed Injection leads to a varying hydrogen content, both in different regions of gas network, and in different time-steps.

In both injection cases, the volume of gas injected was set at 20% of the volumetric flow of gas at the injection point at all time steps. The total daily volume of hydrogen injected is the same in both case studies. What differentiates the two case studies is the location of hydrogen injection. In the 20% Centralised Injection, injection sites are located near natural gas supply points, while in the 20% Distributed Injection, the injection sites are co-located with wind generation sites across GB.

This difference in location causes two other key differences between the cases.

One) In both injections, hydrogen is always kept at 20% volumetric of flow at the site. In 20% Centralised Injection, all injection sites are close to natural gas supply points, meaning that the gas prior to reaching the injection site has zero hydrogen content. In 20% Distributed Injection, the locations are within the gas network and much further away from natural gas supply points. Here, the 20% volumetric cap, ensures no excess gas is injected at that site. It however cannot monitor the hydrogen already existing in the gas stream from the previous injections. Therefore, the hydrogen content exceeds the 20% volumetric limit. The cascading effect causes varying hydrogen content at different locations of the gas network.

Two) To ensure gas is always at 20% volumetric at the site of injection, the volume of gas injected is varying according to the flow of gas stream at that location. In 20% Centralised Injection, the flow of gas prior injection is constant at every time step, because natural gas supply point has a constant flow rate during the day. In 20% Distributed Injection, as the injection site is located within the network, the flow is varying at every time step. This combined with the effect explained above, causes temporal variations in hydrogen content in the gas network.

The only other parameter that could have an impact was the variations in pressure levels. If that was the case however, as pressure levels are varying in 20% Centralised Injection, the hydrogen content should have also varied. That however is not the case.

To better understand the extent of these variations in Figure 4.11 three arbitrary characteristics need to be discussed for every region: 1) largest variation of hydrogen content over time; 2) technical hydrogen limit violation, which is the ratio of nodes in each region with

hydrogen content above the technical operational limit (20% volumetric); and 3) homogeneity of gas composition, which is the standard deviation of hydrogen content in every region.

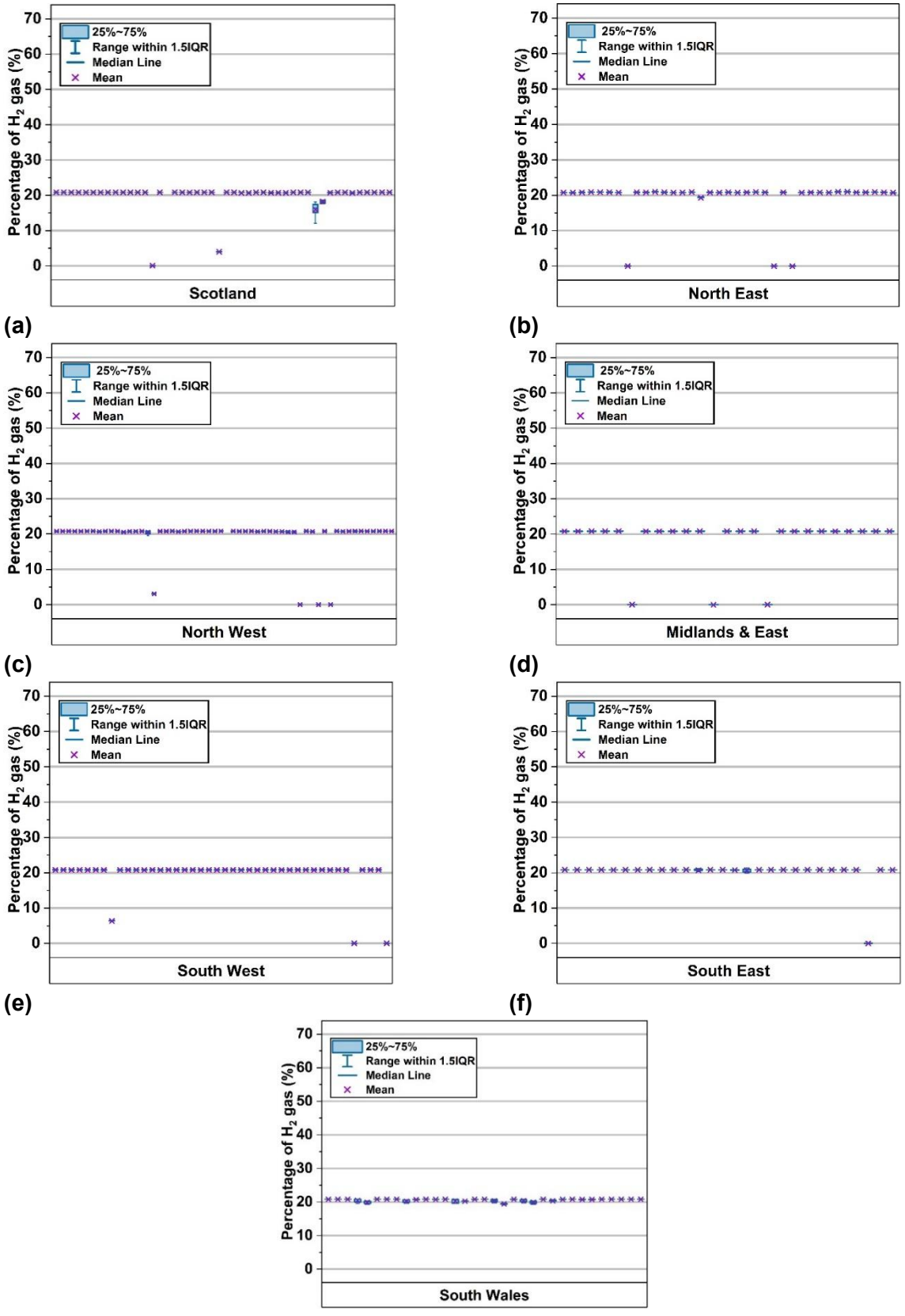

(g)

Figure 4.10. Hydrogen content at each node at each time step of the simulation in the 20% Centralised Injection case.

4.2.2.3. Largest variation of Hydrogen content over time

All regions host nodes with varying hydrogen content over time. In addition, most nodes in these regions have variable hydrogen content, as evident in Figure 4.11. The largest variation occurs in a node located in South Wales. Over the 24 hours of simulation, the hydrogen content in this node varies by 28% volumetric.

The variations in four other regions are also high. The Southwest region hosts nodes with up to 18% volumetric variations in hydrogen content, followed by the Southeast region, where a node has a variation of up to 14.7% volumetric. Scotland also hosts a node with a hydrogen content variation of up to 11%. Finally, the Northwest hosts a node with a hydrogen content variation of up to 7%. In these regions, the large variations are caused by the geographical location of hydrogen injection points. Furthermore, since the hydrogen injection points are distant from the natural gas supply points, the flow rate of the natural gas supply and hydrogen injection do not match every time step, causing variations.

Two regions have small variations; The largest hydrogen content variation in nodes located Midlands & East region is only 4% volumetric. In addition, the largest hydrogen content variation in nodes located in Northeast region is only 4.9% volumetric. In the Midlands and East region, variations are small because injection points are geographically located close to supply points in the region. In the Northeast region, however, variations are even smaller because there is no functioning compressor during the simulation and most of the injection points are also geographically close to natural gas supply points.

Under 20% Distributed injection, hydrogen content varies in all regions during the 24 hours and at different rates. Power stations are the most sensitive consumers to variation in hydrogen content in the gas. Industrial consumers, and households can tolerate variations in hydrogen content in the gas, however it is increasingly difficult to bill their gas consumption. This is since, the gas consumption is billed according to volume of gas delivered to the consumer, and not the energy content delivered. None of such variations exist under 20% Centralised Injection.

4.2.2.4. Technical hydrogen limit violation

In the Southwest and Northeast regions, over 50% of the nodes have hydrogen content above 20% volumetric. Over-limit nodes are also high in Scotland, taking up 42% of the nodes.

Three regions have small violations: only 12.5% of nodes in the Northwest are above 20% volumetric, while the Southeast region and the Midlands and East region both have no violations.

The regions with large violations have hydrogen injection points located in pipelines far away from supply terminals. This resulted in hydrogen oversupply in some branches, while also causing hydrogen undersupply in others. In addition, the regions in the second category have a total oversupply of hydrogen due to the many hydrogen injection points in these regions. On the other hand, there is a total undersupply of hydrogen in Northwest, Southeast, and Midlands and East regions due to the lack of hydrogen injection points in these regions.

Under 20% distributed injection, the technical limit for hydrogen content is significantly violated. This has consequences for both the network and gas consumers.

The gas network can operate safely only when the hydrogen content remains below 20% by volume. Exceeding this threshold increases the risk of embrittlement in steel pipelines and compressor stations with steel impellers and is therefore prohibited under current HSE regulations. Similarly, domestic gas appliances are designed to handle hydrogen concentrations of up to 20% by volume. The findings suggest that, in most regions, the gas network cannot safely support domestic use due to elevated hydrogen levels.

4.2.2.5. Homogeneity of gas composition

The other important characteristic is the homogeneity of hydrogen content in each region. This is different from the previous characteristics because it measures level of similarity the hydrogen content across nodes of each region and it disregards how high or low the overall hydrogen content is. Furthermore, the regional homogeneity is measured with each region's standard deviation of hydrogen content.

South Wales has the highest standard deviation of 15.6 %. This high standard deviation is caused by both high node variations and many nodes with zero hydrogen content. Northeast, Northwest, Scotland, Southeast, and Southwest regions have standard deviations between 7–12.5%. Like South Wales, these regions do not have homogeneous gas content; however, since they have fewer nodes with zero hydrogen content, their standard deviation decreases substantially.

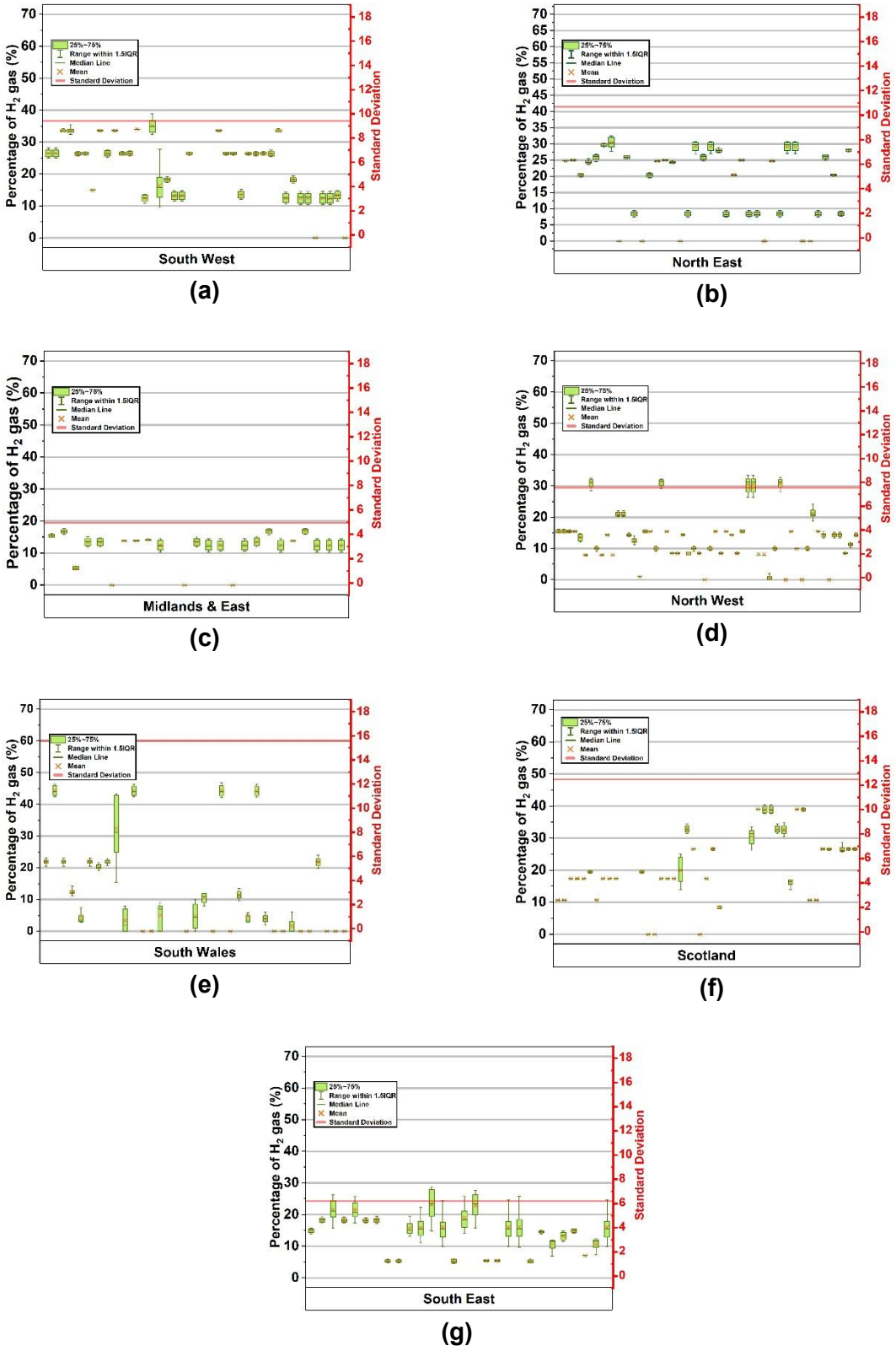

Figure 4.11. Hydrogen content at each node at each time step of the simulation under the 20% Distributed Injection case.

The Midlands & East region has the lowest standard deviation of 4.5 %. Therefore, it can be argued that only Midlands & East region has a gas composition that can be described

as homogeneous. This is because Midlands & East region hosts the Bacton supply terminal, which has the largest natural gas supply gas. This abundance of natural gas supply and presence of hydrogen injection points close to Bacton supply point resulted in a low standard deviation of hydrogen content.

The homogeneity of hydrogen in a region is only related to the proximity of hydrogen injection point to a supply terminal or the primary location of the gas supply to the region. Regions with low standard deviation, such as the Midlands & East region, have hydrogen injection points close to the Bacton supply point, while in the other regions, some of hydrogen injection points are located on pipelines away from the main supply point.

The homogeneity metric measures how evenly hydrogen is distributed across a region. It reveals that hydrogen levels are not only high but also vary from node to node, meaning the network delivers gas with different energy content to consumers within the same area.

4.3. Conclusions

Since the GB high-pressure gas network operator uses the gas network for hydrogen transmission, the observations from this research bring insight into how the gas network can operate. These observations can be summarised as follows:

- The case studies demonstrated that the high-pressure gas network at its existing stage could host 20% volumetric hydrogen without compromising operating pressure levels and compressor energy consumption, regardless of the mode of hydrogen injection. Linepack levels are also not significantly affected by the presence of 20% volumetric hydrogen; this was the same for both injection case studies.
- The mode of hydrogen injection into the grid significantly affects the levels of hydrogen at each node of the network. In the 20% Centralised Injection case, the daily rate of hydrogen injection at each node was volumetrically proportional to natural gas entering the network from the related supply node and the daily rate was set at 20% volumetric. This centralised injection of hydrogen, led to a homogenous mix of hydrogen and natural gas across the network. This was not the case in 20% Distributed Injection, and hydrogen was proportional to the generation capacity of windfarms corresponding to the location of hydrogen injection. This distributed injection of hydrogen led to a nonhomogeneous mix of hydrogen and natural gas across the network.
- For 100% hydrogen transmission, pressure levels can be kept as same as the existing levels. However, to transport 100% hydrogen, a significantly large compressor energy consumption will be required, up to 3.9 times that of typical levels in the existing

network. By keeping the pressure levels the same as existing levels, linepack levels will drop to a quarter of the existing linepack levels. This means that the network will have much lower within-day flexibility than today.

This research can be further developed by finding accurate means of simulating hydrogen injection into the high-pressure grid, especially the hydrogen generated from intermittent and variable sources such as wind and solar.

Furthermore, by developing a real-time simulation method that monitors gas flow in every time step, the hydrogen content in the network can be actively measured and the volume of hydrogen injected could be adjusted accordingly. Here, real-time means the time when the simulation is running.

The key improvement to the simulation is that the gas composition should be monitored and the volumetric injection rate adjusted at every timestep. At each timestep, the simulation pauses so that gas compositions can be recalculated, and injection rates adjusted. The simulation then resumes for the next timestep, and this process repeats until the end of the simulation. To perform such a process, Synergi Gas must be coupled with a scripting interface that automates these iterations. Because this procedure is computationally intensive, it should be executed on a high-performance computer.

Since linepack levels in the 100% H_2 case are significantly lower than existing levels, the gas network's within-day flexibility will be compromised. Therefore, it is crucial to know how the gas network's resilience to external events will be compromised when transporting 100% hydrogen. It is also crucial to understand how the network's reliability will be compromised when facing system failures (i.e., internal events).

A question that may arise is whether these conclusions have been found elsewhere. In the public domain, results describing the impact of hydrogen injection on high-pressure gas networks are relatively new. National Gas has previously undertaken studies on this topic but has only disclosed limited details — for example, brief mentions in its Future Operability Planning[94] — suggesting that much of its analysis has been conducted privately. Publicly, the company’s focus has been on demonstrating that the transmission network can operate safely with hydrogen blends of up to 20%.[98] The FutureGrid project is designed to prove the safety and performance of hydrogen blends within high-pressure gas transmission assets[25], while the 2025 Hydrogen Acceptability Study**,** commissioned by National Gas, found that blending up to around 20% hydrogen by volume into the natural gas network is technically feasible for most industrial users, provided some equipment and safety modifications are

made. Therefore, the findings of this chapter remain novel from both an academic and industrial perspective[95][99]

Chapter 5. Deblending hydrogen and natural gas in the high-pressure gas network

This chapter attempts to answer three research questions:

1. If the National Gas NTS incorporates deblending technology for delivering modified concentrations of hydrogen and natural gas to consumers, what is the energy consumption of the gas network with multiple deblending facilities?
2. Since deblending stations are sensitive to hydrogen concentration and the volumetric flow rate at the inlet, how do seasonal variations in NTS operation affect the energy consumption of deblending facilities?
3. Do the deblending customers' requirements, such as a specific quality of gas or the volume of gas, affect the operation of the deblending site?

Two case studies were designed to investigate these points. The combination of compressors operating, the flow levels, and the flow directions in the network will be different in the two cases. This difference allows the deblending sites to be studied in two contrasting cases:

- Winter Deblending case study, which simulates the NTS on a winter day in the year 2035.
- Summer Deblending case study, which simulates the NTS on a summer day in the year 2035.

The case studies are assumed to be in the year 2025 because it is estimated that there will be enough hydrogen produced in GB to be injected into the grid[96]. Furthermore, it is assumed that hydrogen is injected at a 20% volumetric rate at a point co-located with wind farms across the GB. Both case studies investigate the same use cases of deblending technology in the NTS. These use cases are:

Deblending could realise two fundamental requirements for domestic consumption of hydrogen: Firstly, by fixing the hydrogen content at 20% volumetric, it satisfies the boundary declared by the HSE, which states that hydrogen in gas consumed in a domestic setting should be less than 23% volumetric[20]. Secondly, fixing the hydrogen content at 20% volumetric enables accurate billing of domestic gas consumers based on the volume of gas consumed.

Industrial consumers who require pure hydrogen could utilise blending technology to withdraw hydrogen directly from the high-pressure gas network. In Steel production, to produce carbon-neutral steel, direct reduced Iron (DRI) is produced by reducing iron ore using pure hydrogen as a reducing agent. [21]. In Ammonia production, pure hydrogen is mixed with N_2 gas to react under high temperatures. [22].

For now, CCGT power stations can only operate safely with a hydrogen content of less than 1% volumetric. Therefore, Deblending technology could be a necessary part, ensuring that the high-pressure gas network and CCGTs stay connected after hydrogen injection into the grid.[26]

Although there is no defined industry strategy for deblending, the motivation for investigating the technology is clear. National Gas aims to ensure that all existing gas consumers can continue to be supplied following the introduction of hydrogen blends into the grid

Figure 5.1depicts three types of gas consumers and their requirements:

1. deblending for power stations, which provides natural gas with no hydrogen.
2. deblending for industrial sites, which provides pure hydrogen.
3. deblending for LDZ sites, which provides natural gas with a fixed 20% hydrogen volumetric rate.

The choice of which LDZ, industrial site, or power station node, is dictated by the pre-requisite criteria. These are criteria for running a physically feasible simulation.

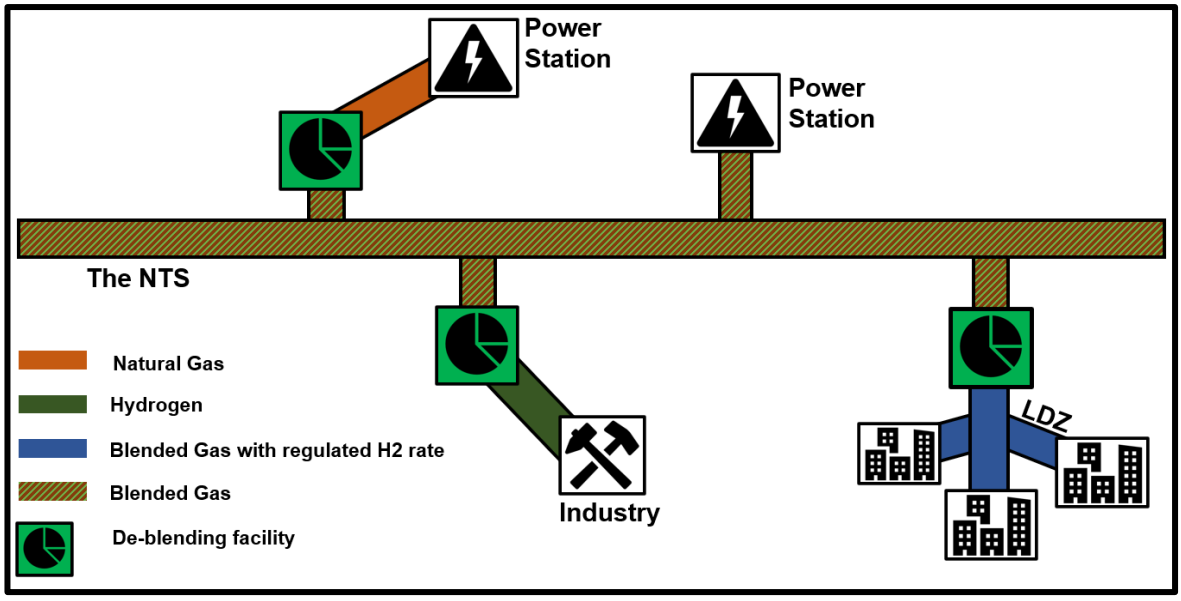

Figure 5.1. Schematic of the GB gas network utilising deblending facilities.

5.1. Methodology

This study is conducted in two parts. The first part is the simulation study, as seen in Figure 5.2, in which Synergi Gas software is used to model gas networks operating with deblending sites. The second part is a post-simulation analysis, which is conducted using Microsoft Excel 2022.

5.1.1. Simulation process

The study process uses the following steps:

1. Adjust daily demand of nodes in the model: In this step, demand levels of The Winter Model were multiplied by 0.58, projecting demand for each node on a winter's day in 2035. For projecting demand for the summer day, demand levels for The Summer Model were multiplied by 0.44. Both conversion factors are taken from National Gas's 10-year statement[97].
2. Adjust daily supply of nodes in the model. This process is the same as the first step, and the conversion factors are also the same.
3. Adjust compressor station combination: Since demand and supply of gas is much lower in 2035 than 2018, some of the compressors used in the Winter Model may not be of use. Therefore, the combination of compressors used were changed. The same is done for the Summer Model.
4. Adjust the compressor station setups:
    a. Adjust the compressor station's set pressure to support lower flow levels.

b. Adjust the compressor station's control model to support lower flow levels.

5. Set hydrogen injection volume at each injection site: hydrogen injection at each of the busbars was capped not to exceed 20% of gas mix at the point of injection.
6. Select deblending site: Deblending sites were chosen based on pre-requisite criteria. These criteria are explained in Section 5.1.2.
7. Run a daily steady-state simulation with a single time step.
8. Check if the operation of deblending sites still observes the pre-requisite criteria, as explained in Section 5.1.2. If not, go back to step six. If so, save the modelling results.

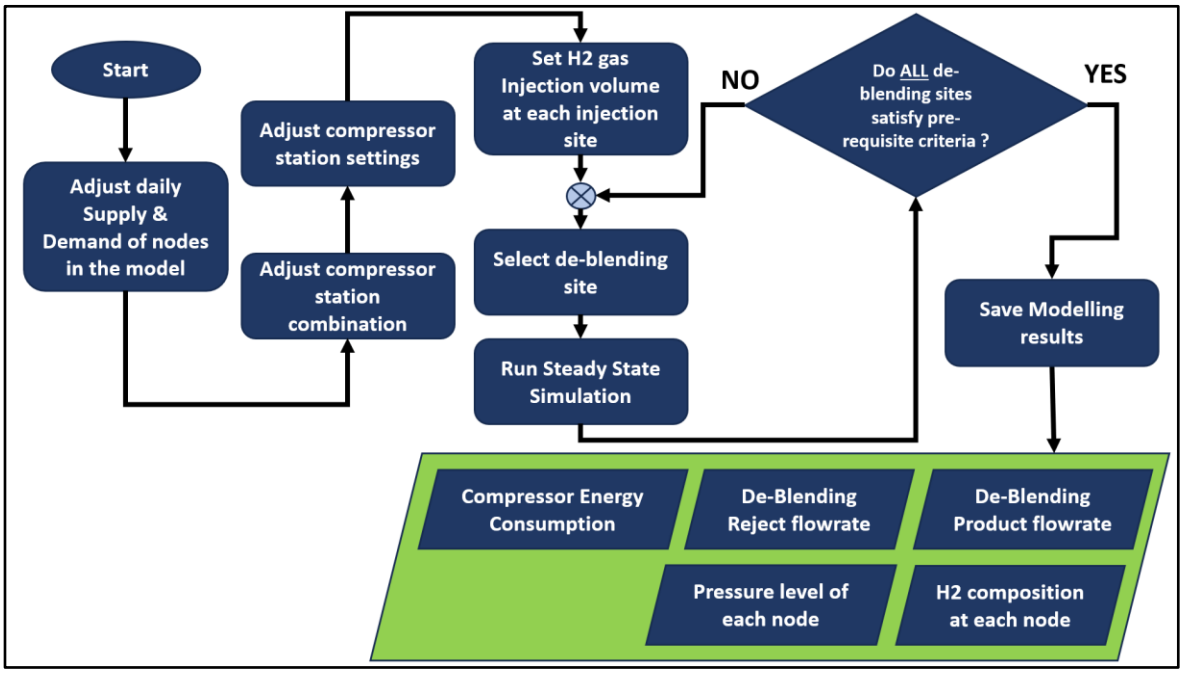

Figure 5.2. Post-analysis process

5.1.2. Prerequisites for deblending

For a deblending site to be practically operable, four prerequisites were introduced. The deblending site was deactivated and removed from the simulation if it did not meet one of these criteria. The criteria are as follows:

1. The deblending customer must have demand above zero.
2. The deblending inlet node must not be located at the end of the pipeline branch; otherwise, no physical space will be available for reinjecting the reject gas into the high-pressure network.
3. The deblending customer's demand flow rate should not be so high as to cause all the gas flow streams to be redirected towards the deblending site to meet this high demand. This phenomenon prevents the reinjection of the reject gas back into the high-

pressure gas network. The simulation was repeated several times to determine if demand was too high for a particular site. Finally, the deblending site with too high demand was removed.

4. The hydrogen content at the deblending site's inlet should be above zero; otherwise, the simulation cannot be conducted.

5.1.3. Post-analysis process

The aim of the post-analysis is to estimate the energy consumption of deblending sites, and it has the following steps:

In the study conducted by national gas [47]., deblending technologies were categorised using three criteria. A) Feed flowrate, which is the total gas feed into the deblending site. B) volumetric percentage of hydrogen present in the feed gas C) Type of deblending technology used.

Feed flowrate and percentage of hydrogen present in the feed gas, are data taken from the simulation. National gas has tested two types of deblending technologies, i) cryogenic deblending and ii) PSA plus membrane technology. It is assumed that either all sites use cryogenic deblending or PSA plus membrane.

The post-analysis consists of estimating the energy consumption of each de-blending site based on the three criteria mentioned above. To conduct the estimation, the criteria categorise the deblending sites into 2 X 8 categories, eight categories for cryogenic deblending and another eight categories PSA plus membrane.

Each site’s specific energy consumption (SEC) was calculated by comparing the total energy consumption to the deblending product flowrate. The methodology for SEC calculations is given in section 5.2.3.

In addition, each sites reject-to-product ratio was calculated by comparing the volume of gas rejected by the deblending site compared to the volumetric demand of deblending consumer that was satisfied. The reject-to-product ratio is calculated using methodology explained in Section 5.2.1.

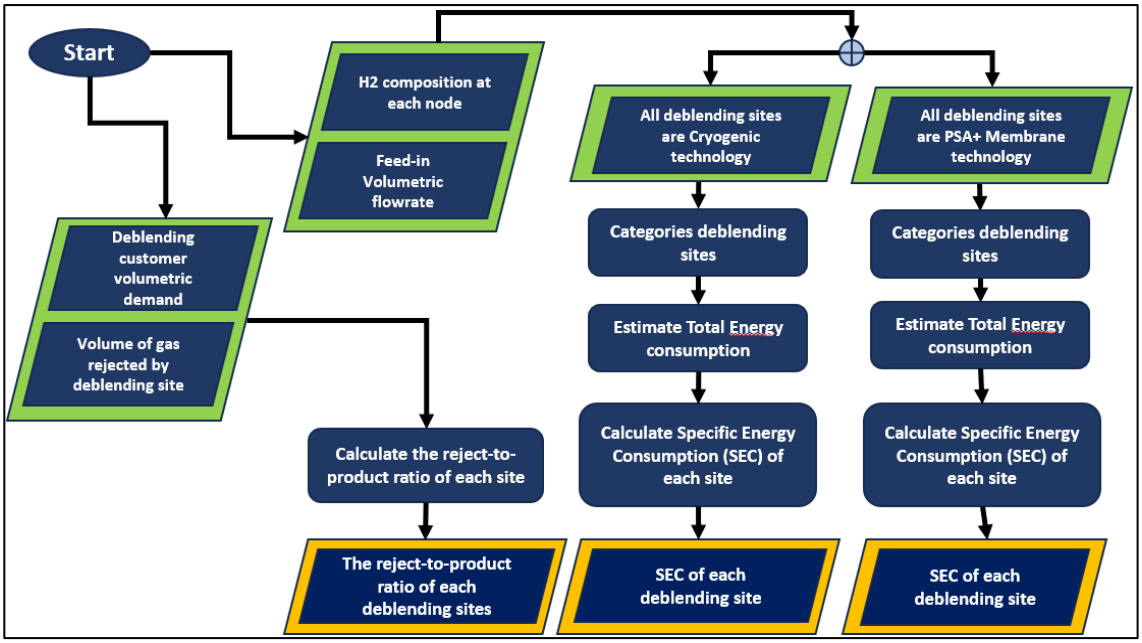

Figure 5.3. Post-simulation process.

5.1.4. Reject-to-product ratio

This ratio represents how much gas needs to be rejected to reach the production quota set by the offtake demand:

$$r_p^r = \frac{Q_r}{Q_p} \tag{6}$$

5.1.5. Categorising deblending sites and calculating their energy consumption

Two variables define every deblending site:

$$W_d = f(Q_f, N_h) \tag{7}$$

where Q_f is the deblending site's feed gas and $N_h$is the volumetric percentage of hydrogen at the hydrogen at feed.

Data from National Grid's deblending report [47]has been used to calculate energy demand. According to this report, the energy demand of a deblending site is sensitive to the volumetric flow rate and the hydrogen content of the feed gas. Figure 5.4 shows the energy demand for two station setups: one is a cryogenic separator, and the other is a combination of PSA and membrane. Energy demand is plotted at two feed-flowrates: 1 Mm^3/d and $3Mm^3/d$.

Each line has four data points, representing energy demand when exposed to 5, 10, 20, and 40 % of hydrogen in feed.

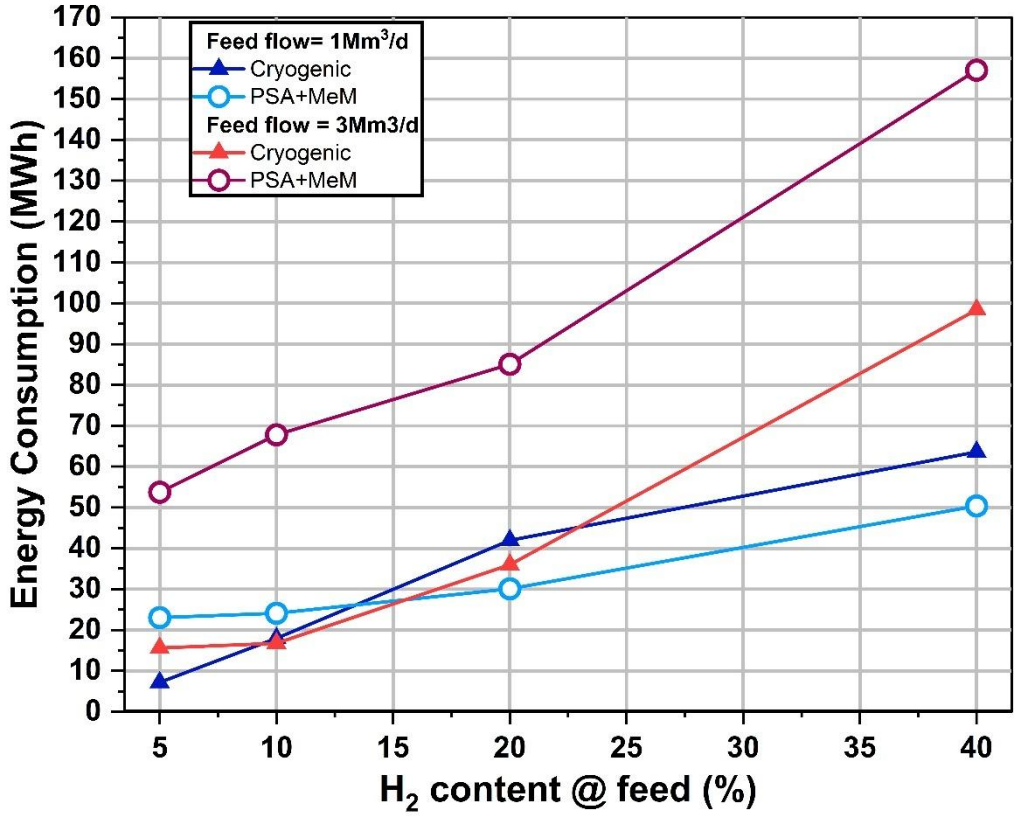

Figure 5.4. Relationship between feed flow, hydrogen content in feed, and energy consumption of deblending sites.[98]

As seen in the figure 5.4, there are eight distinct points, where the hydrogen content and volume of gas at feed define the energy consumption of the deblending site.

These eight points were used in the post-analysis, and the energy consumption of each deblending site was estimated by grouping the deblending sites into eight categories.

As presented in Table 5.1, feed gas volumes Q_f below 1.75 Mm³ were classified as low flow and denoted by the abbreviation “lo”. Volumes exceeding this threshold were categorised as high flow, indicated by “hi”. The hydrogen content, N_h, was discretised into representative values for modelling purposes: concentrations between 0–7.5% were assumed to be 5%; those between 7.5–17.5% were assigned a value of 10%; concentrations from 17.5–30% were represented as 20%; and values ranging from 30–100% were approximated as 40%. each deblending site is categorised based on the two variables to estimate the deblending site’s energy consumption.

Table 5.1. Categorising deblending sites based on feed flow and feed hydrogen content.

Feed Flow	Vol % of hydrogen at Feed	Assigned Group	Energy Consumption	
			Cryogenic Separation	PSA Plus Membrane
$Q_f < 1.75 Mm^3$	$0 < N_h \leq 7.5$	Lo-5	7.2	23.04
	$7.5 < N_h \leq 17.5$	Lo-10	18	24.12
	$17.5 < N_h \leq 30$	Lo-20	42	30.12
	$30 < N_h \leq 100$	Lo-40	63.6	50.4
$Q_f \geq 1.75 Mm^3$	$0 < N_h \leq 7.5$	Hi-5	15.6	53.76
	$7.5 < N_h \leq 17.5$	Hi-10	16.8	67.8
	$17.5 < N_h \leq 30$	Hi-20	36	85.08
	$30 < N_h \leq 100$	Hi-40	98.4	157.08

5.1.6. Specific energy consumption of deblending sites

The SEC for the deblending sites is the ratio of the product of the deblending sites and the energy consumed for delivering that product.

$$E_w^q = \frac{Q_p}{W_p} \quad (8)$$

5.2. Description of case studies

Supply levels to the gas network are different in the two cases. Hydrogen is injected at 20% volumetric of total gas supply. The total volume of hydrogen injected into the network was also differs because of the different natural gas supply levels between the two case studies.

For both of these case studies, the hydrogen is injected from 28 injection points connected to wind generation. These injection points inject at 20% volumetric of total gas at the location of injection. This is the same as Distributed Injection case in chapter four.

By choosing distributed injection The hydrogen content in the network therefore varies at different locations. Introducing deblending to the distributed injection case automatically studies the impact of hydrogen content higher and lower than the 20% volumetric limit.

Table 5.2 Provides an overview of the two case studies:

Table 5.2. summary of the case studies

Case Study	Year	Duration of Simulation	Supply (Mm^3/d)	
			Natural Gas	Wind-generated hydrogen
Summer Deblending	2035	Single day	92	23
Winter Deblending	2035	Single day	127	32

In the Summer Deblending case study, demand for gas is met with a high LNG supply from Milford Haven in South Wales, Teesside in Northeast England, and the Isle of Grain in Southeast England. LNG constitutes 40% of the total supply into the NTS. The continental shelf, St Fergus in Scotland and Easington in Northeast England constitutes 31% of the total supply. The contribution of each supply point is shown in Figure 5.5 (a), and the percentage contribution of each supply type is presented in Figure 5.5 (b).

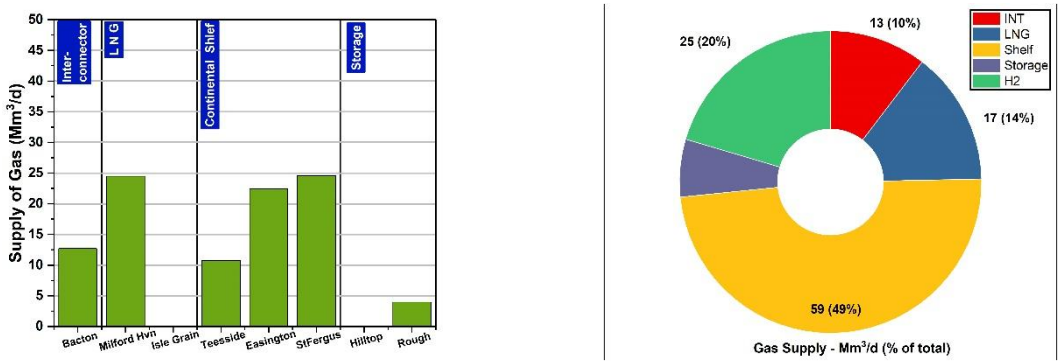

(a) **(b)**

Figure 5.5. Supply of gas in the Summer Deblending case

In the Winter Deblending case study, the continental shelf has the largest proportion of the total NTS supply, constituting 40% of the total supply. This is followed by the Bacton interconnector supply, constituting 22% of the total supply. Therefore, most of the gas supply comes from St Fergus in Scotland, Easington in Northeast England and Bacton in East England. The flow of each supply point on a Winter Deblending is shown in Figure 5.6 (a), and the proportion of each type of supply to the total supply is represented in Figure 5.6 (b).

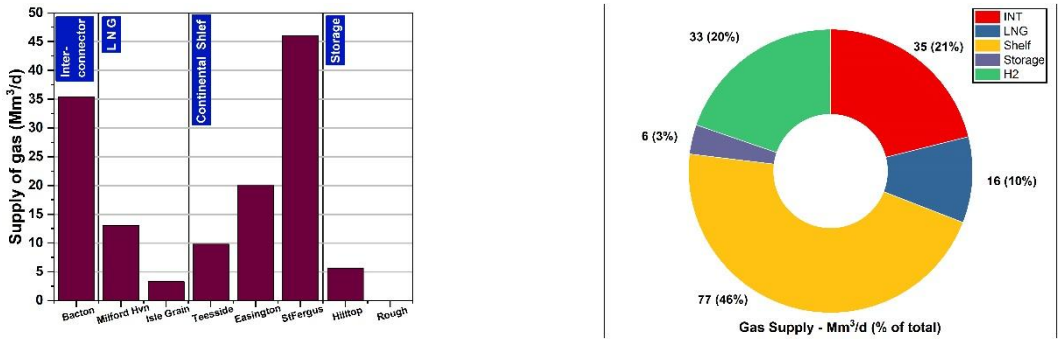

(a) **(b)**

Figure 5.6. Supply of gas in the Winter Deblending case

Demand levels in every region differ from summer to winter days. Most of the gas demand on a Summer Deblending case comes from the Midlands and East of England. However, most of the demand for a Winter Deblending comes from Northwest and Southeast England. This difference changes the gas flow direction in the high-pressure network between the two cases. Figures 5.7 (a) and (b) demonstrate the volumetric demand for gas in every region of the high-pressure gas network, and the percentage on top of each column represents the proportion of the region's demand to the total demand for gas.

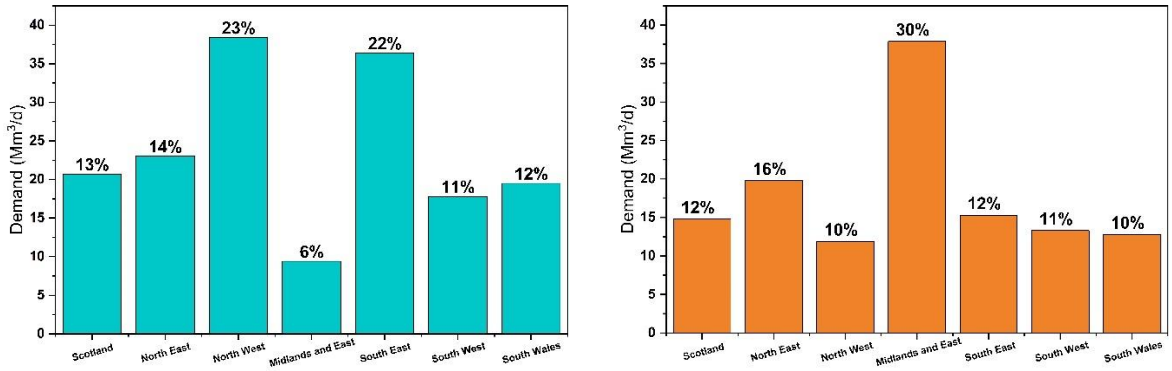

(a) **(b)**

Figure 5.7. Volumetric demand for gas in (a) the Winter Deblending case and (b) the Summer Deblending case.

The differences in supply and demand between cases lead to different levels of hydrogen injection in every region. Hydrogen is injected into the network via 28 injection points scattered across the NTS. The location of these injection points corresponds to 28 busbars of the electrical grid. The hydrogen injected at each point constitutes 20% of the volumetric flow of the gas stream at the injection point.

Figure 5.8. demonstrates the aggregate volume of hydrogen injected in each region of GB. In both summer and winter, the highest hydrogen injection happens in Scotland. Scotland hosts St Fergus, a major NTS supplier in both cases. In summer, the second largest hydrogen

injection happens in the Northeast, followed by South Wales, Midlands, and East. In winter, however, the largest hydrogen injection happens in the Southeast, followed by South Wales and Southwest.

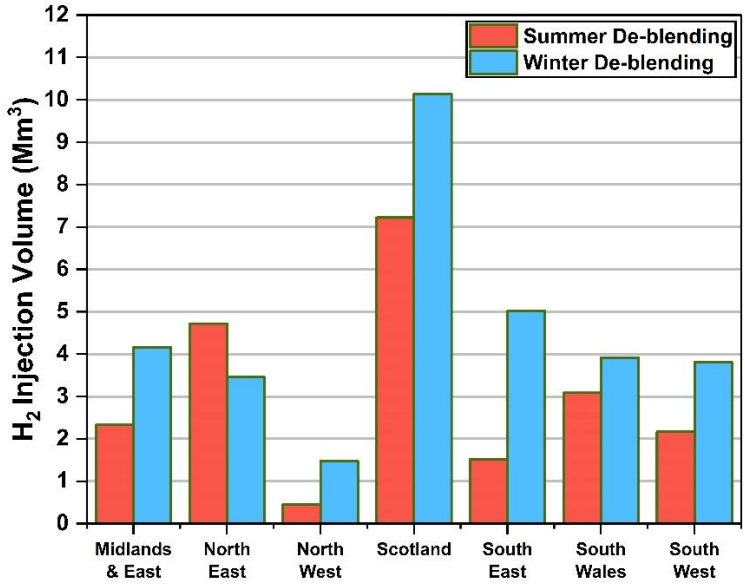

Figure 5.8. Hydrogen Injection in different regions in two case studies.

5.2.1. Compressor Setup

The combination of compressor stations used in the summer deblending case depends on the direction of gas flow and the total level of gas flow. Table 5.3 summarises the compressors used for the summer deblending case.

Table 5.3. Compressor setup in the summer deblending case

Name	Purpose	Set Pressure
Wormington	Keeping pressure levels below 70 bar-g between Felindre and Wormington. Directing the flow of gas from South Wales to Southwest England	50 bar-g @ Inlet
Felindre	Boosting pressure levels at Milford Haven LNG terminal	50 bar-g @ Inlet
St Fergus	Boosting pressures at St Fergus Terminal	45 bar-g @ Inlet
Aberdeen	Directing flow from St Fergus towards Scotland and the North of England Keeping pressures below 65 bar-g between St Fergus and Aberdeen	55 bar-g @ Inlet

The combination of compressor stations used in the Winter Deblending case depends on the direction of gas flow, as well as the total level of gas flow. Table 5.4 summarises the compressors used for the Winter Deblending case:

Table 5.4 Compressor setup in the Winter Deblending case

Name	Purpose	Set Pressure
St Fergus	Boosting pressures at St Fergus Terminal	55 bar-g @ Inlet
Aberdeen	Directing flow from St Fergus towards Scotland and the North of England Keeping pressures below 65bar-g between St Fergus and Aberdeen	70 bar-g @ Outlet
Nether Kellet	Supporting pressures at network extremities, Blackrod and Blackburn	75 bar-g @ Outlet
Kings Lynn	Delivering gas away from Bacton supply point	70 bar-g @ Outlet
Diss	Delivering gas away from Bacton supply point	65 bar-g @ Outlet
Alrewas	Delivering gas from Midlands to North West	65 bar-g @ Outlet

5.2.2. Prerequisite screening and deblending setup

A multi-stage screening process was used to identify suitable nodes for deblending sites. Each stage is outlined below.

Stage 1. Exclusion of one-way branches

The initial screening stage filtered out nodes located at the end of a one-way network branch. A deblending site requires a 'reject' outlet to return the non-compliant gas mixture back to the network. Locating this outlet at a one-way branch is operationally unfeasible, as the rejected gas would flow back into the site's own feed, creating an unproductive operational loop. These terminal nodes were identical for both Winter and Summer Deblending cases, resulting in the exclusion of 27 demand nodes.

Stage 2. Exclusion of zero-flow nodes

Nodes with zero gas flow were excluded. In the Winter Deblending case, this accounted for 47 nodes. The number was higher in the summer Deblending cases, with 71 nodes excluded due to zero flow.

Stage 3. Exclusion based on hydrogen content

The third stage screened the remaining nodes based on the hydrogen content of their feed gas, as determined by steady-state simulations. Nodes were eliminated if the feed gas

contained no hydrogen, as deblending would be redundant. Similarly, nodes where the hydrogen concentration was already at the 20% volumetric limit for Local Distribution Zones (LDZs) were also excluded, as no further deblending was necessary. This resulted in the exclusion of 53 nodes in the Winter Deblending case and 8 in the Summer Deblending cases. The lower figure for Summer is attributed to the larger number of nodes previously eliminated in Stage 2.

Stage 4. Exclusion of Sites Causing Flow Convergence

In the final stage, potential sites that caused network flow convergence during simulations were eliminated. flow convergence describes an incident where the high gas volume required for the deblending process diverted all regional gas flow towards the deblending site. The phenomena prevented the effective reinjection of the rejected gas stream, as reinjection brings the reject gas back into the deblending site's feed. A total of 9 nodes in the Winter Deblending case and 4 in the Summer Deblending cases was removed for this reason.

The final list of deblending sites were shown in *Table 5.5* and *Table 5.6* :

Table 5.5. Deblending setup in the Summer Deblending case

Offtake Name	**Demand Volume (Mm3/d)**	**Type of Offtake**	**Demand Type**
Elton	1.342	Local Distribution Zones (LDZ)	Gas with 20% volumetric hydrogen and 80% natural gas
Pannal	3.801		
Eccleston	0.716		
Dowlais	1.371		
Staythorpe	2.055		
Alrewas	1.194		
Bishop Auckland	0.708		
Warburton	3.091		
Grain	1.248		
Epping Green	1.094		
Damhead Creek	2.365	Power Station (PS)	Only natural gas
Didcot	2.678		
Keadby	1.865		
Peterhead	2.614		
Stallingborough	1.918		

Thornton Court	2.179
Paul-Saltned	2.319

Table 5.6. Deblending sites in the Winter Deblending Case

Offtake Name	Volumetric Demand (Mm^3/d)	Type of Offtake	Demand Type
Gooleglass	0.2	Industrial (Ind)	Only hydrogen
Horndon	1.537	Local Distribution Zones (LDZ)	Gas with 20% volumetric hydrogen and 80% natural gas
Mappowder	1.326		
Samlesbury	2.694		
Leamington	0.124		
LtBurdon	0.373		
Drum	0.783		
Balgray	0.44		
Audley	0.285		
Ispden	0.197		
Burnhervie	0.888		
Fiddington	0.623		
Pucklechurch	0.875		
Ilchester-Coffinswell	0.915 0.195		
Staythorpe	3.137	Power Station (PS)	Only natural gas
Peterhead	2.409		
Grain	2.721		
Cottam	0.996		
LtBarford	1.065		
DamhdCreak	1.016		
Carrington	0.091		
Langage	0.436		

5.3. Results

The result was divided into two parts: the first part focuses on the operation of the network by looking at pressure levels and compressor operation, while the second part focuses on the operation of the deblending sites.

5.3.1. Operation of the network

5.3.1.1. Pressure levels

Figure 5.9 plots pressure levels against the daily demand at the extremities of the model for both case studies. Extremities refer to nodes located at the very end of pipeline branches.

The vertical axis shows that the largest demand at the extremities in the Winter Deblending case is 6 Mm^3/d. Moreover, the total demand of the extremities in the Winter Deblending case is 30 Mm^3/d. In the Summer Deblending case, the largest demand in the extremities is 2.5 Mm^3/d, and the total demand of the extremities is 11.1 Mm^3/d.

In the winter deblending case, the pressure of extremities range between 75–59 bar-g. In the Summer Deblending case, the pressure of the extremities range between 63 –53 bar-g.

As seen Figure 5.9, extremities in the Winter Deblending have larger demand levels than in the Summer Deblending. The large demand levels in Winter Deblending cause large variations between pressure levels in each of the extremities. The standard deviation of pressure levels of the Winter Deblending case is 4 bar-g

In contrast, smaller demand in extremities of Summer Deblending cause smaller variation in pressure levels in extremities as the standard deviation of pressure levels in Summer Deblending is 2.3 bar-g.

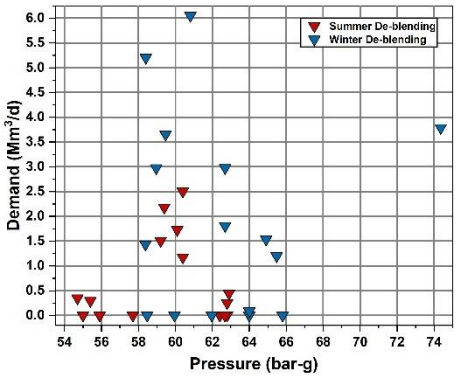

Figure 5.9. Pressure vs Demand at the extremities in both Summer and Winter deblending cases.

5.3.1.2. Compressors

Figure 5.10 demonstrates each compressor station's energy consumption against its overall utilisation. The plots are colour-mapped, and the colour corresponds to the total flow of gas passing through the compressor station.

Figure 5.10 (a) shows that Aberdeen and St Fergus compressors in Scotland have the largest energy consumption in the Winter Deblending case; Aberdeen with 227MWh and St Fergus with 166MWh. Kings Lynn follows this in East England with an energy consumption of

94MWh. Furthermore, in the Winter Deblending, the compressors consume a total of 508 MWh, compressing a total of 119 Mm^3/d of gas.

Figure 5.10(b) shows the large energy consumption in Kings Lynn's for the Summer Deblending case, 528 MWh. However, the rest of the compressor stations have much lower energy consumption. St Fergus comes second with 165 MWh and Hatton third with 105MWh. Since the Summer Deblending is modelled based on the Summer Model (see Chapter 2), it too hosts large exports of gas to the European continent via the Bacton interconnector. Therefore, Kings Lynn has an exceptionally high energy consumption. In the Summer Deblending, the compressors consume a total of 1010MWh of energy, compressing a total of 181 Mm^3/d of gas.

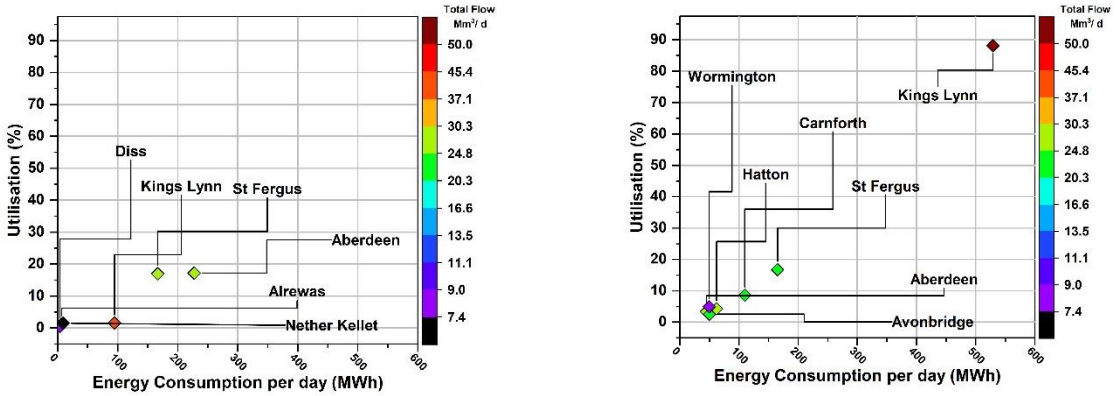

Figure 5.10. Compressor station utilisation vs energy consumption in (a) the Winter Deblending case and (b) the Summer Deblending case

5.3.2. Operation of deblending sites

5.3.2.1. Deblending reject-to-product ratio

The reject-to-product ratio reflects the intensity of the physical process. Unlike the energy consumption—which is based on an estimation in this study—the reject-to-product ratio is a direct output of the simulation. It is the ratio the rejected gas by the deblending site over the product gas as demanded by the consumer. These ratios indicate the demand sites where the most processing is required to separate hydrogen from natural gas.

Figure 5.12 demonstrates the volume of gas rejected and produced after deblending from the deblending station. Figure 5.11(a) shows the Winter Deblending case, and Figure

5.12 (b) shows the Summer Deblending case. The line with the circle symbols drawn in Figures 5.12 (a) and 5.12 (b) demonstrates the reject-to-product gas ratio.

According to Figure 5.11(a), deblending sites connected to LDZ offtakes in the Winter Deblending case have a reject-to-product ratio between 0.1 and 1.9 Moreover, deblending sites connected to power stations have a reject-to-demand ratio between 0.1 and 0.8. However, the deblending site connected to industrial offtake have significantly larger reject-to-demand ratio of 8.2 .

According to Figure 5.11(b), deblending sites connected to LDZ offtakes in the Summer Deblending case have a reject-to-product ratio between 0.03 to 1.49. Moreover, deblending sites connected to power stations have a reject-to-demand ratio between 0.04 to 0.74.

Amongst all the deblending sites, those that connect to the industrial offtakes have large reject-to-product ratios. This means that reaching a specific quota of pure hydrogen using deblending of gas in the NTS requires large quantities of gas being processed and large quantities of gas being sent back to the NTS after rejection. This raises the question of whether deblending effectively meets a quota for pure hydrogen.

Some deblending sites connected to LDZ offtakes also exhibit large reject-to-product ratios, such as Leamington in the Winter Deblending case and Elton and Pannal in the Summer Deblending case. These LDZ sites are in regions where hydrogen concentration is significantly below 20% volumetric. Therefore, they must reject relatively large volumes of natural gas to deliver gas with a fixed 20% hydrogen concentration to the LDZ offtake.

The power stations Langage and Carrington in Winter Deblending case, and Grain in Summer Deblending case are in regions of the NTS with exceptionally large hydrogen concentrations. Therefore, the deblending sites connected to these power stations must also reject a relatively large volume of gas to deliver the natural gas demanded.

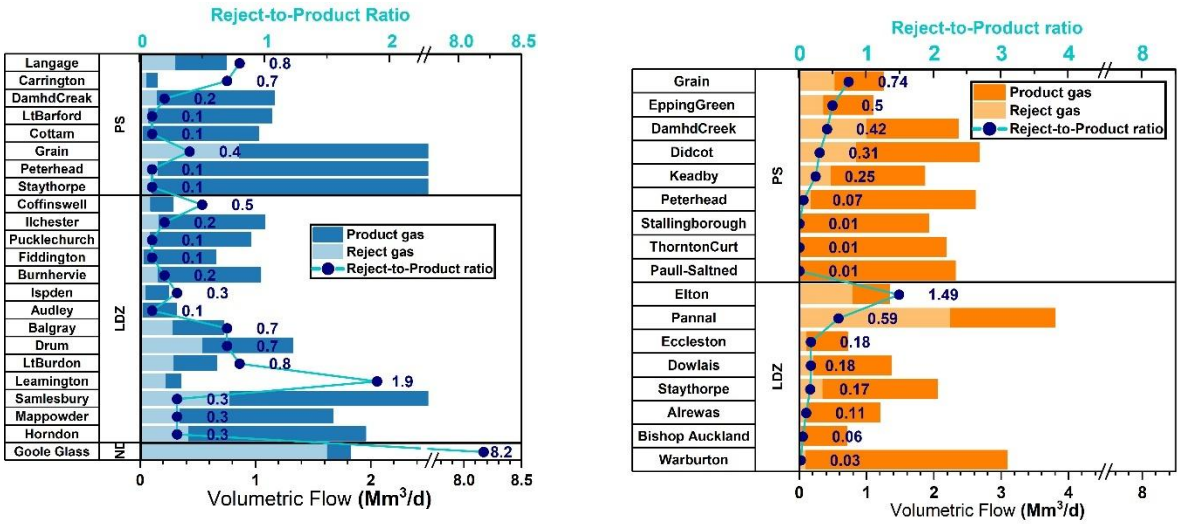

(a) **(b)**

Figure 5.11. Reject-to-product ratio in (a) the Winter Deblending and (b) in the summer deblending case.

5.3.2.2. Energy consumption of deblending sites

The deblending sites are divided into eight categories. Figure 5.12(a) demonstrates the categorisation for the Winter Deblending and Figure 5.13 (b) demonstrates the categorisation for the summer deblending case.

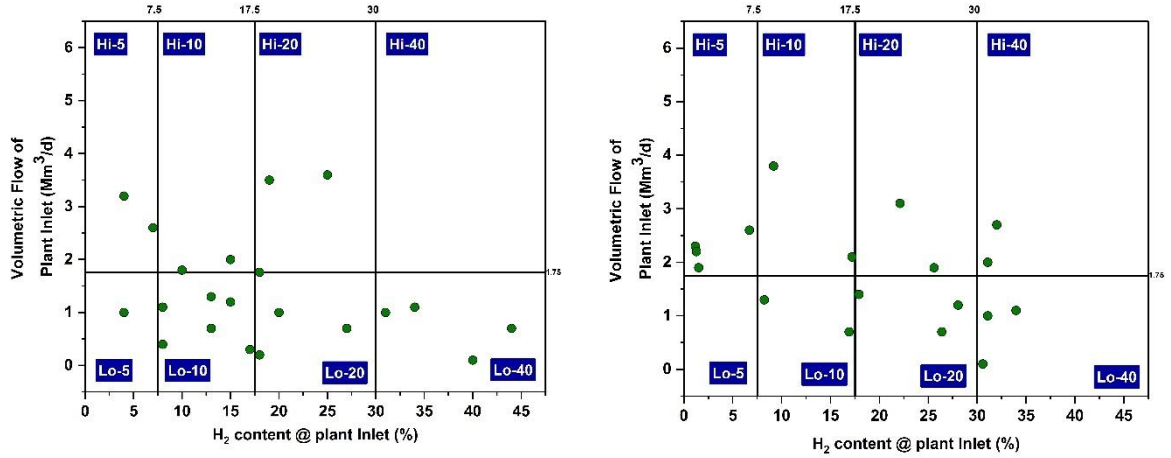

(a) (b)

Figure 5.12. Categorising deblending sites (a) in the Winter Deblending and (b) in the Summer Deblending case

As a result, the deblending sites that fall under the same category have the same energy demand. Here, it is assumed that all deblending sites are either cryogenic or PSA plus membrane setups. Therefore, the energy consumption levels are reported for either cryogenic or PSA plus membrane.

Figure 5.13 demonstrates the total energy consumption of deblending sites, categorised by deblending technology and the type of offtake to which the site delivers. The plots are colour-mapped and deblending sites from the same category have the same colour.

Figure 5.13 (a) demonstrates the energy consumption of deblending sites in Winter Deblending when they all use a cryogenic separation setup. Figure 5.14 (a) shows that the deblending site delivering gas to an industrial offtake has of 16.8 MWh of energy consumption. In addition, deblending sites delivering gas to LDZ offtakes have a total of 519.6 MWh of energy consumption. Finally, deblending sites delivering gas to power stations have a total of 238.8 MWh of energy consumption.

Figure 5.13 (b) demonstrates the energy consumption of deblending sites in Winter Deblending when they all use PSA plus membrane setup. Furthermore, this figure demonstrates that using PSA plus membrane technology, deblending site delivering gas to an industrial offtake require energy 4 times that of cryogenic technology. The trend repeats as deblending sites connected to LDZ offtakes require energy 1.16 times that of cryogenic technology. The deblending sites connected to power stations require energy 1.58 times that of cryogenic technology.

Figure 5.13 (c) demonstrates the energy consumption of deblending sites in Summer Deblending when they all use the cryogenic separation setup. Figure 5.14 (c) shows that deblending sites delivering gas to LDZ offtakes have a total of 325 MWh of energy consumption. In addition, deblending sites delivering gas to power stations have a total of 320MWh of energy consumption.

Figure 5.13 (d) demonstrates the energy consumption of deblending sites in summer if all of them are PSA plus membrane technologies. Furthermore, this figure shows that using PSA plus membrane setup, deblending sites connected to the LDZ offtakes require energy 1.6 that of cryogenic technology. Finally, by using PSA plus membrane setup, deblending sites connected to power stations require energy 1.8 times that of cryogenic technology.

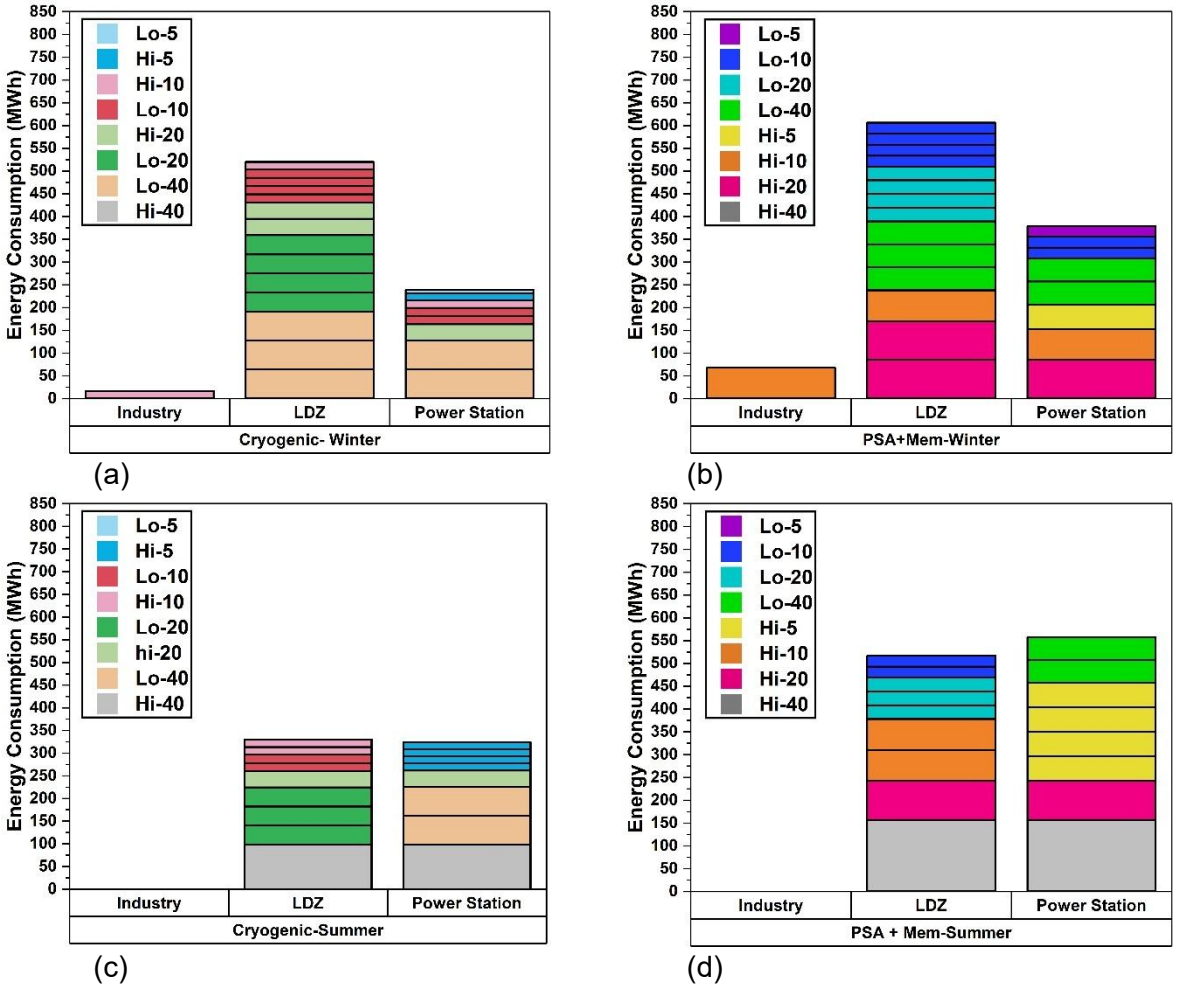

Figure 5.13. Energy consumption of deblending sites (a) in Winter Deblending case using cryogenic separation (b) in Winter Deblending case using PSA plus membrane (c) in Summer Deblending case using cryogenic separation (d) in summer deblending case using PSA plus membrane.

The results demonstrate that the total energy consumption of deblending sites are significantly large. For comparison, the total energy consumption for compression in winter is half that of deblending sites. Use of PSA plus Membrane technology increases the deblending energy consumption further.

All gas consumers, regardless of their deblending requirements, could potentially suffer from exceptionally high energy consumption cost. As the hydrogen content in the network varies in different times of the day, as shown in the previous chapter, all industries could struggle with high processing energy consumption at a point of time in the year.

5.3.2.3. Specific energy consumption of deblending sites

The SEC for the deblending sites is the ratio of the product of the deblending sites and the energy consumed for delivering that product. Figure 5.14 demonstrates the SEC of deblending sites using box and whisker plots.

Figure 5.14 (a) belongs to the Winter Deblending case, and Figure 5.15. (b) belongs to the Summer Deblending case. The box plots are categorised by the deblending type and the type of customer to which they deliver gas.

According to Figure 5.14. (a), in the Winter Deblending case, the use of cryogenic separation for delivering gas to industry offtakes has a SEC calculated at 84 MWh/Mm^3. The use of cryogenic separation technology for delivering gas to LDZ offtakes led to a mean SEC calculated at 89.3 MWh/Mm^3. Finally, cryogenic separation technology for delivering gas to power stations led to a mean SEC calculated at 114.2 MWh/Mm^3.

According to Figure 5.14. (a), in the Winter Deblending, the use of PSA plus membrane technology for delivering gas to industry offtakes has a SEC is calculated at 339 MWh/Mm^3. The use of PSA plus membrane technology for delivering gas to LDZ offtakes led to a mean SEC calculated at 85.5 MWh/Mm^3. Finally, cryogenic separation technology for delivering gas to power stations led to a mean SEC calculated at 101.8 MWh/Mm^3.

According to Figure 5.14. (b) in the Summer Deblending case, use of cryogenic separation for delivering gas to LDZ offtakes led to a mean calculated at 28 MWh/Mm^3. Cryogenic separation for delivering gas to power stations led to a mean calculated at 33 MWh/Mm^3.

According to Figure 5.14. (b), in the Summer Deblending case, using PSA plus membrane for delivering gas to a mean calculated at 32.5 MWh/Mm^3. Using PSA plus membrane for delivering gas to power stations led to a mean SEC calculated at 62 MWh/Mm^3.

In the Winter Deblending case, the mean SEC for delivering gas to industry using PSA plus membrane is 1.83 times that of cryogenic separation. The mean SEC for delivering gas to LDZ offtake using PSA plus membrane is 1.56 times that of cryogenic separation. Finally, the mean SEC for delivering gas to power stations using PSA plus membrane is 0.99 times that of cryogenic separation.

In the Summer Deblending case, the mean SEC for delivering gas to LDZ offtakes using PSA plus membrane is 1.16 times that of cryogenic separation. Finally, the mean SEC for delivering gas to power stations using PSA plus membrane is 1.9 times that of cryogenic separation.

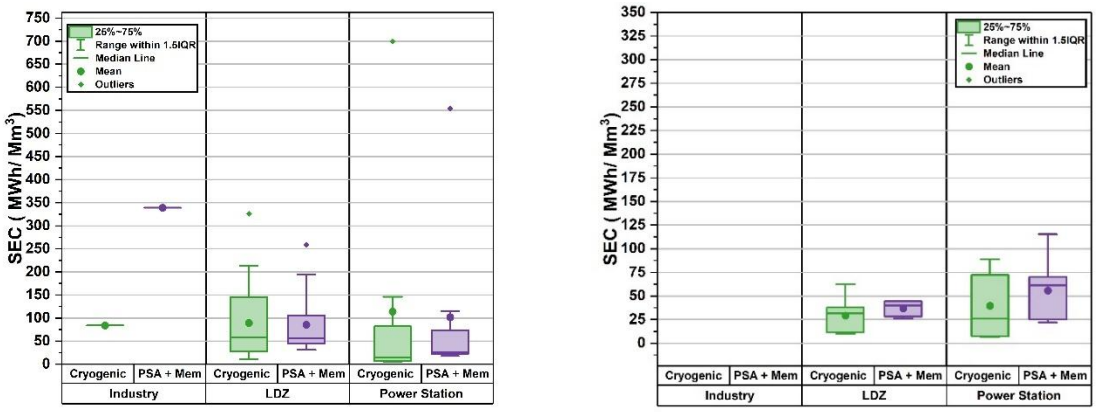

(a) **(b)**

Figure 5.14. SEC in (a) Winter Deblending case and (b) Summer Deblending case.

The SEC showed how much energy is consumed per product. The industrial site in the winter case has a high SEC. This is since the industry requires pure hydrogen, which is usually the minority gas in the network with 20% blending target. To reach demand quota for the industry site, large amounts of mix gas should be processed, and majority of the gas will be rejected back into the network. This makes the end-product energy intense.

Although no consumer is immense to these phenomena in a network with varying hydrogen content, the industries will always experience the high SEC value, while other consumers will periodically face high SEC values.

5.4. Conclusions

Based on the analysis, the following conclusions are drawn regarding the potential use of deblending technologies in the NTS:

- The prerequisite screening showed that, in both Summer and Winter Deblending cases, there are many customers that cannot use deblending due to the physical structure of the NTS preventing operation of a deblending site. If this issue is resolved, significant volume of gas could be deblended; In Winter Deblending, a total of 33Mm^3 of and in the Summer Deblending, a total of 15Mm^3.

- The energy consumption of deblending is directly related to hydrogen content and volume of gas at feed. In wintertime, when demand for gas is higher than summer, the energy consumption of deblending sites are also higher. Furthermore, the total energy consumption of deblending is larger, 1.3 to 1.7 times, in Winter Deblending compared with Summer Deblending.

- The cryogenic technology is more established that PSA plus membrane, and the energy consumption of the technology is generally lower than PSA plus membrane.

The results also reflect this, and the total energy consumption of each case is 1.1 to 1.9 times larger with PSA plus membrane technology compared with cryogenic technology.

- Different customers have different requirements for deblending. Local distribution sites require hydrogen fixed at 20% volumetric, power stations require gas with no hydrogen, and Industries require pure hydrogen. Despite this, the mean SEC of deblending is similar in both Summer Deblending and Winter Deblending cases when comparing the same types of customers (i.e. when comparing LDZ deblending together and power station deblending together).
- Deblending for industrial sites where pure hydrogen is demanded from customers results in high SEC values. As hydrogen is the minority in the mix-gas, large volumes of gas should be processed to extract pure hydrogen in large volumes. The large feed flow leads to large energy consumption. Finally, comparing the small volume of extracted hydrogen to the energy consumption leads to a substantial SEC value.

Chapter 6. Conclusions and suggestions for future research

The studies conducted in this thesis have yielded significant findings on the use of the GB high-pressure gas network for hydrogen transmission. These findings confirm that in its current state the high-pressure gas network can transport a blend of up to 20% hydrogen. Moreover, studies have verified that the high-pressure gas network can transport pure hydrogen, operating in the same manner as it does today.

Additionally, this thesis has delved into deblending technologies in the high-pressure gas network for delivering a specific type of gas to certain customers. This study has revealed that using cryogenic separation is a less energy intense option than a combination of membrane and PSA technology. Importantly, this study has shown that the energy intensity of operating the deblending site is dependent on the type of gas that the customer is demanding, with delivering to industries requiring pure hydrogen being the most expensive and delivering natural gas with no hydrogen being the least expensive process.

This chapter details the conclusions of each previous chapter in chronological order. At the end of this chapter, the authors will offer several suggestions for improving the research.

6.1. Conclusions

6.1.1. Calibration of the GB high-pressure gas network model

GB's high-pressure gas network was modelled using Synergi Gas 4.9.4 software. The model simulates both the gas network's steady-state and unsteady-state behaviour. The unsteady-state analysis provides insight into the network's within-day behaviour, with an hourly resolution.

The Winter and Summer Models are the basis of all the case studies in Chapters Four and Five. Because of their crucial role in developing the rest of the models, the Winter and Summer Model were reviewed in detail. Furthermore, the Winter Model and Summer Model’s calibration was assessed by comparing their calculated linepack with the seasonal linepack range of every region of GB. The seasonal linepack range was taken from National Gas’ public database. The high-pressure gas network model was divided into 12 Linepack Zones based on geographical locations to assess calibration. The conclusions are as follows:

1. Nine out of 11 zones were assessed to be calibrated well against the seasonal linepack range, indicating that their calculated linepack was near seasonal linepack levels.

2. Amongst the 12 Linepack Zones, Zone 11 in South Wales, Zone 2 in Scotland, and Zone 4 in Northwest England were uncalibrated. This was due to the exclusion of gas regulator stations, making it impossible to simulate large pressure differences between these linepack zones and the adjacent regions. Consequently, the linepack levels in these linepack zones were outside the seasonal linepack range.
3. Regulator stations in the model were excluded because operational data were lacking. It is crucial to re-emphasise that all the nodes in all the linepack zones, even the uncalibrated linepack zones, operate within the pressure ranges suggested by National Gas.

6.1.2. Operation of GB high-pressure gas network with hydrogen

Four studies were conducted:

1. Winter Model: This depicts the gas network operation on a typical winter's day in 2018.

2. 20% Centralised Injection: This represents the operation of the GB gas network in a day in 2035, with a centralised method for injecting hydrogen. In this injection method, hydrogen is injected at a 20% volumetric rate of the total gas mix. The injection points are located at eight natural gas entry points into the gas network.

3. 20% Distributed Injection: This represents the operation of the GB gas network in a day in 2035 with a distributed method for injecting hydrogen. In this injection method, hydrogen is injected at a 20% volumetric rate of the total gas mix. There are 28 injection points co-located with wind farms dispersed across GB.

4. 100% H_2: This represents the operation of the high-pressure gas network with 100% hydrogen in 2050. Just like the previous case studies, the main assumption is that the gas network operates with the same facilities as today (i.e. same number of compressor stations and same number of pipelines and demand nodes).

The conclusions are as follows:

1. The case studies demonstrated that the GB high-pressure gas network, like other networks of the scale, could host 20% volumetric hydrogen without compromising operating pressure levels and compressor energy consumption. The Linepack levels are also not significantly affected by the presence of 20% volumetric hydrogen gas; this was the same for both injection case studies.

2. The case studies also demonstrated that the method of injection does not affect the gas network operational metrics. And the pressure, linepack and compressor energy consumption is similar regardless of the location of hydrogen injection.
3. The method of hydrogen injection into the high-pressure gas grid significantly affects the levels of hydrogen at each node of the network:

    a. In 20% Centralised Injection, two factors defined the mode of hydrogen injection: first, hydrogen was injected into the grid from points of natural gas supply. Second, the hourly rate of hydrogen injection was set to be volumetrically proportional to natural gas supplied to the network from the related supply node, with hydrogen consisting of 20% volumetric mix-gas and natural gas the remaining 80%. This injection mode led to a homogenous mix of hydrogen and natural gas across the network.

    b. The 20% Distributed Injection case was characterised as follows: first, H_2 gas injection was proportional to the generation capacity of wind farms corresponding to the location of hydrogen injection; second, the hourly injection rate was capped at most 20% of mix-gas. This distributed injection of hydrogen led to a nonhomogeneous mix of hydrogen and natural gas across the network. Furthermore, hydrogen content in the nodes varied temporally during the day. Also, different locations of the gas network had different hydrogen content.

4. For 100% H_2 case, the operating pressure was kept at levels comparable to those currently used in the GB high-pressure gas network. Despite maintaining similar pressures, compressor energy consumption increased substantially—up to 3.9 times higher than typical levels in the existing natural gas network. This reflects the greater molecular volume of hydrogen compared with methane. To the authors' knowledge, this impact on compressor energy at current GB pressure levels has not been previously evaluated.

5. Under 100% H_2 case, maintaining present-day pressure levels would reduce the network's energetic linepack to roughly one-quarter of current levels. This would significantly limit the system's within-day flexibility to accommodate sudden demand spikes or supply disruptions. The implications of this reduction in linepack capacity for the GB high-pressure system have not been considered in prior assessments.

6. When transporting 100% hydrogen, the rate of change of linepack is faster than in a network operating with natural gas. The linepack peaks and troughs approximately 1.5 times faster than in the current system, indicating greater sensitivity to within-day supply-

demand imbalances. This dynamic behaviour has not yet been examined for the GB high-pressure gas network.

7. These findings highlight a key trade-off regarding the feasibility of maintaining existing pressure levels. Reducing pressure would help lower compressor energy consumption; however, it would also further reduce linepack capacity and diminish the system's ability to manage within-day fluctuations in supply and demand. In effect, improvements in energy efficiency may come at the expense of operational flexibility.

6.1.3. Deblending hydrogen and natural gas in the GB high-pressure gas network

The GB high-pressure gas network operation with compressor stations and deblending sites was simulated using steady-state analysis. Deblending sites are setups used to separate hydrogen from natural gas. Two case studies were considered for simulation:

1. Winter Deblending: This represents the operation of the gas network on a typical winter's day in 2035.
2. Summer Deblending: This represents the operation of the gas network on a typical summer day in 2035.

In both case studies, 20% volumetric hydrogen was injected from 28 injection points co-located with wind farms dispersed across GB. A post-simulation analysis was conducted to estimate the energy consumption of deblending sites. The energy consumption was estimated for two deblending setups:

1. Cryogenic separation technology.
2. PSA plus membrane technology.

The conclusions are as follows:

1. Deblending has no adverse effects on the operation of the network. Pressure levels at the extremities remain within acceptable range. Compressor operation depends on different flow directions in typical Winter Deblending and Summer Deblending cases.
2. winter deblending requires 1.5 to 1.7 times the energy consumption of a Summer Deblending case. The sites deblending larger gas volumes in winter than in summer.
3. The average energy consumption of deblending remains similar between summer deblending and winter deblending cases. The energy consumption of deblending is largely sensitive to the type of product (i.e. whether hydrogen or natural gas is the

demanded product). Furthermore, deblending for industrial sites is expensive. In these sites, the volume of rejected natural gas is much larger than the product, which is pure hydrogen. Because of the large reject volume, the total feed flow is also substantial, leading to a large energy consumption. Moreover, since the product is of a small volume, the calculated SEC is much larger than sites delivering to other offtakes.

6.2. Suggestions for future research

6.2.1. Calibration of the GB high-pressure gas network model

Three actions can be taken to improve the high-pressure gas network model developed using Synergi Gas software, all within the software's capabilities. At the time that the model was being developed, a lack of data prevented taking these actions:

1. To increase accuracy, regulator stations should be included in the high-pressure gas network model. This would enable accurate modelling of linepack levels in South Wales, the Northwest, and Scotland.
2. To accurately estimate the energy consumption of compressor stations, operational maps of each compressor station in GB should be used to simulate centrifugal compressor operation.
3. Each compressor station in GB consists of several compressor units. Choosing different combinations of units affects the station's operation. Incorporating compressor units in the gas network model will improve the accuracy of the results generated.

6.2.2. Operation of GB high-pressure gas network with hydrogen

The study of the operation of the high-pressure gas network with hydrogen can be improved by considering the following points:

1. A real-time simulation model that monitors gas flow at every step should be developed. The network's hydrogen content must also be measured in real-time. Finally, hydrogen can be injected according to these two real-time parameters.
2. More focus needs to be given to optimising the geographical location of hydrogen injection so that hydrogen reach-out and homogeneity improve in various regions of the high-pressure gas network.
3. Since linepack levels in the 100% H_2 case are significantly lower than existing levels, the gas network's within-day flexibility will be compromised. Therefore, it is crucial to know how the gas network's resilience to external events will be compromised when transporting 100% hydrogen and how the network's reliability will be compromised when facing system failures.

6.2.3. Deblending hydrogen and natural gas in the GB high-pressure gas network

Developing a transient model that can carry a deblending simulation is vital for further study of the within-day operation of deblending technology in the high-pressure gas network. Furthermore, using a transient model makes it possible to study the impact of deblending on pressure and linepack levels within a day. In addition, a transient model will better estimate compressor energy consumption. Combined with more accurate deblending energy consumption, this leads to an accurate estimate of the gas network's overall energy expenditure when operating with deblending sites.

References

[1] UK Government. UK becomes first major economy to pass net zero emissions law 2019. https://www.gov.uk/government/news/uk-becomes-first-major-economy-to-pass-net-zero-emissions-law (accessed November 1, 2022).

[2] BEIS. UK hydrogen strategy. vol. 85. 2021. https://doi.org/10.1002/cind.859_6.x.

[3] National Grid. Future Energy Scenarios 2022. http://fes.nationalgrid.com.

[4] Szablowski L, Wojcik M, Dybinski O. Review of steam methane reforming as a method of hydrogen production. Energy 2025;316:134540. https://doi.org/10.1016/j.energy.2025.134540.

[5] International Energy Agency. Towards hydrogen definitions based on their emissions intensity. 2023.

[6] Guo X, Zhu H, Zhang S. Overview of electrolyser and hydrogen production power supply from industrial perspective. Int J Hydrogen Energy 2024;49:1048–59. https://doi.org/10.1016/j.ijhydene.2023.10.325.

[7] National Grid Gas Transmission. Gas Ten Year Statement. 2022.

[8] National Gas. Gas Ten Year Statement. 2018.

[9] BEIS. Digest of the UK Energy Statistics, Chapter 4: Natural Gas. 2021.

[10] National Grid Gas Transmission. FutureGrid Progress Report 2021.

[11] National Gas. Closure Report Phase 1 Facility. 2024.

[12] National Grid Gas Transmission. Project Union: Launch Report 2022 2022.

[13] Hydrogen Council. Path to hydrogen competitiveness: a cost perspective 2020:88.

[14] Department of Energy Security and Net Zero. Hydrogen Transport and Storage Costs. 2023.

[15] - International Energy Agency I. Global Hydrogen Review 2022. 2022.

[16] Hydrogen Europe. | Hydrogen Infrastructure: The Recipe For Hydrogen Grid Plan. 2024.

[17] Van Rossam R, Jens J, La Guardia G, Wang A, Kühnen L, Overgaag M. European Hydrogen Backbone. 2022.

[18] ACER. Repurposing existing gas infrastructure to pure hydrogen: ACER finds divergent visions of the future | www.acer.europa.eu 2021. https://www.acer.europa.eu/news-and-events/news/repurposing-existing-gas-infrastructure-pure-hydrogen-acer-finds-divergent-visions-future (accessed April 22, 2023).

[19] National Gas. Gas Ten Year Statement 2023. https://www.nationalgas.com/sites/default/files/documents/GTYS-2023_1.pdf (accessed February 10, 2025).

[20] Hodges J, Geary W, Graham S, Hooker P, Goff R. Injecting hydrogen into the gas network – a literature search. Health and Safety Laboratory 2015:1–53.

[21] WorldSteel. Hydrogen (H2)-based ironmaking 2022. https://worldsteel.org/wp-content/uploads/Fact-sheet-Hydrogen-H2-based-ironmaking.pdf (accessed February 10, 2025).

[22] The Royal Society. Green Ammonia Production 2022. https://royalsociety.org/news-resources/projects/low-carbon-energy-programme/green-ammonia/#:~:text=Ammonia%20is%20a%20pungent%20gas,to%20use%20low%2Dcarbon%20hydrogen.https://royalsociety.org/news-resources/projects/low-carbon-energy-programme/green-ammonia/#:~:text=Ammonia%20is%20a%20pungent%20gas,to%20use%20low%2Dcarbon%20hydrogen. (accessed February 10, 2025).

[23] British Ceramics Confederation. Hydrogen for the Ceramics Sector 2023. https://assets.publishing.service.gov.uk/media/649aa7eede86820013bc8e8f/British_Ceramic_Confederation_-_Hydrogen_for_the_Ceramics_Sector_-_IFS_Feasibility_Report.pdf (accessed January 30, 2025).

[24] Michelmersh. HyBrick Feasibility Study Press Release n.d. https://www.mbhplc.co.uk/sustainability/hybrick/ (accessed January 30, 2025).

[25] National Gas. Future Grid Phase 1 Closure Report 2024. https://www.nationalgas.com/sites/default/files/documents/FutureGrid%20Phase%201%20Closure%20Report%20July%202024.pdf (accessed January 28, 2025).

[26] HydrogenUK. Hydrogen to Power Report 2025. https://hydrogen-uk.org/wp-content/uploads/2025/01/HUK-Hydrogen-to-Power-Report-FINAL.pdf (accessed February 10, 2025).

[27] Adam P, Heunemann F, Von dem Bussche C, Engalshove S, Thiemann T. Hydrogen infrastructure-the pillar of energy transition. 2021.

[28] Adam P, Bode R, Groissboeck M. HYDROGEN TURBOMACHINERY Readying Pipeline Compressor Stations For 100% Hydrogen. 2020.

[29] National Gas. Future Grid Project 2025. https://www.nationalgas.com/future-energy/futuregrid (accessed April 8, 2025).

[30] Zabrzeski Ł, Janusz P, Liszka K, Łaciak M, Szurlej A. The effect of hydrogen transported through a gas pipeline on the functioning of gas compression station work. AGH Drilling, Oil, Gas 2017;34:959–68.

[31] Dong J, Song B, Yuan X, Jin W, Wang J. Research on aerodynamic performance of centrifugal compressors for hydrogen-mixed natural gas. PLoS One 2024;19:e0312829. https://doi.org/10.1371/journal.pone.0312829.

[32] Xiong Z, Liu Y, Cai Y, Chang W, Wang Z, Li Z, et al. Research on the effect of green hydrogen blending on natural gas centrifugal compressor performance. Renew Energy 2025;242:122378. https://doi.org/10.1016/j.renene.2025.122378.

[33] Bainier F, Kurz R. Impacts of H2 Blending on Capacity and Efficiency on a Gas Transport Network. Volume 9: Oil and Gas Applications; Supercritical CO2 Power Cycles; Wind Energy, American Society of Mechanical Engineers; 2019. https://doi.org/10.1115/GT2019-90348.

[34] Zhou D, Yan S, Huang D, Shao T, Xiao W, Hao J, et al. Modeling and simulation of the hydrogen blended gas-electricity integrated energy system and influence analysis of hydrogen blending modes. Energy 2022;239:121629. https://doi.org/https://doi.org/10.1016/j.energy.2021.121629.

[35] Witek M, Uilihoorn F. Impact of hydrogen blended natural gas on linepack energy for existing high pressure pipelines. Archives of Thermodynamics 2023. https://doi.org/10.24425/ather.2022.143174.

[36] National Grid Gas Transmission. GFOP study: Delivering within-day customer needs now and into the future 2021. https://www.nationalgas.com/insight-and-

innovation/gas-future-operability-planning-gfop/understanding-within-day-behaviour (accessed April 22, 2023).

[37] Wang C, Zhou D, Xiao W, Shui C, Ma T, Chen P, et al. Research on the dynamic characteristics of natural gas pipeline network with hydrogen injection considering line-pack influence. Int J Hydrogen Energy 2023;48:25469–86.

[38] Wesselink O, Krom A, van Agteren M. Balancing Hydrogen Networks Safely: A Method for Calculating Linepack Potential Without Causing Integrity Risk Due to Hydrogen-Enhanced Fatigue. International Pipeline Conference, vol. 86564, American Society of Mechanical Engineers; 2022, p. V001T08A003.

[39] Wu C, Li W, Qian T, Xie X, Wang J, Tang W, et al. Optimal scheduling of hydrogen blended integrated electricity–gas system considering gas linepack via a sequential second-order cone programming methodology. J Energy Storage 2024;76:109718.

[40] Jiang Y, Ren Z, Dong ZY, Sun Z, Terzija V. An Optimal Dispatch Method of Integrated Electricity and Gas Systems Incorporating Hydrogen Injection Flexibility. International Journal of Electrical Power & Energy Systems 2024;155:109662.

[41] Melaina M W., Antonia O., Penev M. Blending hydrogen into natural gas pipelines networks: A review of key issues. Tecnical Report NREL/TP-500-51995 2013.

[42] Fernandes LA, Marcon LRC, Rouboa A. Simulation of flow conditions for natural gas and hydrogen blends in the distribution natural gas network. Int J Hydrogen Energy 2024;59:199–213. https://doi.org/https://doi.org/10.1016/j.ijhydene.2024.01.014.

[43] Khabbazi AJ, Zabihi M, Li R, Hill M, Chou V, Quinn J. Mixing hydrogen into natural gas distribution pipeline system through Tee junctions. Int J Hydrogen Energy 2024;49:1332–44. https://doi.org/https://doi.org/10.1016/j.ijhydene.2023.11.038.

[44] Ekhtiari A, Flynn D, Syron E. Investigation of the Multi-Point Injection of Green Hydrogen from Curtailed Renewable Power into a Gas Network. Energies 2020, Vol 13, Page 6047 2020;13:6047. https://doi.org/10.3390/EN13226047.

[45] Saedi I, Mhanna S, Mancarella P. Integrated electricity and gas system modelling with hydrogen injections and gas composition tracking. Appl Energy 2021;303:117598. https://doi.org/https://doi.org/10.1016/j.apenergy.2021.117598.

[46] Allden J. Hydrogen deblending future and emerging technology watch 2022. https://doi.org/10.47120/npl.ENV45.

[47] National Grid Gas. HYDROGEN DEBLENDING IN THE GB NETWORK FEASIBILITY STUDY 2021. https://smarter.energynetworks.org/projects/nggtgn04/ (accessed December 27, 2023).

[48] DNV Energy Systems. Deblending phase 2: Conceptual Design and Network Considerations 2022. https://smarter.energynetworks.org/projects/nia_nggt0177/ (accessed December 27, 2023).

[49] Frontier Economics. Future Cost Trajectory for Gas Deblending 2022. https://smarter.energynetworks.org/projects/nia_nggt0177/ (accessed December 27, 2023).

[50] Arvesen Ø, Medbø V, Fleten S-E, Tomasgard A, Westgaard S. Linepack storage valuation under price uncertainty. Energy 2013;52:155–64. https://doi.org/https://doi.org/10.1016/j.energy.2012.12.031.

[51] Tran TH, French S, Ashman R, Kent E. Linepack Planning Models for Gas Transmission Network 2018. https://doi.org/10.1016/j.ejor.2018.01.033.

[52] Ettouney RS, El-Rifai MA. Quick estimation of gas pipeline inventory. J Pet Sci Eng 2009;69:139–42. https://doi.org/https://doi.org/10.1016/j.petrol.2009.08.004.

[53] Keyaerts N, Hallack M, Glachant J-M, D'haeseleer W. Gas market distorting effects of imbalanced gas balancing rules: Inefficient regulation of pipeline flexibility. Energy Policy 2011;39:865–76. https://doi.org/https://doi.org/10.1016/j.enpol.2010.11.006.

[54] Chaudry M, Jenkins N, Qadrdan M, Wu J. Combined gas and electricity network expansion planning. Appl Energy 2014;113:1171–87.

[55] Qadrdan M, Chaudry M, Jenkins N, Baruah P, Eyre N. Impact of transition to a low carbon power system on the GB gas network. Appl Energy 2015;151:1–12. https://doi.org/https://doi.org/10.1016/j.apenergy.2015.04.056.

[56] Qadrdan M, Chaudry M, Ekanayake J, Wu J, Jenkins N. Impact of wind variability on GB gas and electricity supply. 2010 IEEE International Conference on Sustainable Energy Technologies (ICSET), IEEE; 2010, p. 1–6.

[57] Qadrdan M, Chaudry M, Wu J, Jenkins N, Ekanayake J. Impact of a large penetration of wind generation on the GB gas network. Energy Policy 2010;38:5684–95.

[58] Qadrdan M, Abeysekera M, Chaudry M, Wu J, Jenkins N. Role of power-to-gas in an integrated gas and electricity system in Great Britain. Int J Hydrogen Energy 2015;40:5763–75. https://doi.org/10.1016/J.IJHYDENE.2015.03.004.

[59] Mi J, Khodayar ME. Operation of natural gas and electricity networks with line pack. Journal of Modern Power Systems and Clean Energy 2019;7:1056–70. https://doi.org/10.1007/s40565-019-0547-0.

[60] Schwele A, Ordoudis C, Kazempour J, Pinson P. Co-ordination of Power and Natural Gas Systems (Schwele A 2019). Proceedings of IEEE PES PowerTech 2020.

[61] Chaudry M, Jenkins N, Strbac G. Multi-time period combined gas and electricity network optimisation. Electric Power Systems Research 2008;78:1265–79. https://doi.org/10.1016/j.epsr.2007.11.002.

[62] Clegg S, Mancarella P. Integrated electrical and gas network modelling for assessment of different power-and-heat options. n.d.

[63] Clegg S, Mancarella P. Storing renewables in the gas network: Modelling of power-to-gas seasonal storage flexibility in low-carbon power systems. IET Generation, Transmission and Distribution 2016;10:566–75. https://doi.org/10.1049/iet-gtd.2015.0439.

[64] Clegg S, Mancarella P. Integrated electricity-heat-gas modelling and assessment , with applications to the Great Britain system . Part II : Transmission network analysis and low carbon technology and resilience case studies. Energy 2019;184:191–203. https://doi.org/10.1016/j.energy.2018.02.078.

[65] Zhou S, Pei R, Xie J, Gu W, Chen X. Integrated energy system operation optimization with gas linepack and thermal inertia. IET Renewable Power Generation 2021;15:3743–60. https://doi.org/10.1049/rpg2.12271.

[66] Hyett C, Pagnier L, Alisse J, Sabban L, Goldshtein I, Chertkov M. Control of Line Pack in Natural Gas System: Balancing Limited Resources under Uncertainty 2023.

[67] dos Santos PL, Azevedo-Perdicoulis T-P, Ramos JA, de Carvalho JLM, Jank G, Milhinhos J. An LPV Modeling and Identification Approach to Leakage Detection in High Pressure Natural Gas Transportation Networks. IEEE Transactions on Control Systems Technology 2011;19:77–92. https://doi.org/10.1109/TCST.2010.2077293.

[68] Sunday OI, Sunday BI, Oluwatoyin OA. Pressure transient analysis of multiple leakages in a natural gas pipeline. Journal of Petroleum and Gas Engineering 2014;5:1–8. https://doi.org/10.5897/JPGE203.0176.

[69] Z L, D H. Issues Surrounding Multiple Frame of Reference Models for Turbo Compressor Applications. International Compressor Engineering Conference, 2000.

[70] Liu J, Fan X, Tang X. Development of Automated Processes for Three-Dimensional Numerical Simulation of Compressor Performance Characteristics. Applied Sciences 2024;14:623. https://doi.org/10.3390/app14020623.

[71] Woldeyohannes AD, Majid MAA. Simulation model for natural gas transmission pipeline network system. Simul Model Pract Theory 2011;19:196–212. https://doi.org/https://doi.org/10.1016/j.simpat.2010.06.006.

[72] Clegg S, Mancarella P. Integrated electricity-heat-gas modelling and assessment, with applications to the Great Britain system. Part II: Transmission network analysis and low carbon technology and resilience case studies. Energy 2019;184:191–203. https://doi.org/10.1016/j.energy.2018.02.078.

[73] Ameli H, Qadrdan M, Strbac G. Value of gas network infrastructure flexibility in supporting cost effective operation of power systems. Appl Energy 2017;202:571–80. https://doi.org/https://doi.org/10.1016/j.apenergy.2017.05.132.

[74] Ryan MJ, Mailloux RL. Methods for performing composition tracking for pipeline networks. PSIG Annual Meeting, PSIG; 1986, p. PSIG-8609.

[75] Chaczykowski M, Sund F, Zarodkiewicz P, Hope SM. Gas composition tracking in transient pipeline flow. J Nat Gas Sci Eng 2018;55:321–30. https://doi.org/10.1016/j.jngse.2018.03.014.

[76] Zhang Z, Saedi I, Mhanna S, Wu K, Mancarella P. Modelling of gas network transient flows with multiple hydrogen injections and gas composition tracking. Int J Hydrogen Energy 2022;47:2220–33. https://doi.org/10.1016/J.IJHYDENE.2021.10.165.

[77] Tackie-Otoo BN, Mahmoud M, Murtaza M, Raza A, Kamal MS, Patil S, et al. An Integrated Experimental and Simulation Study for the Feasibility of Underground H 2 Production from Natural Gas Reservoirs. ACS Omega 2025;10:24510–9. https://doi.org/10.1021/acsomega.5c01056.

[78] Naeiji E, Noorpoor A, Ghanavati H. Energy, Exergy, and Economic Analysis of Cryogenic Distillation and Chemical Scrubbing for Biogas Upgrading and Hydrogen Production. Sustainability 2022;14:3686. https://doi.org/10.3390/su14063686.

[79] Maqsood K, Ali A, Nasir R, Abdulrahman A, Mahfouz A Bin, Ahmed A, et al. Experimental and simulation study on high-pressure V-L-S cryogenic hybrid network for CO2 capture from highly sour natural gas. Process Safety and Environmental Protection 2021;150:36–50. https://doi.org/10.1016/j.psep.2021.03.051.

[80] Erdöl HB, Şahin Fİ, Acaralı N. Novel Study on Cryogenic Distillation Process and Application by Using CHEMCAD Simulation. ACS Omega 2024;9:15165–74. https://doi.org/10.1021/acsomega.3c09490.

[81] Sutradhar P, Maity P, Kar S, Poddar S. Modelling and Optimization of PSA (Pressure Swing Adsorption) Unit by using Aspen Plus® and Design Expert®. International Journal of Inovative Technology and Exploring Engineering 2019.

[82] Ahmad F, Lau KK, Shariff AM, Murshid G. Process simulation and optimal design of membrane separation system for CO2 capture from natural gas. Comput Chem Eng 2012;36:119–28. https://doi.org/10.1016/j.compchemeng.2011.08.002.

[83] SIMONE. SIMONE software n.d. https://www.simone.eu/simone-simonesoftware-simulation.asp (accessed April 7, 2025).

[84] DNV. Hydraulic modelling software | hydraulic simulation software | Synergi Gas 2023. https://www.dnv.com/services/hydraulic-modelling-and-simulation-software-synergi-gas-3894 (accessed April 22, 2023).

[85] Microsoft. Power Query n.d. https://learn.microsoft.com/en-us/power-query/power-query-what-is-power-query (accessed April 7, 2025).

[86] OriginLab. Origin n.d. https://www.originlab.com/index.aspx?go=PRODUCTS/Origin (accessed April 7, 2025).

[87] NAN Steel. Pipe Roughness n.d. https://www.nan-steel.com/news/pipe-roughness.html (accessed January 28, 2025).

[88] Lielmezs J. Comparison of benedict-webb-rubin and starling equations of state for use in p-v-t calculations of binary mixtures. Thermochim Acta 1989;152:341–58. https://doi.org/10.1016/0040-6031(89)85403-6.

[89] National Grid Gas Transmission. Compressor Supporting Information December. 2019.

[90] National Grid Gas Transmission. Data Item Explorer n.d. https://mip-prd-web.azurewebsites.net/DataItemExplorer (accessed April 22, 2023).

[91] National Grid Gas Transmission. Data Item Explorer n.d. https://mip-prd-web.azurewebsites.net/DataItemExplorer (accessed April 22, 2023).

[92] National Grid Gas Transmission. St Fergus Investment Programme Engineering. n.d.

[93] National Grid Gas Transmission. Transmission Planning Code. 2015.

[94] National Gas. Hydrogen Blends in the NTS: A theoretical exploration. Gas Future Operability Planning. 2021. https://www.nationalgas.com/sites/default/files/documents/Hydrogen%20Blends%20in%20the%20NTS.pdf (accessed October 24, 2025).

[95] National Gas. Hydrogen Acceptability Study 2025. https://www.nationalgas.com/sites/default/files/documents/Hydrogen%20Acceptability%20Summary%20Report.pdf (accessed October 23, 2025).

[96] National Grid. Future Energy Scenarios 2022. http://fes.nationalgrid.com.

[97] National Grid Gas Transmission. Gas Ten Year Statement. 2022.

[98] National Grid Gas Transmission. Hydrogen Deblending in the GB Gas Network 2020.

Appendix A

Table A.1. Demand of nodes of the network in Winter Case.

Zone 0- Scotland								
Name	**Demand (GWh/d)**	**Profile**	**Name**	**Demand (GWh/d)**	**Profile**	**Name**	**Demand (GWh/d)**	**Profile**
Shell Backhaul	0	IND	Aberdeen	18.9	IND	Avonbridge inlet	1.8	IND
Balgray	47.6	IND	Blackness	0	IND	Burnhervie	0	IND
Careston	2.8	IND	Crieff	0	IND	Drum	5	IND
Gowkhall	0.8	IND	Kinknockie	0	IND	Kirriemuir inlet	1.6	IND
Kirriemuir outlet	0	IND	St Fergus	166.9	INT			
Zone 1- Scotland								
Name	**Demand (GWh/d)**	**Profile**	**Name**	**Demand (GWh/d)**	**Profile**	**Name**	**Demand (GWh/d)**	**Profile**
Grangemouth	8.8	LDZ	Moffat	16.8	LDZ	Armadale	1.6	LDZ
Avonbridge outlet	2.4	LDZ	Broxburn	8.4	LDZ	Coldstream	15.4	LDZ
Elvanfoot	0	LDZ	EX Saltwick	0	LDZ	Glenmavis	0	LDZ
Humbleton	0	LDZ	Hume	0	LDZ	Keld	0	LDZ
Langholm	0.7	LDZ	Lockerbie	0	LDZ	Longtown	0	LDZ
Lupton	0.1	LDZ	Melkinthorpe	0	LDZ	Moffat	4.2	LDZ
NetherHwclgh	0	LDZ	Soutra	0.1	LDZ	Towlaw	2.5	LDZ
Wetheral	33.8	LDZ						
Zone 2- Scotland								
Name	**Demand (GWh/d)**	**Profile**	**Name**	**Demand (GWh/d)**	**Profile**	**Name**	**Demand (GWh/d)**	**Profile**
Aberdeen	23.3	LDZ	Aberdeen Outlet	49.9	LDZ	Bishop Auckland	0	LDZ
Corbridge	0	LDZ	Guyzance	0	LDZ	Lochside	0	LDZ
Wooler	0	LDZ	Wooler	8.8	LDZ			
Zone 3- North East								
Name	**Demand (GWh/d)**	**Profile**	**Name**	**Demand (GWh/d)**	**Profile**	**Name**	**Demand (GWh/d)**	**Profile**
Gooleglass	0	LDZ	ICI BILLINGHAM	0	LDZ	Immingham	0	LDZ
Saltned	1.5	LDZ	Tees Phil BOC	0.1	LDZ	Aldbrough	0	LDZ
Asselby	0	LDZ	Baldersby	38	LDZ	Beeford	25.8	LDZ
Bishop Auckland	0	LDZ	Blyborough	7.1	LDZ	BurleyBank	2.7	LDZ
Cowpen Bewley	12.2	LDZ	Elton	0.7	LDZ	Ganstead	27.9	LDZ
LtBurdon	4.9	LDZ	Pannal	0	LDZ	Pickering	0	LDZ
Rawcliffe	8.8	LDZ	Scunthorpe	2.1	LDZ	Sproatley	38.3	LDZ

Susworth Trent E.	0	LDZ	Susworth Trent W.	0	LDZ	Thrintoft	0	LDZ
Towton	2.1	LDZ	Walesby	0.6	LDZ	Brigg	23.6	LDZ
Coryton &&	82.5	LDZ	Keadby	0	LDZ	Paull && Saltned	0	LDZ
Saltend	0	LDZ	Stallingbor1	0	LDZ	Teesside	49.9	LDZ
Thornton Curt	0	LDZ	West Burton	0	LDZ			

Zone 4- North West

Name	Demand (GWh/d)	Profile	Name	Demand (GWh/d)	Profile	Name	Demand (GWh/d)	Profile
Blackburn M &&	0	LDZ	Bridgewater	0	LDZ	Shellstar	0	LDZ
HaysChem	0	LDZ	ICIRuncorn Rocksavage	0	LDZ	Alrewas	81.9	LDZ
Alrewas Comp	12.3	LDZ	Aspley	5.6	LDZ	Audley	0	LDZ
Austrey	0	LDZ	Birch Heath	0	LDZ	Bridgefarm	0	LDZ
Burscough	0	LDZ	Carnforth	17	LDZ	Carnforth	0	LDZ
Churchover Comp	0	LDZ	Deeside	56.9	PS	Drointon	0.5	LDZ
Eccleston	0	LDZ	Elworth	8.9	LDZ	Entry Node	43.5	LDZ
EX Maelor	49.9	LDZ	Ferney Knoll	0	LDZ	Hawarden	46.8	LDZ
Helsby	46.2	LDZ	Holmes Chapel	0	LDZ	Malpas	0	LDZ
Mawdesley	0	LDZ	MickleTrafd	0	LDZ	Milwich	0	LDZ
Nether Kellet	0	LDZ	Nether Kellet	51.1	LDZ	No115	29.5	LDZ
No119	0	LDZ	Pennington	0	LDZ	Pickmere	4.2	LDZ
Samlesbury	0	LDZ	Shocklach	0	LDZ	Shustoke	0	LDZ
Treales	37.4	LDZ	Warburton	7.5	LDZ	Warnington	7	LDZ
Warnington	0	LDZ	WestonPoint	0	LDZ	Wheelock	11.8	LDZ
BurtonPoint	0	LDZ	Carrington	0	LDZ	EX Blackrod && blkburn	1.3	LDZ
Sellafield	0	LDZ						

Zone 5- Midlands

Name	Demand (GWh/d)	Profile	Name	Demand (GWh/d)	Profile	Name	Demand (GWh/d)	Profile
Alrewas Comp	6.2	LDZ	Blaby	0	LDZ	Brisley	0	LDZ
Caldecott	0	LDZ	Churchover	37.2	LDZ	Hatton	2.4	LDZ
Hatton	3	LDZ	Kings Lynn	0	LDZ	Kings Lynn	4.3	LDZ
Market Harboro'	0	LDZ	PeterborEye	0	LDZ	Peterborough	17.7	LDZ
Peterborough	0	LDZ	Peterborough Tee	11.8	LDZ	Saddle Bow	0	LDZ
Tur Langton	2.5	LDZ	West Winch	0	LDZ	Wisbech Nene E.	0	LDZ
Wisbech Nene W.	59	LDZ	Corby	0	LDZ	Cottam	24.7	LDZ
Kings Lynn	53.1	LDZ	Palmpaper	0	LDZ	Peterborough	14.3	LDZ
Staythorpe &&	1.1	LDZ						

Zone 6- South Wales

Name	Demand (GWh/d)	Profile	Name	Demand (GWh/d)	Profile	Name	Demand (GWh/d)	Profile
Aberdulais	4.3	LDZ	Churchover Comp	0	LDZ	Cirencester	30.1	LDZ
Clifrew	0	LDZ	Dowlais	0	LDZ	DyffrynClyd	0	LDZ
Easton Grey	0.4	LDZ	Evesham	9.5	LDZ	EX Seabank	0	LDZ
Fiddington	0	LDZ	Gilwern	0	LDZ	Honeybourne	0	LDZ

Leamington	0	LDZ	Littletn Drew	0	LDZ	Llanvetherine	0	LDZ
LowerQuinton	0	LDZ	Newbold Pacey	0	LDZ	Ross	0	LDZ
Rugby	62	LDZ	Sapperton	0	LDZ	StratfrdAvon	0	LDZ
Tirley Pri	0	LDZ	Treadow	0	LDZ	Wormington	3.7	LDZ
Wormington	0	LDZ	BaglanBay	76.1	LDZ	Seabank	4.2	LDZ
Zone 7- South West								
Name	**Demand (GWh/d)**	**Profile**	**Name**	**Demand (GWh/d)**	**Profile**	**Name**	**Demand (GWh/d)**	**Profile**
Centrax O/T	25.2	LDZ	Ayelsbury	17.3	LDZ	Ayelsbury	0	LDZ
Aylesbeare	0	LDZ	Barnington	11.3	LDZ	Braishfield	12.5	LDZ
Centrax Tee	0	LDZ	Chalgrove	3.4	LDZ	Coffinswell	16.4	LDZ
East Ilsley	0	LDZ	Choakford	29.9	LDZ	Gosberton	19.9	LDZ
Hardwick	67.2	LDZ	Horndon	0	LDZ	Huntingdon	14.3	LDZ
Huntingdon	0	LDZ	Ilchester	1.5	LDZ	Ispden	0	LDZ
Kenn (South)	112.2	LDZ	Kirkstead	0	LDZ	Lockerley	23.7	LDZ
Lockerley	0	LDZ	Lutton	0	LDZ	Mappowder	0	LDZ
Marchwood	0	LDZ	Michelmersh	0	LDZ	Nutfield	0	LDZ
Ottery St. Mary	117.2	LDZ	Pucklechurch	95.4	LDZ	Slapton	23.6	PS
Steppingley	11.2	PS	Sutton Bridge	0	PS	Theddlethorpe	97.4	PS
Tydd St. Giles	43.1	PS	Tydd St. Giles	21.2	PS	Willington	1.2	PS
Winkfield	25.6	PS	Didcot	6	PS	Langage	16.8	PS
Spalding	0.4	PS	Sutton Bridge	0	PS			
Zone 8- South Eeast								
Name	**Demand (GWh/d)**	**Profile**	**Name**	**Demand (GWh/d)**	**Profile**	**Name**	**Demand (GWh/d)**	**Profile**
Cambridge Comp Tee	0	PS	Peters Green	2	PS	Great Wilberham	3.3	PS
No198	6.2	PS	Roudham Heath	81.1	PS	Royston	22.2	PS
Whitwell	0	PS						
Zone 9- South East								
Name	**Demand (GWh/d)**	**Profile**	**Name**	**Demand (GWh/d)**	**Profile**	**Name**	**Demand (GWh/d)**	**Profile**
Diss Comp Tee	0	PS	Diss Tee	70	PS	EX Tatsfield	3.4	PS
Farmingham	0	PS	Gravesend Thames Sth	0	PS	Roxwell	5.5	PS
Roxwell	0	PS	Shorne	39.9	PS	Stanford Le Hope	10.2	PS
Yelverton	0	PS	Grain	0	PS	GTYarmouth	60.4	PS
Marchwood	38.2	PS	Medway	10.6	PS			
Zone 10- South East								
Name	**Demand (GWh/d)**	**Profile**	**Name**	**Demand (GWh/d)**	**Profile**	**Name**	**Demand (GWh/d)**	**Profile**
Matching Green	4.4	LDZ	Stapleford	0.8	LDZ	Tilbury Thames Nth	1.2	LDZ
Epping Green	0.3	LDZ	Lt Barford	0.9	LDZ	Rye House	13.5	LDZ
Zone 11- South Wales								
Name	**Demand (GWh/d)**	**Profile**	**Name**	**Demand (GWh/d)**	**Profile**	**Name**	**Demand (GWh/d)**	**Profile**
Felindre	0.9	LDZ	Felindre	0.1	LDZ	Three Cocks	0	LDZ
Blackbridge	14.4	LDZ						

Table A.2. Demand of nodes in Summer Case

Zone 0- Scotland								
Name	**Demand (GWh/d)**	**Profile**	**Name**	**Demand (GWh/d)**	**Profile**	**Name**	**Demand (GWh/d)**	**Profile**
Aberdeen	**8.282**	LDZ	**Aberdeen**	0	LDZ	**Aberdeen Inlet**	0	LDZ
Avonbridge Inlet	**0**	LDZ	**Balgray**	2.121	LDZ	**Blackness**	0	LDZ
Burnhervie	**0**	LDZ	**Careston**	0.707	LDZ	**Crieff**	0	LDZ
Drum	**0**	LDZ	**Gowkhall**	0	LDZ	**Kinknockie**	0.303	LDZ
Kirriemuir Inlet	**0**	LDZ	**Kirriemuir Outlet**	0	LDZ	**No65**	0	LDZ
Shell Backhaul	**0**	LDZ	**St Fergus**	0	LDZ			
Zone 1- Scotland								
Name	**Demand (GWh/d)**	**Profile**	**Name**	**Demand (GWh/d)**	**Profile**	**Name**	**Demand (GWh/d)**	**Profile**
Armadale	1.111	LDZ	**Hume**	0.101	LDZ	**NetherHwclgh**	0	LDZ
Avonbridge outlet	0	LDZ	**Keld**	0.606	LDZ	**No71**	0	LDZ
Broxburn	8.686	LDZ	**Langholm**	0	LDZ	**Peterhead**	52.722	PS
Coldstream	0.707	LDZ	**Lockerbie**	1.515	LDZ	**Saltwick**	0	LDZ
Elvanfoot	0	LDZ	**Longtown**	0	LDZ	**Soutra**	0	LDZ
Glenmavis	34.138	LDZ	**Lupton**	5.858	LDZ	**Towlaw**	0.101	LDZ
Grangemouth	0	Ind	**Melkinthorpe**	0.505	LDZ	**Wetheral**	0	LDZ
Humbleton	0	LDZ	**Moffat**	188.264	INT			
Zone 2- Scotland								
Name	**Demand (GWh/d)**	**Profile**	**Name**	**Demand (GWh/d)**	**Profile**	**Name**	**Demand (GWh/d)**	**Profile**
Aberdeen Outlet	0	LDZ	**Corbridge**	0	LDZ	**Guyzance**	0.303	LDZ
Lochside	0	LDZ	**No68**	0	LDZ	**Wooler**	0	LDZ
Wooler	0	LDZ						
Zone 3- North East								
Name	**Demand (GWh/d)**	**Profile**	**Name**	**Demand (GWh/d)**	**Profile**	**Name**	**Demand (GWh/d)**	**Profile**
Tees Phil BOC	2.626	Ind	**Gooleglass**	1.111	Ind	**ICIBillnghm**	0	Ind
Immingham	40.501	Ind	**Saltned**	0	Ind	**Asselby**	0.808	LDZ
Auckland	14.443	LDZ	**Baldersby**	0.202	LDZ	**Beeford**	0	LDZ
Bishop Auckland	14.443	LDZ	**Blyborough**	0	LDZ	**Brigg**	1.212	LDZ
BurleyBank	1.212	LDZ	**Cowpen Bewley**	10.403	LDZ	**Elton**	10.706	LDZ
Ganstead	4.545	LDZ	**Injection Easington**	0	LDZ	**LtBurdon**	0	LDZ
Pannal	30.603	LDZ	**Pickering**	0.707	LDZ	**Rawcliffe**	1.111	LDZ
Saltend	0	LDZ	**Scunthorpe**	0	LDZ	**Sproatley**	0	LDZ
Susworth Trent E.	0	LDZ	**Susworth Trent W.**	0	LDZ	**Thrintoft**	0.909	LDZ

Towton	0	LDZ	**Walesby**	0.202	LDZ	**Keadby**	34.946	PS
Stallingbor1	38.784	PS	**Thornton Curt**	44.238	PS	**WestBurton**	0	PS
Coryton	0	PS	**Paull & Saltned**	47.066	PS	**Teesside NSMP**	0.707	PS
Aldbrough	43.733	Storage						
Zone 4 – North West								
Name	**Demand (GWh/d)**	**Profile**	**Name**	**Demand (GWh/d)**	**Profile**	**Name**	**Demand (GWh/d)**	**Profile**
Alrewas	23.533	LDZ	**Alrewas**	0	LDZ	**Aspley**	0	LDZ
Audley	1.515	LDZ	**Austrey**	0.505	LDZ	**Birch Heath**	0	LDZ
Bridgefarm	0	LDZ	**Bridgewater**	0	Ind	**Burscough**	0	LDZ
BurtonPoint	42.319	LDZ	**Carnforth**	0	LDZ	**Carrington**	38.279	LDZ
Churchover Comp	0	LDZ	**Deeside**	0	PS	**Drointon**	0	LDZ
Eccleston	12.423	LDZ	**Elworth**	0	LDZ	**Blackrod &blkburn**	0	PS
Helsby	0	LDZ	**EX Maelor**	10.504	LDZ	**Shellstar**	0	Ind
WestonPoint	0.101	LDZ	**Ferney Knoll**	0	LDZ	**Hawarden**	0	LDZ
Holford	0	LDZ	**Holmes Chapel**	3.838	LDZ	**Blackburn M**	0	Ind
Ind HaysChem	0	Ind	**Injection**	0	LDZ	**Injection Deesside**	0	LDZ
Injection Hiltop	0	LDZ	**Malpas**	0	LDZ	**Mawdesley**	0	LDZ
MickleTrafd	0	LDZ	**Milwich**	0	LDZ	**Nether Kellet**	0	LDZ
No115	0	LDZ	**No119**	0	LDZ	**Pennington**	0	LDZ
Pickmere	0	LDZ	**Rocksavage**	16.059	Ind	**Samlesbury**	0	LDZ
Sellafield	0	PS	**Shocklach**	0	LDZ	**Shustoke**	0	LDZ
St Fergusublach	0	LDZ	**BurtonPoint**	0	LDZ	**Treales**	0	LDZ
Virtual Demand	0	LDZ	**Warburton**	64.438	LDZ	**Warmingham**	0	LDZ
Warnington	0	LDZ	**Wheelock**	0	LDZ	**Winnington**	0	LDZ
Zone 5- Midlands								
Name	**Demand (GWh/d)**	**Profile**	**Name**	**Demand (GWh/d)**	**Profile**	**Name**	**Demand (GWh/d)**	**Profile**
Alrewas Comp	0	LDZ	**Bacton**	634.886	INT	**BactonBBL**	162.004	INT
Blaby	6.666	LDZ	**Brisley**	0.505	LDZ	**Caldecott**	0	LDZ
Churchover	0	LDZ	**Corby**	0	PS	**Cottam**	0	PS
Hatton	0	LDZ	**Hatton**	0	LDZ	**Hatton**	0	LDZ
Kings Lynn	0	LDZ	**Kings Lynn**	0	LDZ	**KingsLynn**	0	PS
MktHarborough	0	LDZ	**Palmpaper &**	2.929	Ind	**Palmpaper &&**	2.222	LDZ
PeterborEye	3.232	LDZ	**Peterborough**	3.333	LDZ	**Peterborough**	0	LDZ
Peterborough	0	PS	**Peterborough Tee**	0	LDZ	**Saddle Bow**	0	LDZ
Staythorpe &&	39.087	LDZ	**TurLangton**	0	LDZ	**WestWinch**	1.919	LDZ
Wisbech Nene	0	LDZ	**Wisbech Nene W.**	0	LDZ			
Zone 6 – South Wales								
Name	**Demand (GWh/d)**	**Profile**	**Name**	**Demand (GWh/d)**	**Profile**	**Name**	**Demand (GWh/d)**	**Profile**
Aberdulais	0	LDZ	**Avonmouth**	0	LDZ	**Churchover Comp**	0	LDZ
Cirencester	0.404	LDZ	**Clifrew**	0	LDZ	**Dowlais**	23.836	LDZ

DyffrynClyd	5.555	LDZ	**EastonGrey**	0	LDZ	**Evesham**	0.808	LDZ
EX Seabank-Slack	35.249	LDZ	**Fiddington**	5.252	LDZ	**Gilwern-**	6.666	LDZ
Honeybourne	0	LDZ	**Leamington**	0	LDZ	**LittletnDrew**	0	LDZ
Llanvetherine	0	LDZ	**Lower Quinton**	0	LDZ	**Newbold Pacey**	0	LDZ
Pucklechurch	6.767	LDZ	**Ross**	0.909	LDZ	**Rugby-**	45.854	LDZ
Sapperton	0	LDZ	**Seabank**	35.249	LDZ	**StratfrdAvon**	1.01	LDZ
Tirley Pri	0	LDZ	**Treadow**	0	LDZ	**Wormington**	0	LDZ
Wormington	0	LDZ	**BaglanBay**	0	PS			

Zone 7- South West

Name	**Demand (GWh/d)**	**Profile**	**Name**	**Demand (GWh/d)**	**Profile**	**Name**	**Demand (GWh/d)**	**Profile**
Ind Centrax O/T	0	Ind	**Ayelsbury**	1.818	LDZ	**Ayelsbury**	0	LDZ
Aylesbeare	1.818	LDZ	**Barnington**	0	LDZ	**Barton Stusacey**	0	LDZ
Braishfield	42.42	LDZ	**Centrax Tee**	0	LDZ	**Chalgrove**	0	LDZ
Coffinswell	0.707	LDZ	**East Ilsley**	0	LDZ	**EX Choakford**	0	LDZ
Gosberton	0	LDZ	**Hardwick**	0	LDZ	**Horndon**	0	LDZ
Humbley	0	LDZ	**Huntingdon**	0	LDZ	**Huntingdon**	0	LDZ
Ilchester	0	LDZ	**Ipsden**	0	LDZ	**Kenn**	9.191	LDZ
Kirkstead	0.101	LDZ	**Langage- PS**	38.683	LDZ	**Lockerley**	0	LDZ
Lockerley	0	LDZ	**Lutton**	0	LDZ	**Mappowder**	4.444	LDZ
Marchwood	0	LDZ	**Michelmersh**	0	LDZ	**Nutfield**	0	LDZ
Ottery St Fergus. Mary	0	LDZ	**Spalding- PS**	37.673	LDZ	**Stseppingley**	0	LDZ
SuttonBridge	0.404	LDZ	**Theddlethorpe**	0	LDZ	**Tydd St Fergus. Giles**	0	LDZ
Tydd St Fergus. Giles	0	LDZ	**Willington**	0	LDZ	**Winkfield**	0	LDZ
Didcot -PS	49.086	PS	**Sutton Bridge -PS**	0.303	PS			

Zone 8- South East

Name	**Demand (GWh/d)**	**Profile**	**Name**	**Demand (GWh/d)**	**Profile**	**Name**	**Demand (GWh/d)**	**Profile**
Cambridge Comp Tee	0	LDZ	**EX PetersGrn**	21.311	LDZ	**Gt Wilbraham**	2.929	LDZ
RoudhamHeath	6.464	LDZ	**Royston**	1.313	LDZ	**Whitwell**	26.159	LD

Zone 9- South East

Name	**Demand (GWh/d)**	**Profile**	**Name**	**Demand (GWh/d)**	**Profile**	**Name**	**Demand (GWh/d)**	**Profile**
Diss Comp Tee	0	LDZ	**Diss Inlet**	0	LDZ	**Tatsfield**	34.542	LDZ
Farningham	0	LDZ	**Grain**	18.382	LDZ	**Grain**	18.382	PS
Gravesend Thames St Fergush	0	LDZ	**GTYarmouth**	0	PS	**Injection Kemsley**	0	LDZ
Marchwood	0	PS	**Medway**	0	PS	**Roxwell**	0	LDZ
Roxwell	0	LDZ	**Sellindge**	0	LDZ	**Shorne**	0	LDZ
St Fergusanford Le Hope	0	LDZ	**Grain**	0	LDZ	**Yelverton**	0	LDZ

Zone 10- South East

Name	**Demand (GWh/d)**	**Profile**	**Name**	**Demand (GWh/d)**	**Profile**	**Name**	**Demand (GWh/d)**	**Profile**

EppingGreen	17.675	PS	**Matching Green**	0	LDZ	**Tilbury Thames Nth**	0	LDZ
LuxboroughLn	0	LDZ	**RyeHouse**	0	PS			
LtBarford	0	PS	**Stapleford**	0	LDZ			
Zone 11- South Wales								
Name	**Demand (GWh/d)**	**Profile**	**Name**	**Demand (GWh/d)**	**Profile**	**Name**	**Demand (GWh/d)**	**Profile**
Blackbridge	104.232	PS	**Felindre**	0	LDZ	**Injection Milford H**	0	LDZ
Felindre	0	LDZ	**Felindre Valve inlet**	0	LDZ	**Three Cocks**	0	LDZ

Table A.3. Hourly disaggregation profiles

Time	**Profile**				
	Industrial (IND)	**Interconnector (INT)**	**Local Distribution Zone (LDZ)**	**Power Station (PS)**	**Supply**
00:00:00	0.036759	0.039175	0.036248	0.018512	0.041667
01:00:00	0.036036	0.042909	0.035798	0.018058	0.041667
02:00:00	0.036861	0.043403	0.035413	0.016168	0.041667
03:00:00	0.037393	0.041169	0.035709	0.016388	0.041667
04:00:00	0.036045	0.040489	0.035631	0.016648	0.041667
05:00:00	0.037207	0.040309	0.035894	0.016788	0.041667
06:00:00	0.036591	0.036826	0.039975	0.029029	0.041667
07:00:00	0.043836	0.037637	0.044226	0.040773	0.041667
08:00:00	0.043503	0.037867	0.046622	0.047334	0.041667
09:00:00	0.044549	0.037652	0.045355	0.049377	0.041667
10:00:00	0.043968	0.039439	0.043524	0.04838	0.041667
11:00:00	0.044142	0.039563	0.04183	0.04943	0.041667
12:00:00	0.041434	0.040079	0.042048	0.048968	0.041667
13:00:00	0.0419	0.040113	0.040763	0.050295	0.041667
14:00:00	0.042776	0.04341	0.041589	0.053499	0.041667
15:00:00	0.042173	0.043462	0.04189	0.050975	0.041667
16:00:00	0.044793	0.043416	0.043574	0.054825	0.041667
17:00:00	0.044855	0.048934	0.046019	0.057162	0.041667
18:00:00	0.044978	0.042968	0.045378	0.055847	0.041667
19:00:00	0.044978	0.042968	0.045378	0.055847	0.041667
20:00:00	0.044978	0.042968	0.045378	0.055847	0.041667
21:00:00	0.044978	0.042968	0.045378	0.055847	0.041667
22:00:00	0.044978	0.042968	0.045378	0.055847	0.041667
23:00:00	0.040287	0.049307	0.041	0.038156	0.041667
Total	1	1	1	1	1

Appendix B

In this appendix, the linepack and pressure level of each zone are analysed to determine the state of calibration of each zone. The comparison between linepack level results and pressure level results are crucial for understanding why a model linepack does not fall into seasonal range. Therefore, pressure levels and linepack levels are presented together in this section.

The pressure levels are represented using box plots in every other Figures, from Figure B.1 to Figure B.23. Each box represents pressure levels of a single node during the 24-hour simulation. The box is stretched from the minimum pressure level to the maximum pressure level of the node during the simulation. Since the number of data sets is small, there were no whiskers or outliers used in these graphs.

The boxplots shown in every other Figure from Figure B.2 to Figure B.24, demonstrate the zone-by-zone calibration of the high-pressure gas network. The subfigures on the left-hand side represent linepack range for the winter season, while those on the opposite side represent the linepack range for the summer season. The boxes represent the 25%–75% range, the whisker represents the remaining data within the 1.5 quartile range, and the black dots represent outliers.

i. The purple line drawn over the boxplots in every other Figure from Figure B.2 to Figure B.24 represents the result linepack, generated using Winter and Summer Models. If the purple line is placed within the range marked by the box and whiskers, the model is calibrated in that zone. However, if the red line is out of the range marked by box and whiskers in all the time steps, the model behaviour deviates from reality. In that case, the time-series plot of pressure levels of nodes in that zone were plotted to analyse the cause of large deviations.

Zone 0 in Scotland

Zone 0 is in Scotland, enveloping St Fergus supply point, St Fergus compressor, Aberdeen compressor and Avonbridge compressor. The pipelines in Zone 0 have a maximum operating pressure of 75 bar-g. Figure B.1depicts the pressure levels of nodes in Zone 0, Figure B.1(a) belongs to the Winter Model, and Figure B.1(b) belongs to the Summer Model. The pressure levels in both Winter and Summer Models are within the operational range. Furthermore, in the Winter Model, the smallest median is 45 bar-g, and the largest median is 65 bar-g. In the Summer Model, the smallest median is 45 bar-g, and the largest median is 60 bar-g. As seen in Figure B.1, pressure levels in the Winter Model have a larger variation than

in the Summer Model. In Zone 0, the largest variation in a single node in the Winter Model is 5 bar-g; however, in the Summer Model, the largest variation is less than 0.25 bar-g.

Both variation and level of pressure are reflected in the result linepack levels. According to Figure B.2(a), the starting linepack level in the Winter Model is 43.5 Mm3. The closing linepack level in the Winter Model is at 45 Mm3. The linepack swing, which is the difference between the maximum and minimum linepack level, is 2Mm3. However, the pressure levels are lower in the Summer Model than in the Winter Model. In addition, according to Figure B.2(b), the starting linepack level in the Summer Model is also lower at 43 Mm3 and the finishing linepack level at 43 Mm3. Moreover, since pressure variations are lower than the Winter Model, the linepack swing is also lower at 0.5 Mm3.

Comparing the Winter Model result linepack to the winter linepack range, the largest deviation from the season median is 5%. The smallest deviation from the season median is 0.4%. The largest deviation from the winter season's interquartile range is 6.1%. Comparing the Summer Model result linepack to the summer linepack range, the largest deviation from the season median is 3.6 %. The smallest deviation from the season median is 2.6%. The largest deviation from the winter season's interquartile range is 5.9%. Therefore, Zone 0 in both models is calibrated.

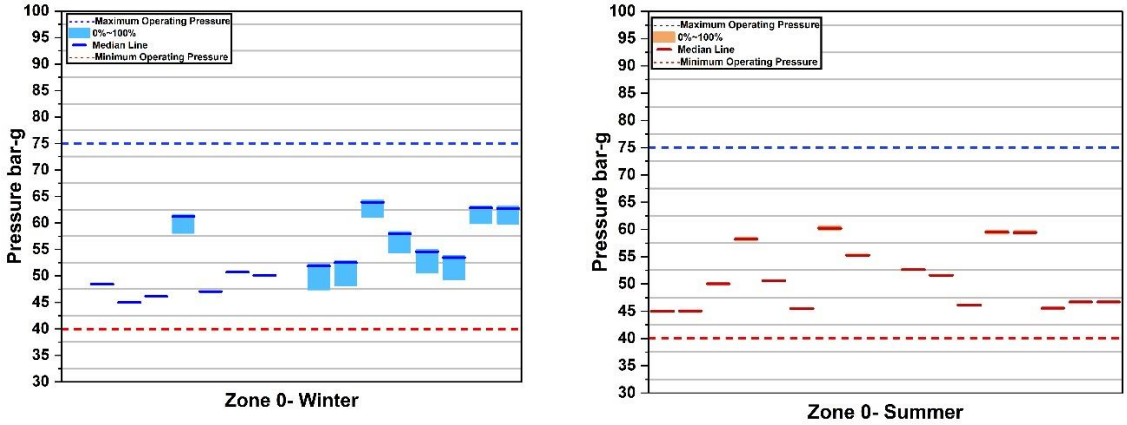

(a) **(b)**

Figure B.1. Pressure levels in each node in Zone 0 (a) in Winter Model and (b) in Summer Model.

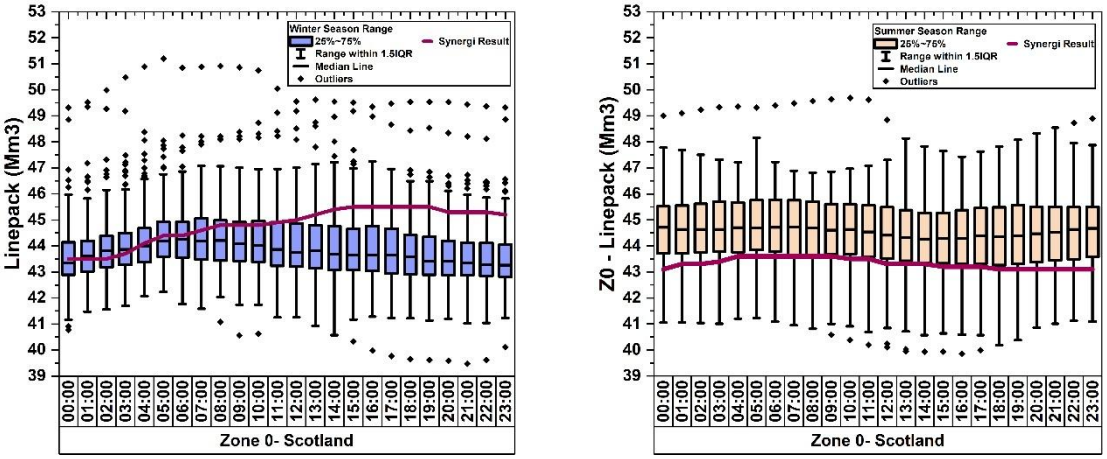

(a) **(b)**

Figure B.2. Result linepack versus seasonal linepack range in Zone 0 in (a) in Winter Model and (b) in Summer Model.

Zone 1 in Scotland

Zone 1 has two branches. The first branch connects Scotland to ortheast England, stretching from Avonbridge compressor to Lupton in Northeast England. The pipelines in this branch of Zone 1 have an maximum operational pressure (MOP) of 84 bar-g.

Figure B.3 depicts the pressure levels of nodes in Zone 1, Figure B.3(a) belongs to the Winter Model, and Figure B.3(b) belongs to the Summer Model. The pressure levels in both Winter and Summer Models are within the operational range. Furthermore, in the Winter Model, the smallest median is 52.5 bar-g, and the largest median is 70 bar-g. In the Summer Model, the smallest median is 57.5 bar-g, and the largest median is 67.5 bar-g. As seen in Figure B.3, pressure levels in the Winter Model have a larger variation than in the Summer Model. In Zone 1, the largest variation in a single node in the Winter Model is 5 bar-g; however, in the Summer Model, the largest variation is less than 2.5 bar-g.

According to Figure B.4(a), the starting linepack level in the Winter Model is 31.5 Mm3. The closing linepack level in the Winter Model is also at 31.5 Mm3. The linepack swing is less than 0.2 Mm3. According to Figure B.4(b), the starting linepack level in the Summer Model is also lower than in Winter Model at 32 Mm3, and the finishing linepack level is also at 32 Mm3. The linepack swing is 0.5 Mm3.

In the Winter Model, a comparison of the result linepack with the seasonal linepack range shows that the largest deviation from the winter season median is 4.8%. The smallest deviation from the season median is 1.5 %. The largest deviation from the winter season's interquartile range is 7.8%. In the Summer Model, comparing the result linepack with the seasonal linepack range shows that the largest deviation from the season median is 3.1%.

The smallest deviation from the season median is 0.6 %. The largest deviation from the winter season's interquartile range is 9.1%. Therefore, Zone 1 in both models is calibrated.

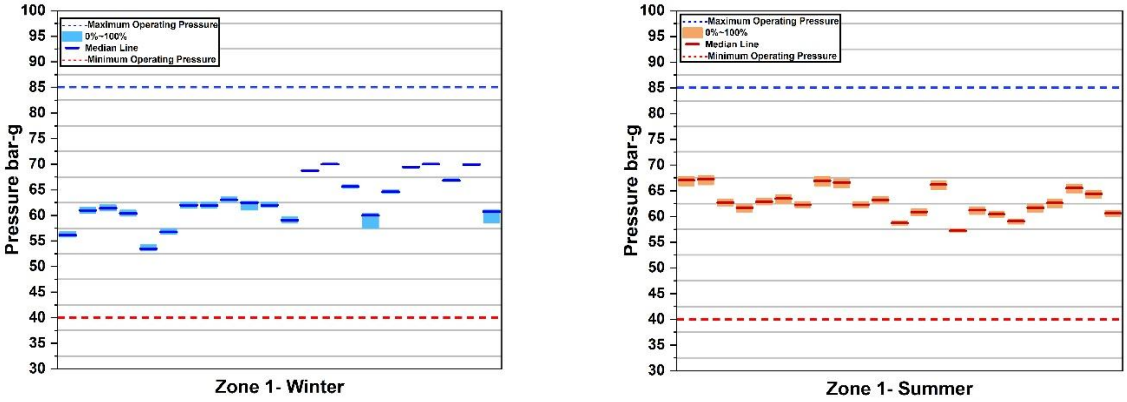

(a) **(b)**

Figure B.3. Pressure levels in each node in Zone 1 in (a) Winter Model and (b) in Summer Model.

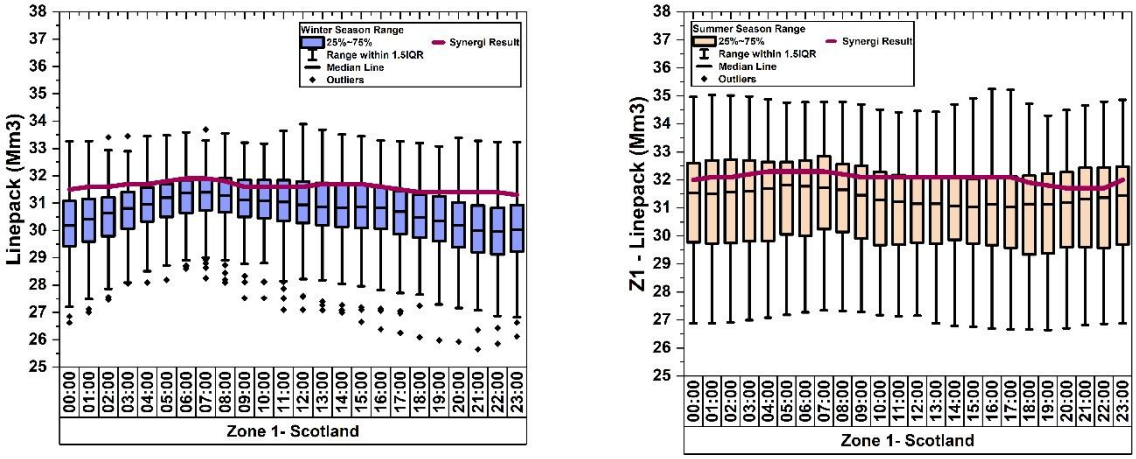

(a) **(b)**

Figure B.4. Result linepack versus seasonal linepack range in Zone 1 in (a) in Winter Model and (b) in Summer Model.

Zone 2 in Scotland

Figure B.5 illustrates the pressure levels of nodes in Zone 2, with Figure B.5 (a) representing the Winter Model and Figure B.5 (b) the Summer Model. Notably, the pressure levels in both models consistently fall within the operational range, indicating the system's reliability. In the Winter Model, the pressure medians range from 60 bar-g to 70 bar-g, while in the Summer Model, they span from 61.5 bar-g to 63 bar-g. As depicted in Figure B.5, the Winter Model exhibits a slightly larger variation in pressure levels than the Summer Model, but both remain within acceptable limits. In Zone 2, the largest variation in a single node in the Winter Model is 2.5 bar-g, while in the Summer Model it is less than 0.1 bar-g.

Figure B.6 (a) demonstrates the linepack levels in the Winter Model, with a starting level of 29 Mm3 and a closing level of 30 Mm3, resulting in a linepack swing of 1 Mm3.

Similarly, Figure B.6 (b) shows the linepack levels in the Summer Model, with a starting level of 28.8 Mm3 and a closing level of 29 Mm3, resulting in a linepack swing of 0.25 Mm3. These figures highlight the efficient performance of the system, maintaining a consistent linepack swing within acceptable limits.

In the Winter Model, the result linepack of Zone 2 exhibits a deviation from the season median, ranging from 7.4% to 10.4%, demonstrating the system's precision. Similarly, in the Summer Model the result linepack of Zone 2 shows a deviation from the season median, ranging from 0.6% to 8.3%. These figures underscore the system's accuracy in maintaining linepack deviations within predictable and manageable ranges.

Pipelines in Zone 2 have a MOP of 85 bar-g. However, compressing this region to such a high-pressure results in linepack in other regions of Scotland and North England going out of seasonal range. It is speculated that this region is also separated from the rest of the network using regulator stations, which is outside of the scope of this research.

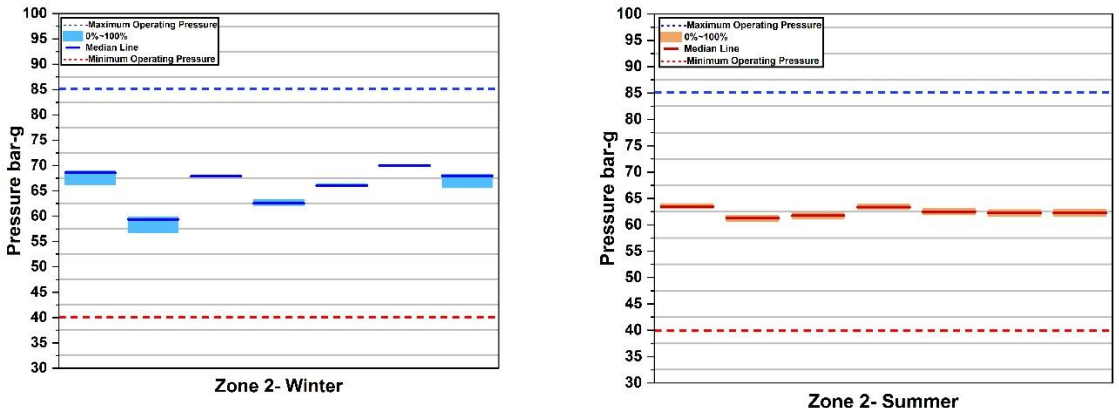

(a) (b)

Figure B.5. Pressure levels in each node in Zone 2 in (a) in Winter Model and (b) in Summer Model.

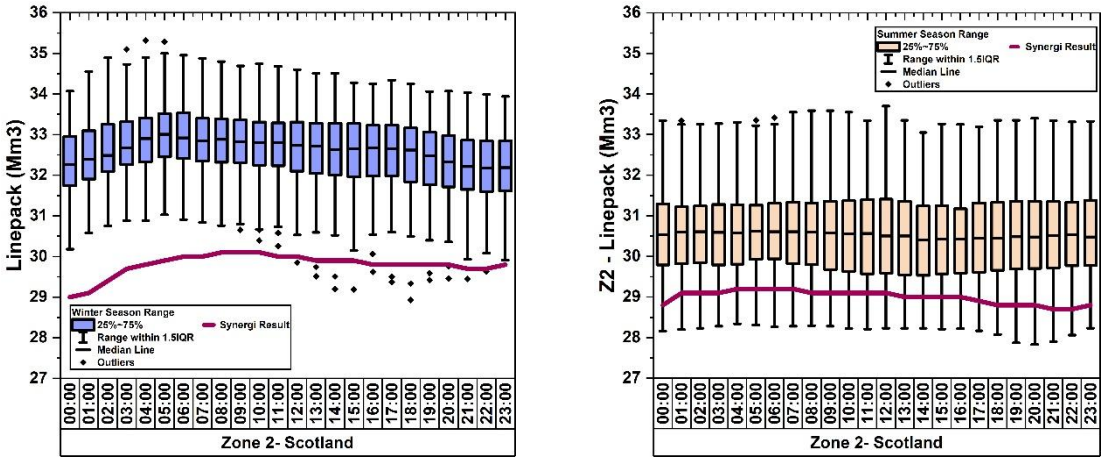

(a) (b)

Figure B.6. Result linepack versus seasonal linepack range in Zone 2 in (a) in Winter Model and (b) in Summer Model.

Zone 3 in Northeast England

Zone 3 envelopes all the pipelines in Northwest England. This region includes Teesside and Easington supply points. It has three entry/exit points: the first is Bishop Auckland compressor station, connecting Zone 3 to Scotland. The second is the Nether Kellet compressor, connecting Zone 3 to the Northwest. Moreover, the Hatton compressor station connects Zone 3 to the Midlands and East of England. The pipelines in this region have an MOP of 70 bar-g.

Figure B.7 depicts the pressure levels of nodes in Zone 3. Figure B.7 (a) belongs to the Winter Model, and Figure B.7(b) belongs to the Summer Model. The pressure levels in both Winter and Summer Models are within the operational range. Furthermore, in the Winter Model, the smallest median is 55 bar-g, and the largest median is 62.5 bar-g. In the Summer Model, the smallest median is 54 bar-g, and the largest median is 61.75 bar-g. As seen in Figure B.7, pressure levels in the Winter Model have a larger variation than in the Summer Model. In Zone 3, the largest variation in a single node in the Winter Model is 1Mm3. In the Summer Model, the largest variation is less than 0.75 bar-g.

According to Figure B.8 (a), the starting linepack level in the Winter Model is 53.5 Mm3. The closing linepack level is 53 Mm3. The linepack swing is 1 Mm3. According to Figure B.8(b), the starting linepack level in the Summer Model is also lower at 52.5 Mm3 and the finishing linepack level is also 53 Mm3. Since pressure variations are lower than in the Winter Model, the linepack swing is 0.5 Mm3.

In the Winter Model, the result linepack of Zone 3, the largest deviation from the season median, is 3.2%. The smallest deviation from the season median is 0.1%. The largest deviation from the winter season’s interquartile range is 4.7%. In the Summer Model, the result linepack of Zone 3, the largest deviation from the season median, is 2 %. The smallest deviation from the season median is 0%. The largest deviation from the winter season’s interquartile range is 4%

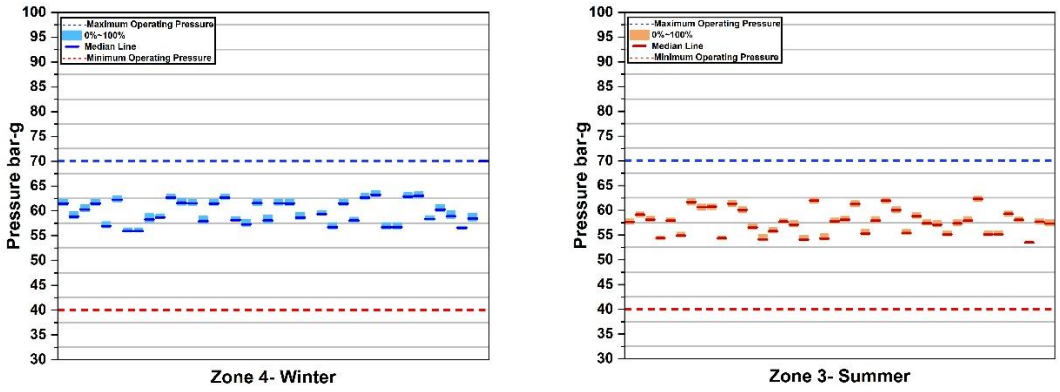

(a) **(b)**

Figure B.7. Pressure levels in each node in Zone 3 in (a)Winter Model and (b) in Summer Model.

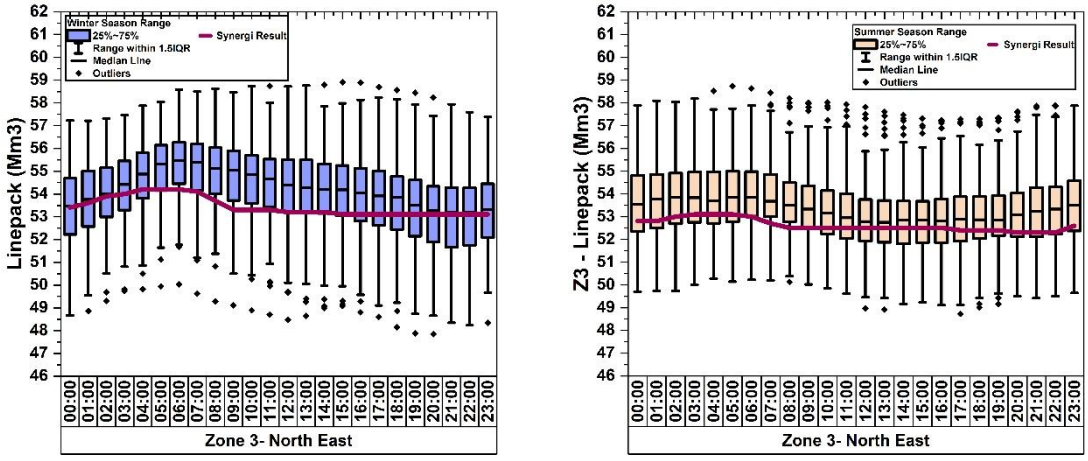

(a) **(b)**

Figure B.8. Result linepack versus seasonal linepack range in Zone 3 in (a) Winter Model and (b) Summer Model.

Zone 4 in Northwest England

Zone 4 envelopes the pipelines in the Northwest of England. It includes Burton Point Barrow Supply points and Hilltop Storage points. The zone has three entry/exit points:

1. Lupton, connecting Scotland and Northwest.
2. The Nether Kellet connects the Northwest to the Northeast.
3. The Church over compressor connects Northwest to Midlands and East.

The pipes in this region have an MOP of 70 bar-g.

Figure B.9(a) illustrates the pressure levels of nodes in Zone 4, with Figure B.9 (a) representing the Winter Model and Figure B.9 (b) the Summer Model. Notably, the pressure

levels in both models consistently fall within the operational range, demonstrating the stability of our operations. In the Winter Model, the median pressure ranges from 40 bar-g to 70 bar-g; in the Summer Model, it varies from 57.5 bar-g to 69 bar-g. The largest variation in a single node is 17.5 bar-g in the Winter Model and 5 bar-g in the Summer Model, further indicating the reliability of our system.

According to Figure B.10 (a), the starting linepack level in the Winter Model is 43 Mm3. The closing linepack level is 41.5 Mm3. The linepack swing is 4 Mm3. According to Figure Figure B.10(b), the starting linepack level in the Summer Model is also lower at 44.5 Mm3, and the finishing linepack level is also 44.5 Mm3. Since pressure variations are lower than in the Winter Model, the linepack swing is at 1.5 Mm3.

In the Winter Model, the result linepack of Zone 4 shows the largest deviation from the season median (i.e., 20.9 %). The smallest deviation is 16.6 %. The largest deviation from the winter season's interquartile range is 24.9%. In the Summer Model, the result linepack of Zone 4 shows the largest deviation from the season median (i.e., 15.4%). The smallest deviation is 13.9 %. The largest deviation from the winter season's interquartile range is 18.8 %.

Based on the linepack results, it is evident that Zone 4 is not calibrated in either of the models. The comparison between seasonal ranges and result linepack levels suggests that the pressure levels in Zone 4 are lower than the model. To address this, a potential solution could be to operate Alrewas and Carnforth compressors as regulator stations, creating an isolated zone with pressures between 45 bar-g and 55 bar-g. This approach falls outside the scope of this research, but may be explored in further study.

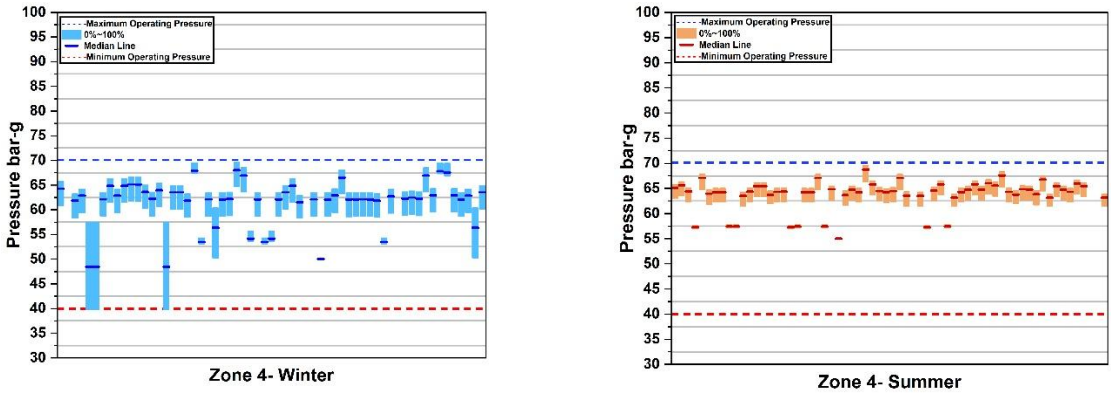

(a) **(b)**

Figure B.9. Pressure levels in each node in Zone 4 in (a) Winter Model and (b) Summer Model.

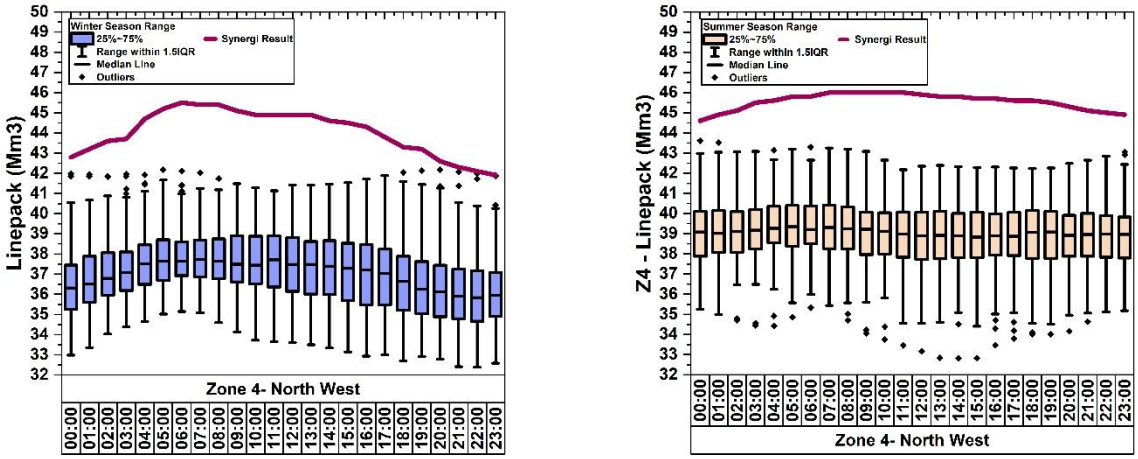

(a) **(b)**

Figure B.10. Result linepack versus seasonal linepack range in Zone 4 in (a) Winter Model and (b) in Summer Model.

Zone 5 in Midlands and East England

Zone 5 envelopes pipelines in the Midlands and East of England, including the Bacton supply point. Zone 5 has multiple entry/exit points. From the Hatton compressor, it connects to the Northeast; from the Alrewas compressor, it connects to the Northwest; from the Peterborough compressor, it connects to the South and Southwest regions; and finally, from the Churchover compressor, it connects to South Wales. The pipelines in this region have an MOP of 70 bar-g.

Figure B.11 depicts the pressure levels of nodes in Zone 5, Figure B.11(a) belongs to the Winter Model, and Figure B.11(b) belongs to the Summer Model. The pressure levels in both Winter and Summer Models are within the operational range. Furthermore, in the Winter Model, the smallest median is 55 bar-g, and the largest median is 67.5 bar-g. In the Summer Model, the smallest median is 49 bar-g, and the largest median is 61 bar-g. In Zone 5, the largest variation in a single node in the Winter Model is 7.5 bar-g. In the Summer Model, the largest variation is 5 bar-g.

According to Figure B.12(a), the starting linepack level in the Winter Model is 39 Mm3. The closing linepack level is 38.5 Mm3. The linepack swing is 3 Mm3. According to Figure B.12(b), the starting linepack level in the Summer Model is also lower, at 36 Mm3, and the finishing linepack level is also 35.5 Mm3. Since pressure variations are lower than in the Winter Model, the linepack swing is 2.5 Mm3.

In the Winter Model, the result linepack of Zone 5, the largest deviation from the season median, is 8.2%. The smallest deviation from the season median is 2.2%. The largest deviation

from the winter season's interquartile range is 10.5%. In the Summer Model, the result linepack of Zone 5, the largest deviation from the season median, is 5.5 %. The smallest deviation from the season median is 3.4%. The largest deviation from the winter season's interquartile range is 7%. Therefore, the model is calibrated in Zone 5

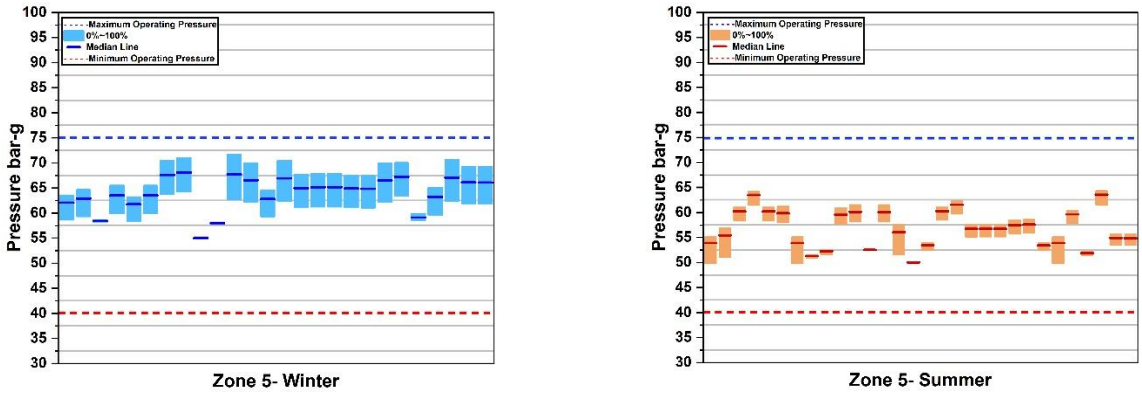

(a) (b)

Figure B.11. Pressure levels in each node in Zone 5 in (a) Winter Model and (b) Summer Model.

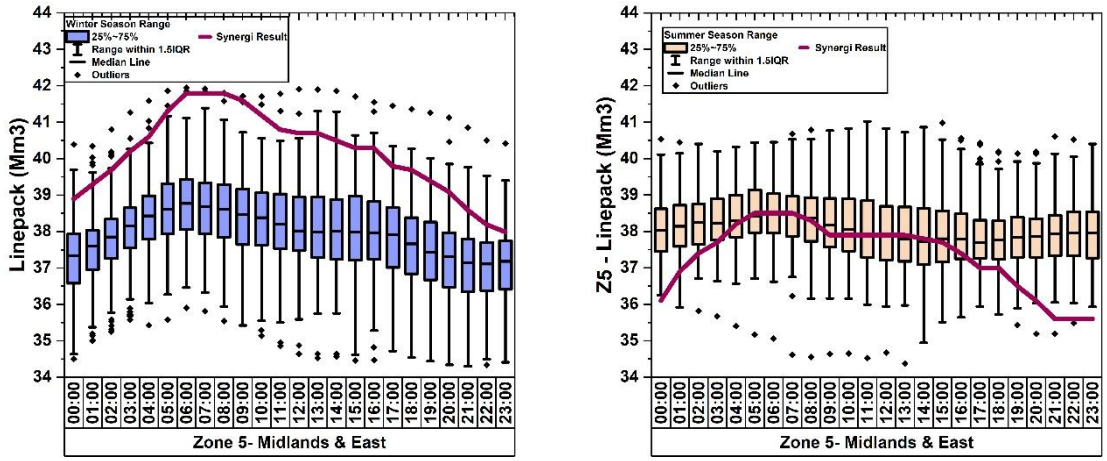

(a) (b)

Figure B.12. Result linepack versus seasonal linepack range in Zone 5 in (a) Winter Model and (b) Summer Model.

Zone 6 in South Wales

Zone 6 has two branches in South Wales and Southwest England. The first branch stretches from Churchover compressor to Pucklechurch junction in Southwest England. The second branch stretches from Felindre compressor to Wormington compressor, connecting South Wales to Southwest England. The pipes in this branch have an MOP of 70 bar-g

Figure B.13 depicts the pressure levels of nodes in Zone 5; Figure B.13(a) belongs to the Winter Model, and Figure B.13(b) belongs to the Summer Model. The pressure levels in

both Winter and Summer Models are within the operational range. Furthermore, in the Winter Model, the smallest median is 52.5 bar-g, and the largest median is 62.5 bar-g. In the Summer Model, the smallest median is 45 bar-g, and the largest median is 65 bar-g. In Zone 6, The largest variation in a single node in the Winter Model is 6 bar-g. In the Summer Model, the largest variation is 10 bar-g.

According to Figure B.14(a), the starting linepack level in the Winter Model is 14.6 Mm3. The closing linepack level is also 14.5 Mm3. The linepack swing is 0.7 Mm3. According to Figure B.14(b), the starting linepack level in the Summer Model is also lower at 13.85 Mm3. The finishing linepack level is also 13.85 Mm3. The linepack swing in the Summer Model is only 0.25 Mm3.

Comparing result linepack levels with the range, in the Winter Model, the result linepack of Zone 6, the largest deviation from the season median, is 2.5%. The smallest deviation from the season median is 0.1 %. The largest deviation from the winter season's interquartile range is 2.5%.

In the Summer Model, the result linepack of Zone 6 shows the largest deviation from the season median (i.e., 5.2%). The smallest deviation is 3 %. The largest deviation from the winter season's interquartile range is 7.7%.

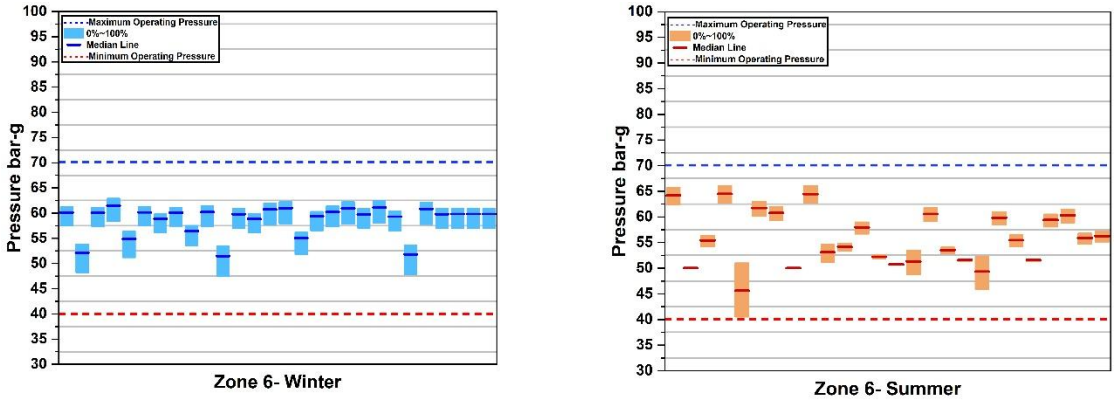

(a) **(b)**

Figure B.13. Pressure levels in each node in Zone 6 in (a) Winter Model and (b) Summer Model.

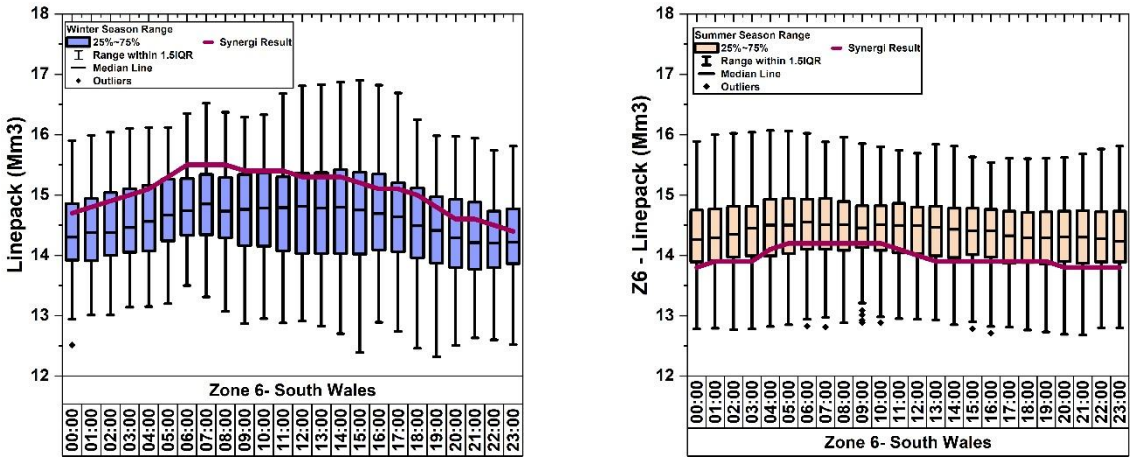

(a) **(b)**

Figure B.14. Result linepack versus seasonal linepack range in Zone 6 in (a) Winter Model and (b) Summer Model.

Zone 11 in South Wales

Zone 11, a significant area located in South Wales, encompasses the Milford Haven supply point and is interconnected with Zone 6 through three entry/exit points. These points include the Clifrew, Treadow and Tirley Pri regulator stations. The pipelines in Zone 11 operate at a MOP of 95 bar-g.

Figure B.15 visually represents the pressure levels at various nodes in Zone 11. Notably, the Winter and Summer Models demonstrate pressure levels well within the operational range. In the Winter Model, the median pressure levels range from 60 bar-g to 62.5 bar-g; in the Summer Model, they vary from 60 bar-g to 70 bar-g. The largest variation in a single node is 3 bar-g in the Winter Model and 5 bar-g in the Summer Model.

Figure B.16(a) illustrates the linepack levels in the Winter Model, with a starting level of 23 Mm3 and a closing level of 22 Mm3, resulting in a swing of 1.5 Mm3. In contrast, Figure B.16 (b) shows the linepack levels in the Summer Model, which remain constant at 25.5 Mm3, indicating a swing of only 1 Mm3.

Comparing the result linepack with the season range in the Winter Model, the largest deviation from the season median is 27%. The smallest deviation from the season median is 24.9%. The largest deviation from the winter season's interquartile range is 30.3%. In the Summer Model, the result linepack of Zone 11 shows the largest deviation from the season median, 19.3%. The smallest deviation from the season median is 16.4%. The largest deviation from the winter season's interquartile range is 23.2%.

Zone 11 is, therefore, not calibrated. The result is that linepack levels in Zone 11 are lower than the season range in winter and significantly lower in summer. Zone 11 consists of

pipelines with a MOP of 95 bar-g. These pipelines are separated from the rest of the network using three regulator stations in Clifrew, Treadow and Tireley Pri. Simulating regulator stations is outside of the scope of this thesis. Therefore, linepack levels in Zone 11 cannot imitate seasonal linepack levels.

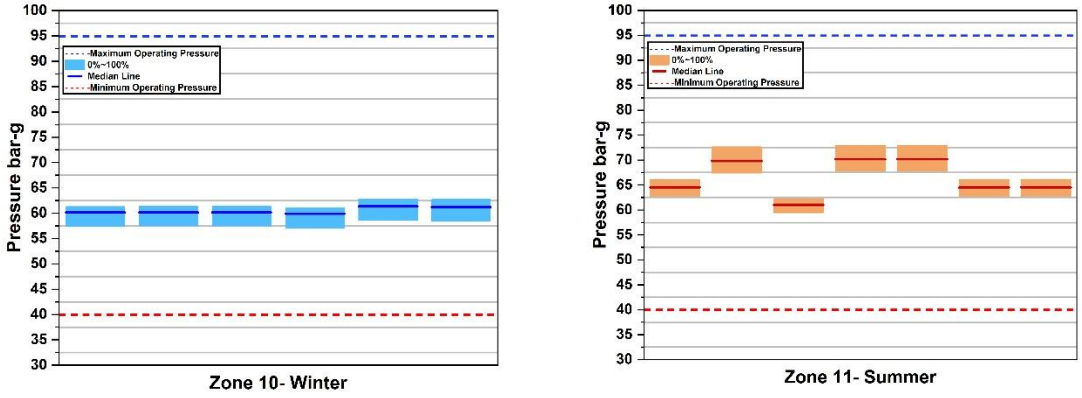

(a) **(b)**

Figure B.15. Pressure levels in each node in Zone 11 in (a) Winter Model and (b) Summer Model.

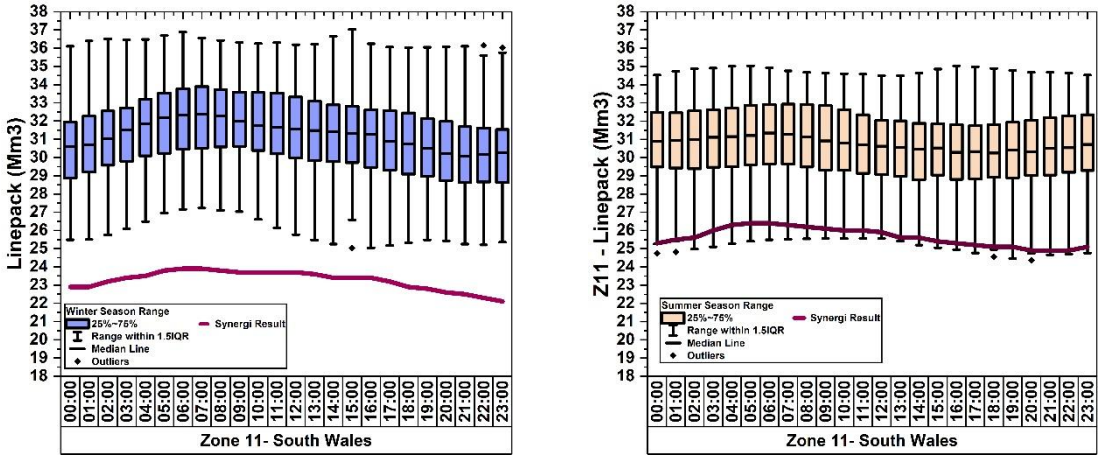

(a) **(b)**

Figure B.16. Result linepack versus seasonal linepack range in Zone 11 in (a) Winter Model and (b) Summer Model.

Zone 7 in Southwest England

Zone 7 stretches from the Midlands and East to Southwest England. It has four entry-exit points. The Hatton compressor connects the zone to the Northeast of England. The Peterborough compressor connects it to Zone 7, also in the Midlands and East. The Huntingdon compressor connects Zone 5 to the Southeast of England. The pipelines in Zone 7 have an MOP of 75 bar-g.

Figure B.17 depicts the pressure levels of nodes in Zone 7, Figure B.17(a) belongs to the Winter Model, and Figure B.17(b) belongs to the Summer Model. The pressure levels in both winter and Summer Models are within the operational range. Furthermore, in the Winter Model, the smallest median is 47.5 bar-g, and the largest median is 67.5 bar-g. In the Summer Model, the smallest median is 47.5 bar-g, and the largest median is 60 bar-g. In Zone 7, The largest variation in a single node in the Winter Model is 7.5 bar-g; in the Summer Model, the largest variation is 8.5 bar-g.

According to Figure B.18(a), the starting linepack level in the Winter Model is 39.5 Mm3. The closing linepack level is 39 Mm3. The linepack swing is 3.5 Mm3. According to Figure B.18(b), the starting linepack level in the Summer Model is also lower, at 37 Mm3. The finishing linepack level is also 37 Mm3. The linepack swing in the Summer Model is 3 Mm3.

In the Winter Model, the result linepack of Zone 7, the largest deviation from the season median, is 2.7%. The smallest deviation from the season median is 0.1%. The largest deviation from the winter season's interquartile range is 6.4%. In the Summer Model, the result linepack of Zone 7, the largest deviation from the season median, is 2.8%. The smallest deviation from the season median is 0.1%. The largest deviation from the winter season's interquartile range is 5.4%. Therefore, Zone 7 is calibrated.

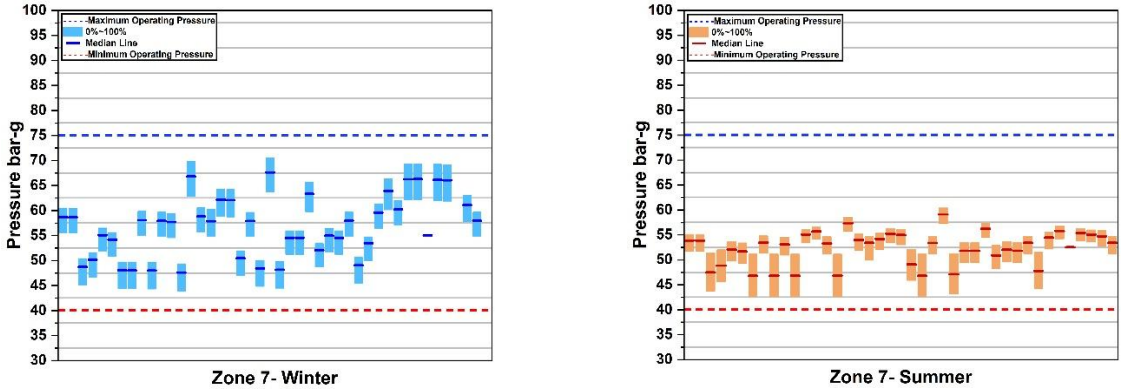

(a) **(b)**

Figure B.17. Pressure levels in each node in Zone 7 in (a) Winter Model and (b) Summer Model.

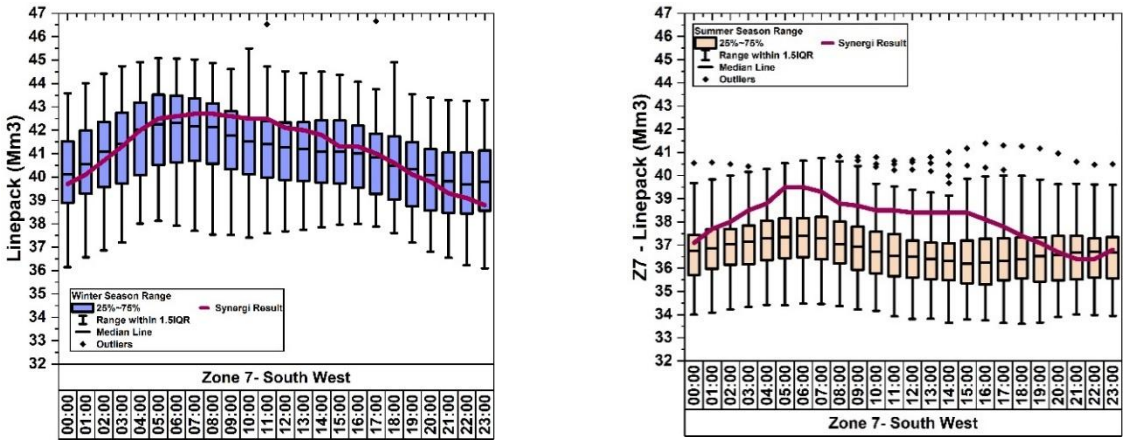

(a) **(b)**

Figure B.18. Result linepack versus seasonal linepack range in Zone 7 in (a) Winter Model and (b) Summer Model.

Zone 8 in Southeast England

Zone 8 stretches from the Bacton supply point to Peters Green in Southeast England. The pipelines have an MOP of 70 bar-g.

Figure B.19 depicts the pressure levels of nodes in Zone 8, Figure B.19(a) belongs to the Winter Model, and Figure B.19(b) belongs to the Summer Model. The pressure levels in both winter and Summer Models are within the operational range. Furthermore, all the medians are at 59.5 bar-g in the Winter Model. In the Summer Model, all the medians are at 54.5 bar-g. In Zone 8, The largest variation in a single node in the Winter Model is 4 bar-g. In the Summer Model, the largest variation is 4 bar-g.

According to Figure B.20(a), the starting linepack level in the Winter Model is 7.6 Mm3. The closing linepack level is 7.5 Mm3. The linepack swing is 0.5 Mm3. According to Figure B.20 (b), the starting linepack level in the Summer Model is 6.4 Mm3, and the closing linepack level is also 6.3 Mm3. The linepack swing in the Summer Model is 0.5 Mm3.

Comparing the result linepack with the seasonal range, the largest deviation from the season median in the Winter Model is 6%. The smallest deviation from the season median is 2.9%. The largest deviation from the winter season's interquartile range is 8.8%. In the Summer Model, the result linepack of Zone 8, the largest deviation from the season median, is 8.9%. The smallest deviation from the season median is 7.6%. The largest deviation from the winter season's interquartile range is 11.6%. Therefore, Zone 8 is calibrated.

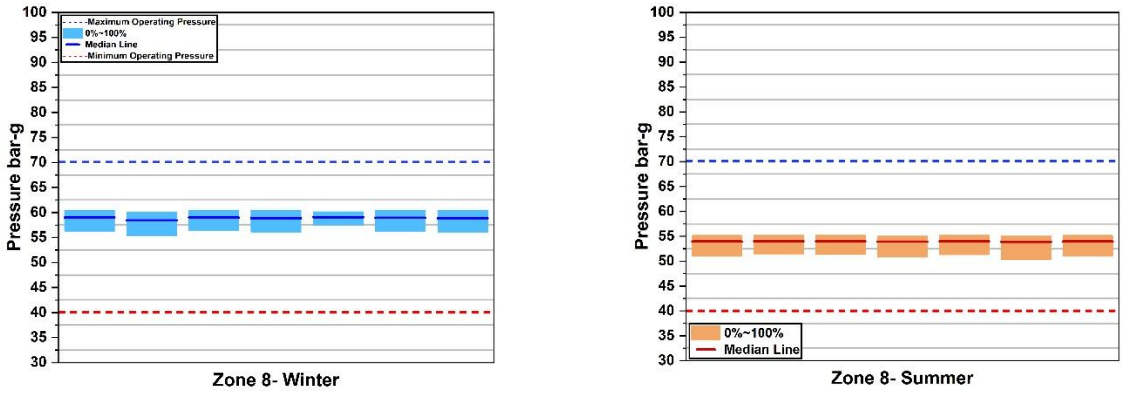

(a) **(b)**

Figure B.19. Pressure levels in each node in Zone 8 in (a) Winter Model and (b) Summer Model.

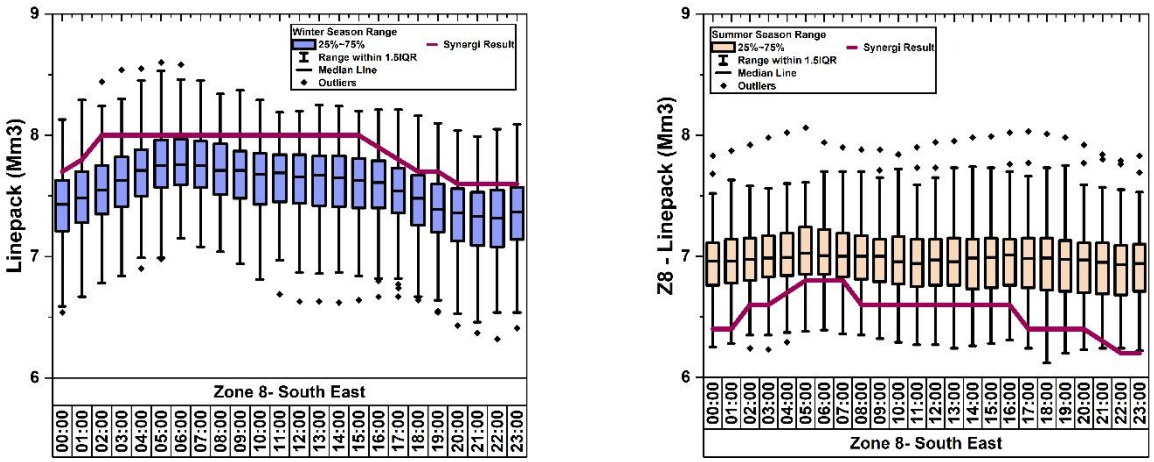

(a) **(b)**

Figure B.20. Result linepack versus seasonal linepack range in Zone 8 in (a) Winter Model and (b) Summer Model.

Zone 9 in Southeast England

Zone 9 stretches from Bacton supply points to Southeast England's Isle of Grain supply point. The pipelines have an MOP of 70 bar-g.

Figure B.21 depicts the pressure levels of nodes in Zone 9, Figure B.21(a) belongs to the Winter Model, and Figure B.21(b) belongs to the Summer Model. In Zone 9, the pressure levels in both winter and Summer Models are within the operational range. Furthermore, in the Winter Model, the smallest median is 52.5 bar-g, and the largest median is 65 bar-g. In the Summer Model, all the medians are at 52.5 bar-g. The largest variation in a single node in the Winter Model is 7 bar-g. In the Summer Model, the largest variation is 4 bar-g.

According to Figure B.22(a), the starting linepack level in the Winter Model is 11.1 Mm3. The closing linepack level is 10.75 Mm3. The linepack swing is 0.75 Mm3. According to

Figure B.22(b), the starting linepack level in the Summer Model is 10.5 Mm3, and the closing linepack level is also 10.25 Mm3. The linepack swing in the Summer Model is 1.25 Mm3.

In the Winter Model, the result linepack of Zone 9, the largest deviation from the season median, is 5%. The smallest deviation from the season median is 0.9%. The largest deviation from the winter season's interquartile range is 7.3%. In the Summer Model, the result linepack of Zone 9, the largest deviation from the season median, is 2.4%. The smallest deviation from the season median is 0.1%. The largest deviation from the winter season's interquartile range is 7.6%. Therefore, Zone 9 is calibrated

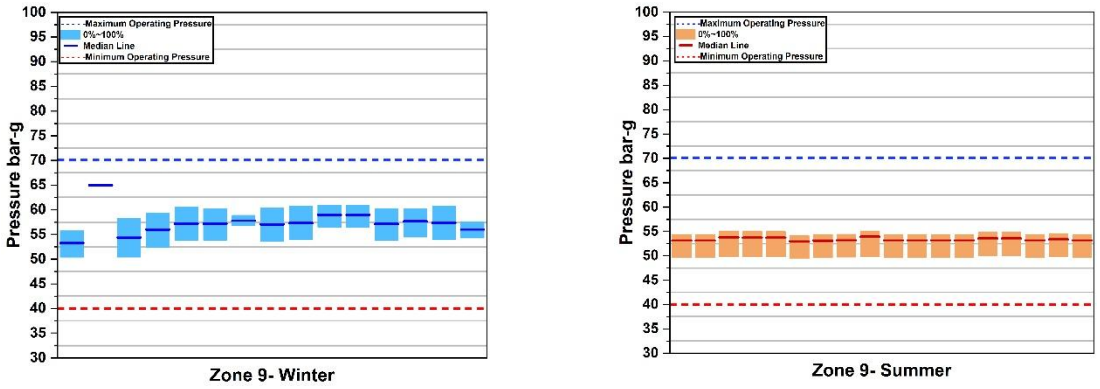

Figure B.21. Pressure levels in each node in Zone 9 in (a) Winter Model and (b) Summer Model.

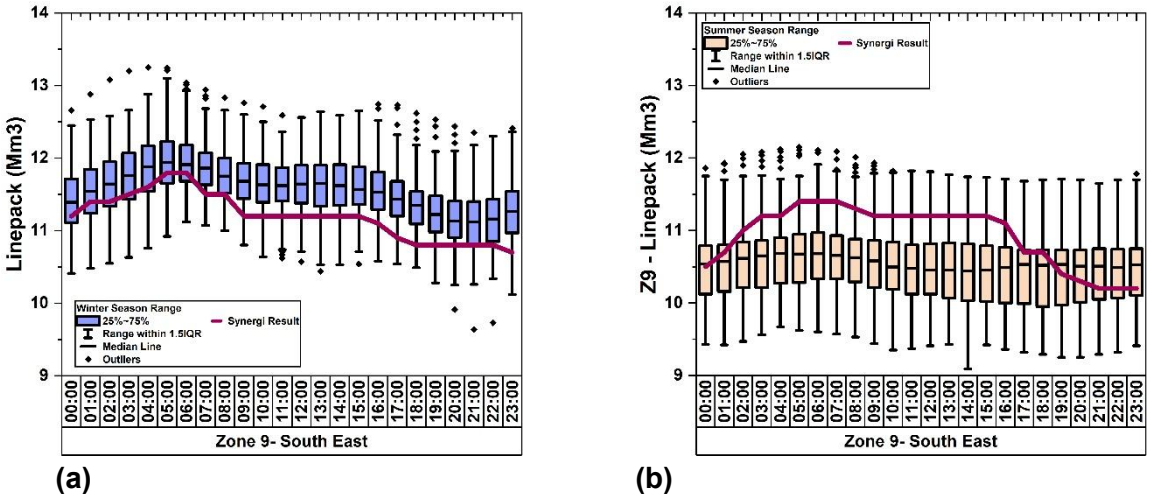

Figure B.22. Result linepack versus seasonal linepack range in Zone 9 in (a) Winter Model and (b) Summer Model.

Zone 10 in Southeast England

Zone 10 stretches from the Huntingdon compressor to the Isle of Grain supply point. The pipelines have an MOP of 70 bar-g. Figure B.23 depicts the result pressure levels of nodes in Zone 10; Figure B.23 (a) depicts the Winter Model, and Figure B.23(b) depicts the

Summer Model. The pressure levels in both winter and Summer Models are within the operational range. Furthermore, all the medians are at 57.5 bar-g in the Winter Model. In the Summer Model, all the medians are at 61.5 bar-g. In Zone 10, The most significant variation in a single node in the Winter Model is 5 bar-g; in the Summer Model, the largest variation is 5 bar-g.

According to Figure B.24(a), the starting linepack level in the Winter Model is 8.5 Mm3. The closing linepack level is 8 Mm3. The linepack swing is 0.75 Mm3. According to Figure B.24(b), the starting linepack level in the Summer Model is 7.75 Mm3, and the closing linepack level is also 7.75 Mm3. The linepack swing in the Summer Model is 0.65 Mm3.

In the Winter Model, the result linepack of Zone 10, the largest deviation from the season median, is 6.3%. The smallest deviation from the season median is 1.5%. The largest deviation from the winter season's interquartile range is 9.2%. In the Summer Model, the result linepack of Zone 10, the largest deviation from the season median, is 1.8%. The smallest deviation from the season median is 0.1%. The largest deviation from the winter season's interquartile range is 5%. Therefore, Zone 10 is calibrated.

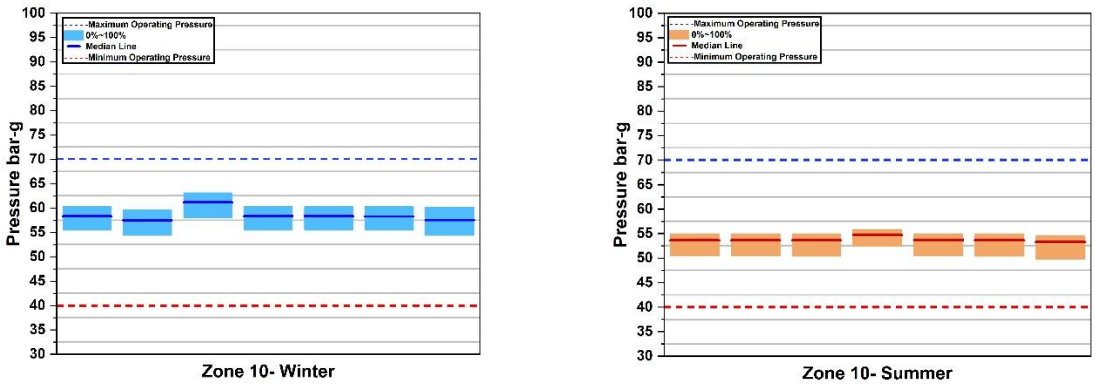

(a) **(b)**

Figure B.23. Pressure levels in each node in Zone 10 in (a) Winter Model and (b) Summer Model.

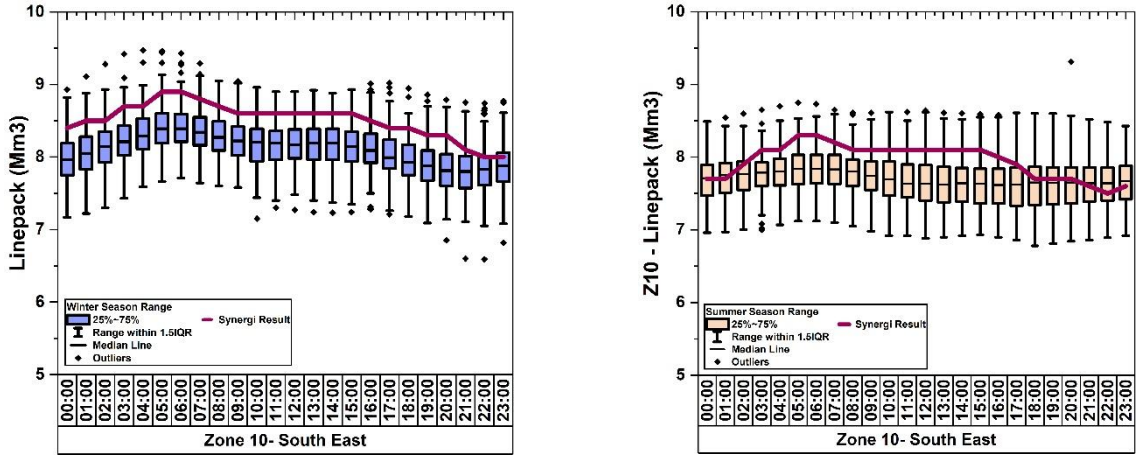

(a) **(b)**

Figure B.24. Result linepack versus seasonal linepack range in Zone 10 in (a) Winter Model and (b) Summer Model.